UNIVERSITY OF CALIFORNIA,
IRVINE

Mechanisms of the Sex-Dependent Effects of Early-Life Adversity on Reward Behaviors

DISSERTATION

submitted in partial satisfaction of the requirements
for the degree of

DOCTOR OF PHILOSOPHY

in Biomedical Sciences

by

Lara Taniguchi

Dissertation Committee:
Professor Tallie Z. Baram, Chair
Professor Christine M. Gall
Assistant Professor Javier Diaz-Alonso

2026

DEDICATION

To

my parents, Jorge, and my friends and family

for their unwavering and unconditional support

TABLE OF CONTENTS

LIST OF FIGURES

Page

LIST OF TABLES

ACKNOWLEDGMENTS

I would like to express my sincere gratitude to the many individuals who have supported me throughout this journey. This work would not have been possible without you.

First and foremost, I would like to thank my advisor, Dr. Tallie Z. Baram. From our very first meeting, I felt genuinely welcomed and supported. Through your continued mentorship and guidance, I have grown tremendously as a scientist and have learned to embrace challenges both in and outside the laboratory. I am deeply grateful for everything you have done for me, and I look forward to our continued work together.

I am grateful to the entire Baram Lab, past and present, for their support, camaraderie, and collegiality. Thank you to Dr. Theresa Auer, Dr. Matthew Birnie, Dr. Yuncai Chen, Dr. Amalia Floriou-Servou, Dr. Rachael Hokenson, Dr. Ryan Weber, Jennifer Daglian, Mason Hardy, Lia Harvey, Jorge Miguel Mendoza, Madison Tetzlaff, James Weinstock, Dr. Noriko Kamei, Dr. Cassie Kooiker, Dr. Sophie Levis, Dr. Annabel Short, Aidan Pham, and Graciella Angeles for your assistance with the laboratory, my experiments, and for the many wonderful conversations along the way. I would especially like to thank Dr. Matthew Birnie for your mentorship and guidance since my very first year of graduate school. Without your support and patience in teaching me the foundations of this research, this work would not have been possible. I also wish to thank Dr. Yuncai Chen for your invaluable support, and for what our lab has come to refer to as "Dr. Chen's magic". Your remarkable ability to troubleshoot experiments and equipment has been an immeasurable asset to this work. I am incredibly grateful to my undergraduate mentees, Amanda, Anamika, Diya, and Anusuya, for the countless hours you devoted to this research. Your hard work, dedication, and growth have been a true joy to witness. I also wish to acknowledge the mice used in this research for their contribution to the advancement of science.

I would like to extend my sincere gratitude to our collaborators, without whom this work would also not have been possible: Dr. Caitlin Goodpaster, Dr. Laura DeNardo, Dr. Gregory Belo de Carvalho, and Dr. Lulu Y. Chen. I am deeply thankful to my advancement committee, Dr. Tallie Z. Baram, Dr. Christine M. Gall, Dr. Robert F. Hunt, Dr. Lulu Y. Chen, and Dr. Stephen Mahler, and to my dissertation committee, Dr. Tallie Z. Baram, Dr. Christine M. Gall, and Dr. Javier Diaz-Alonso, for your guidance and support in my development as a scientist. I would also like to thank my former mentors in science: Dr. Belén C. Guerra-Carrillo, Dr. Wei-Chun Wang, Dr. Silvia A. Bunge, Dr. Ray Lei Zhong, Dr. Lu Chen, Dr. Neir Eshel, Dr. Brandon Bentzley, Dr. Jason Tucciarone, and Dr. Robert C. Malenka. I am grateful for the opportunities each of you provided me to learn, grow, and cultivate my scientific curiosity, and for the wonderful colleagues I met through these experiences.

To my INP cohort, I am so grateful to have shared this journey with such an extraordinary group of people. Your support, encouragement, and camaraderie through both the triumphs and the challenges of graduate school have been invaluable to me. It has been a privilege to witness so many of us reach this milestone, and I look forward to

continuing to celebrate one another's accomplishments for years to come. I would especially like to acknowledge Nini Liu, Daisy Gallardo, Chelsea Callicoatte, and Sarai Santos. You have been there since the very beginning of this journey, and I am truly fortunate to call you, my friends. Through the highs and the lows, your friendship has been a constant source of strength and joy. I am forever grateful that graduate school brought us together, and I look forward to the many adventures that lie ahead. I dearly love you all.

I have been fortunate to meet so many remarkable people through graduate school, and I am deeply grateful for the friendships and experiences we have shared. Your presence has enriched my life in ways I could not have anticipated, and I treasure each of these connections deeply. To my college friends and post-baccalaureate friends, thank you for maintaining our friendships across time and distance. It has been a great joy to reconnect whenever our paths cross, and I have treasured your steadfast friendship and support throughout this journey.

I would like to extend my heartfelt thanks to the entire CNLM team, my K-12 committee co-chairs Alina Tu, Matthew Sandoval, and Jorge Miguel Mendoza, and the CNLM Ambassador Program. I am deeply grateful to Dr. Manuella Yassa, Dr. Morgan Coburn, and Dr. Erin Conway, and to this community for the opportunity to engage in meaningful outreach alongside such a dedicated and supportive group of people. I look forward to our continued work together.

I am also grateful to have been able to continue dancing during graduate school, and to the many wonderful people I met through classes at UCI and through Lost and Thriving and SHUSH dance teams. Thank you for making dance a consistent source of joy and renewal throughout this journey.

I would like to express my gratitude to the musical artists Seventeen and BTS, whose music and performances have provided me with hope, motivation, and comfort throughout the years.

I have also been fortunate to be part of the Fitness on Fire community, and I am particularly grateful to Daisy for the introduction. Thank you all for your friendship, kindness, and encouragement, both during our workouts and beyond. Your support has been a meaningful part of my graduate school experience.

What began as a small group deciding to train for a marathon together has grown into something far greater. Thank you to the Myelin Milers for the training runs, races, and wonderful adventures we have shared. I look forward to many more to come.

I would also like to extend a heartfelt thank you to my plushies, especially to Spot, for the quiet comfort and encouragement you provided throughout this journey. On the most difficult days, your presence was a small but meaningful reminder to keep going.

Jorge, it is difficult to find words adequate to express the depth of my gratitude for your support over these past two and a half years. From a chance conversation about a beloved lab tradition, our relationship and friendship have grown into something I hold very dear, through adventures to national parks, races, and travels abroad. More than the adventures, I am grateful for the steadiness and calm you brought to the more difficult moments of this journey. Thank you for your patience, your kindness, your unwavering support, and your confidence in me, especially during the many moments when I doubted myself. I am so grateful to have shared this journey with you, and I look forward to all that lies ahead. I love you so much. I would also like to thank Jorge's family for their warmth and support.

Finally, to my parents, thank you for your immeasurable sacrifices and tireless dedication. I would not be where I am today without you. You are my greatest role models, and I aspire to one day reflect even a fraction of your strength and resilience. Thank you for working so hard to provide me with every opportunity to learn and grow, and for trusting me to pursue my dreams across an ocean. Though the physical distance between us has at times been great, I have never once doubted your love and support. I love you very, very much, and as my father once said, "we are a family, so we must be together." I look forward to many future adventures together. I would also like to thank my aunts, uncles, and cousins, and my grandmother Maba, who has been cheering me on from Japan. To my grandparents Jiyan, Jichan, and Bachan, I hope you are smiling down and are proud.

To the many others I may not have mentioned by name, please know that I am genuinely grateful for every connection, large or small, that has shaped my path. Thank you all.

This work was supported by National Institutes of Health Grants R01 MH132680 and P50 MH096889, the Bren Foundation, the Dr. Lorna Carlin Scholar Award, and travel awards from the UCI School of Medicine and the Center for the Neurobiology of Learning and Memory.

Chapter 1 of this dissertation is an adaptation of material as it appears in Birnie, M. T., & Baram, T. Z. (2025). The evolving neurobiology of early-life stress. Neuron, 113(10), 1474–1490, used with permission from Cell Press. Chapter 2, originally published in Nature Communications, and Chapters 3 and 4, originally published in the Journal of Neuroscience, are included with the permission of the respective publishers. Co-authors of Birnie et al. 2023, published in Nature Communications, include: Matthew T. Birnie, Annabel K. Short, Gregory B. de Carvalho, Lara Taniguchi, Benjamin G. Gunn, Aidan L. Pham, Christy A. Itoga, Xiangmin Xu, Lulu Y. Chen, Stephen V. Mahler, Yuncai Chen, and Tallie Z. Baram. Co-authors of Taniguchi et al. 2026, published in the Journal of Neuroscience, include: Lara Taniguchi, Caitlin M. Goodpaster, Yuncai Chen, Gregory B. de Carvalho, Matthew T. Birnie, Anamika Paul, Amanda Chiang, Lulu Y. Chen, Tallie Z. Baram, and Laura A. DeNardo. All research included in this dissertation was directed and supervised primarily by Dr. Tallie Z. Baram.

VITA

Lara Taniguchi

EDUCATION

Doctor of Philosophy in Biomedical Sciences — Expected August 2026
University of California, Irvine

Bachelor of Arts in Molecular and Cell Biology, Neurobiology Emphasis — May 2019
University of California, Berkeley

RESEARCH EXPERIENCE

Graduate Student Researcher — 2022–Present
Department of Anatomy & Neurobiology, University of California, Irvine
PI: Dr. Tallie Z. Baram

Life Science Research Professional — 2019–2021
Department of Psychiatry and Behavioral Sciences, Stanford University
PI: Drs. Robert Malenka, Neir Eshel, Brandon Bentzley, Jason Tucciarone

Undergraduate Research Assistant — 2017–2019
Department of Psychology, University of California, Berkeley
PI: Dr. Silvia Bunge

Summer Undergraduate Research Assistant — Jun–Aug 2018
Department of Psychiatry and Behavioral Sciences, Stanford University
PI: Dr. Lu Chen

PUBLICATIONS

- Birnie, M. T., Short, A. K., De Carvalho, G. B., Taniguchi, L., Gunn, B. G., Pham, A. L., Itoga, C. A., Xu, X., Chen, L. Y., Mahler, S. V., Chen, Y., & Baram, T. Z. (2023). Stress-induced plasticity of a CRH/GABA projection disrupts reward behaviors in mice. Nature Communications, 14(1), 1088. https://doi.org/10.1038/s41467-023-36780-x
- Cardozo Pinto, D. F., Taniguchi, L., Norville, Z. C., & Pomrenze, M. B. (2020). A New Look at the Role of Mesoamygdaloid Dopamine Neurons in Aversive Conditioning. The Journal of Neuroscience, 40(40), 7590–7592. https://doi.org/10.1523/JNEUROSCI.1483-20.2020
- Eshel, N., Touponse, G. C., Wang, A. R., Osterman, A. K., Shank, A. N., Groome, A. M., Taniguchi, L., Cardozo Pinto, D. F., Tucciarone, J., Bentzley, B. S., & Malenka, R. C. (2024). Striatal dopamine integrates cost, benefit, and motivation. Neuron, 112(3), 500-514.e5. https://doi.org/10.1016/j.neuron.2023.10.038
- Taniguchi, L., Goodpaster, C. M., Chen, Y., De Carvalho, G. B., Birnie, M. T., Paul, A., Chiang, A., Chen, L. Y., Baram, T. Z., & DeNardo, L. A. (2026). Sex and Stress Govern the Function and Innervation of a Basolateral Amygdala to Nucleus Accumbens Corticotropin-Releasing Hormone/GABA-Expressing Projection. The

Journal of Neuroscience, 46(2), e1239252025. https://doi.org/10.1523/JNEUROSCI.1239-25.2025

- Tian, G., Hui, M., Macchia, D., Derdeyn, P., Rogers, A., Hubbard, E., Liu, C., Vasquez, J. J., Taniguchi, L., Bartas, K., Carroll, S., & Beier, K. T. (2022). An extended amygdala-midbrain circuit controlling cocaine withdrawal-induced anxiety and reinstatement. Cell Reports, 39(5), 110775. https://doi.org/10.1016/j.celrep.2022.110775
- Wang, A. R., Groome, A., Taniguchi, L., Eshel, N., & Bentzley, B. S. (2020). The role of dopamine in reward-related behavior: Shining new light on an old debate. Journal of Neurophysiology, 124(2), 309–311. https://doi.org/10.1152/jn.00323.2020

PRESENTATIONS

- Role of a Novel Amygdala-Accumbens Neuropeptide/Neurotransmitter Expressing Projection in Motivated Behaviors: Effects of Early Life Adversity and Sex Differences. Anatomy and Neurobiology Grad Day. UC Irvine, California, USA. September 2024.
- Sex Dependent Influence of Early Life Adversity on Reward Circuits. DeNardo Lab Meeting. UCLA, California, USA. May 2023. **Invited Talk*
- Sex Dependent Influence of Early Life Adversity on Reward Circuits. Progress in Neuroscience Seminar Series. UC Irvine, California, USA. April 2023. **Competitively selected as Best Pre-Doc PiN Talk of the Year (2022-2023)*
- Sex Dependent Influence of Early Life Adversity on Reward Circuits. Interdepartmental Neuroscience Program Symposium. UC Irvine, California, USA. June 2022.

POSTERS

- Taniguchi, L., Goodpaster, C. M., Chen, Y., De Carvalho, G. B., Birnie, M. T., Paul, A., Chiang, A., Chen, L. Y., Baram, T. Z., & DeNardo, L. A. Sex-Specific Structure And Function Of A CRH/GABAergic Basolateral Amygdala→Nucleus Accumbens (BLA—NAc) Projection Governs The Impact Of Early-Life Adversity On Adult Motivated Behaviors. School of Medicine Grad Day 2026. UC Irvine, California, USA. May 2026.
- Taniguchi, L., Goodpaster, C. M., Chen, Y., De Carvalho, G. B., Birnie, M. T., Paul, A., Chiang, A., Chen, L. Y., Baram, T. Z., & DeNardo, L. A. Sex-Specific Structure And Function Of A CRH/GABAergic Basolateral Amygdala→Nucleus Accumbens (BLA—NAc) Projection Governs The Impact Of Early-Life Adversity On Adult Motivated Behaviors. Society for Neuroscience 2025. San Diego, California, USA. November 2025.
- Taniguchi, L., Goodpaster, C. M., Chen, Y., De Carvalho, G. B., Birnie, M. T., Paul, A., Chiang, A., Chen, L. Y., Baram, T. Z., & DeNardo, L. A. Sex- and Stress-Dependent Plasticity of a Novel CRH/GABA BLA-NAc Projection That Mediates Reward Behaviors. Conte Center at UCI 12th Annual Symposium. Irvine, California, USA. February 2025.
- Taniguchi, L., Goodpaster, C. M., Chen, Y., De Carvalho, G. B., Birnie, M. T., Paul, A., Chiang, A., Chen, L. Y., Baram, T. Z., & DeNardo, L. A. Sex- and Stress-Dependent Plasticity of a Novel CRH/GABA BLA-NAc Projection That Mediates

Reward Behaviors. Society for Neuroscience 2024. Chicago, Illinois, USA. October 2024.

- Taniguchi, L., Goodpaster, C. M., Chen, Y., De Carvalho, G. B., Birnie, M. T., Paul, A., Chiang, A., Chen, L. Y., Baram, T. Z., & DeNardo, L. A. Sex Dependent Influence of Early Life Adversity on Reward Circuits. School of Medicine Grad Day 2024. UC Irvine, California, USA. May 2024.
- Taniguchi, L., Goodpaster, C. M., Chen, Y., De Carvalho, G. B., Birnie, M. T., Paul, A., Chiang, A., Chen, L. Y., Baram, T. Z., & DeNardo, L. A. Sex Dependent Influence of Early Life Adversity on Reward Circuits. Conte Center at UCI 11th Annual Symposium. UC Irvine, California, USA. March 2024.
- Taniguchi, L., Goodpaster, C. M., Chen, Y., De Carvalho, G. B., Birnie, M. T., Paul, A., Chiang, A., Chen, L. Y., Baram, T. Z., & DeNardo, L. A. Sex Dependent Influence of Early Life Adversity on Reward Circuits. Society for Neuroscience 2023. Washington, D.C., USA. November 2023.
- Taniguchi, L., Birnie, M. T., Chen, Y., & Baram, T. Z. Sex Dependent Influence of Early Life Adversity on Reward Circuits. Conte Center at UCI 10th Annual Symposium. UC Irvine, California, USA. March 2023.
- Taniguchi, L., Birnie, M. T., Chen, Y., & Baram, T. Z. Sex Dependent Influence of Early Life Adversity on Reward Circuits. Society for Neuroscience 2022. San Diego, California, USA. November 2022.
- Taniguchi, L., Birnie, M. T., Chen, Y., & Baram, T. Z. Sex Dependent Influence of Early Life Adversity on Reward Circuits. UCI School of Medicine Grad Day 2022. UC Irvine, California, USA. October 2022.
- Taniguchi, L., Birnie, M. T., Chen, Y., & Baram, T. Z. Sex Dependent Influence of Early Life Adversity on Reward Circuits. Conte Center at UCI 9th Annual Symposium. UC Irvine, California, USA. March 2022.
- Taniguchi, L., Wang, W. C., Bunge, S. A. Effects of Prior Knowledge and Development on Memory for Verbal Associations. Molecular and Cell Biology Honors Research Poster Session. UC Berkeley, California, USA. 2019.
- Guerra-Carrillo, B., Taniguchi, L., Bunge, S.A. Eye Gaze Patterns Reflect Individual Differences in Reasoning Improvements. Association for Psychological Science 30th Annual Convention. San Francisco, California, USA. 2018.

HONORS AND AWARDS

- Neurobiology of Stress Workshop Travel Award (June 2026)
- UC Irvine Dr. Lorna Carlin Scholar Award (December 2025)
- UC Irvine Stanley Behrens Health Sciences Research Award (October 2025)
- UC Irvine CNLM Norman M. Weinberger Award (March 2025)
- UC Irvine CNLM John W. Haycock Memorial Graduate Student Award (March 2023)

ABSTRACT OF THE DISSERTATION

Mechanisms of the Sex-Dependent Effects of Early-Life Adversity on Reward Behaviors

by
Lara Taniguchi
Doctor of Philosophy in Biomedical Sciences
University of California, Irvine, 2026
Professor Tallie Z. Baram, Chair

Early-life adversity (ELA) is a risk factor for human affective disorders involving dysregulated reward behaviors. In our limited bedding and nesting mouse model, ELA induces anhedonia-like behaviors in adult male mice while increasing motivation for rewards in adult females, indicating sex-dependent disruption of reward circuit operations. Searching for potential underlying circuit mechanisms of these disruptions of reward behavior, we identified a novel projection from the basolateral amygdala (BLA) to the nucleus accumbens (NAc) that expresses the stress-sensitive neuropeptide corticotropin-releasing hormone (CRH), together with the neurotransmitter GABA.

To test the contribution of this projection to reward deficits in adult male and female mice reared in ELA conditions, we conducted the following experiments: Adult male and female CRH-Cre mice raised in control or ELA conditions received bilateral excitatory or inhibitory Cre-dependent DREADDs in the BLA, with clozapine N-oxide or vehicle delivered bilaterally to the NAc medial shell during reward behaviors. Cell identity was determined via immunostaining and electrophysiology. Tissue clearing, light sheet fluorescence microscopy, and deep learning pipelines were used to map brain-wide CRH BLA axonal projections.

Bilateral chemogenetic manipulations in male mice demonstrated inhibitory effects of the CRH/GABA BLA→NAc projection on reward behaviors in control mice and

inhibiting the projection rescued reward deficits in ELA male mice. In females, neither excitation nor inhibition influenced reward seeking behaviors. Molecular and electrophysiological cell-identities of the projection did not vary by sex. By contrast, comprehensive whole-brain mapping uncovered subtle differences in axonal terminals in the NAc as well as elsewhere, which were both sex- and ELA-dependent. Because these changes did not explain the apparent lack of effect of bilateral chemogenetic manipulations of the projection on female reward behaviors, we tested the hypothesis that ipsilateral and contralateral CRH/GABA BLA→NAc projections may have opposing effects on reward behavior that cancel out when both are manipulated concurrently. Results of ongoing studies support this hypothesis.

In summary, the CRH/GABA BLA→NAc projection that influences reward behaviors in males differs structurally and functionally in females, uncovering potential mechanisms for the profound sex-specific impacts of ELA on reward behaviors. Further investigation of this projection will give us a deeper understanding of intrinsic sex differences in the organization of the reward circuitry and the effects of ELA on reward behaviors that underlie many mood disorders.

Chapter 1 – Introduction

Prevalence and Scope of Early-Life Adversity

Early-life adversity (ELA), encompassing childhood exposure to abuse, neglect, poverty, and chaotic caregiving, affects a majority of the world's children and is among the strongest known risk factors for long-term cognitive and emotional health impairment (Merrick et al., 2018; Short & Baram, 2019). In the United States, more than 60% of adults report at least one type of adverse childhood experience, and nearly one in six report four or more distinct categories (Hughes et al., 2017; Swedo et al., 2023). This burden is not equally distributed: individuals from low socioeconomic communities and racial and ethnic minority groups are disproportionately affected (Liu et al., 2018; Merrick et al., 2018). The consequences of ELA span a wide spectrum of health outcomes, from anxiety, depression, and cognitive dysfunction to obesity and cardiovascular disease (Burke et al., 2011; K. E. Smith & Pollak, 2020; Taylor, 2010).

The foundational large-scale study by Felitti et al. (1998) demonstrated that adverse childhood experiences exert a cumulative, dose-dependent impact on lifetime health outcomes, a finding confirmed across independent cohorts (Baldwin et al., 2021). These findings align with the concept of allostatic load, which describes the progressive physiological dysregulation incurred when repeated stressors prevent full homeostatic recovery across the brain and body (McEwen, 1998; McEwen & Stellar, 1993). This framework motivated the adoption of quantitative ACE scores as clinical screening tools (Dube et al., 2003), yet ACE scores have significant limitations at the individual level: they do not account for gene-environment interactions, omit protective factors embedded in family and social context, and assign equal weight to all adverse

experiences despite evidence that distinct adversity types engage divergent neurobiological pathways (Baldwin et al., 2021; Birnie & Baram, 2025).

Among the adversity dimensions not captured by standard ACE instruments, the unpredictability of sensory signals from caregivers and the proximate environment has emerged as an independently consequential risk factor (Davis et al., 2017; Glynn & Baram, 2019). Human cohort studies across multiple continents demonstrate that unpredictable maternal sensory signals, quantified as entropy, predict adverse neurodevelopmental and psychiatric outcomes in children and adolescents beyond the variance explained by established ACEs (Davis et al., 2017, 2019; Spadoni et al., 2022). A population study of approximately 30,000 children indicated that early unpredictability alone increases the probability of depression approximately 12-fold (Glynn et al., 2026). Because unpredictability of childhood experiences is amenable to behavioral intervention, its neurobiological characterization carries direct clinical urgency (Luby et al., 2020).

Outcomes of ELA: Effects on Reward Circuit Function

ELA is robustly associated with augmented, sex-modulated vulnerability to depression and PTSD (Anda et al., 2006; Green et al., 2010; LeMoult et al., 2020; Tracy et al., 2019). These conditions are defined in part by anhedonia, a diminished capacity to experience pleasure or pursue rewarding stimuli, which reflects early stress-induced disruption of the underlying reward circuitry (Heshmati & Russo, 2015; Nestler & Carlezon, 2006; Pizzagalli, 2022). The clinical stakes of anhedonia extend beyond depression per se. For example, it predicted post-combat PTSD development in U.S.

Marine Corps recruits (Risbrough et al., 2018), is independently associated with suicidal ideation (Ducasse et al., 2018), and forecasted poor treatment outcomes in cocaine dependence (Crits-Christoph et al., 2018).

Human neuroimaging studies directly link ELA to the structural and functional correlates of anhedonia. Smaller right NAc volume correlated with anhedonic symptom burden, and bilateral putamen volume predicted both current and future anhedonic state severity (Auerbach et al., 2017). Functional MRI revealed reduced basal ganglia activity in young adults with histories of early institutional deprivation (Boecker et al., 2014; Mehta et al., 2010), and attenuated ventral striatum activation during reward anticipation was documented in adolescents who experienced ELA, with the effects more pronounced when adversity occurred earlier in development (Corral-Frías et al., 2015).

Whereas there is a strong link between early-life adversity with emotional and cognitive deficits later in life in humans, studies in humans are still correlational. Establishing causality, and, further, identifying underlying mechanisms requires animal experimentation. Our group has generated a rodent model of chronic stress during the first postnatal weeks through the limiting bedding and nesting (LBN) model (see section Animal Models of ELA: Limited Bedding and Nesting Model for more details). LBN-induced ELA produces persistent anhedonia-like deficits in male adult mice and rats, including reduced consumption of palatable food, diminished preference for sex-relevant cues, lowered sucrose preference, and a reduced hedonic set point for cocaine (Birnie et al., 2023; Bolton et al., 2018; Levis et al., 2022; Molet, Heins, et al., 2016; Molet, Maras, et al., 2016). In contrast, adult female LBN rodents exhibit augmented reward motivation, the opposite behavioral profile, demonstrating sex-dependent

divergence from the same early-life experience (Birnie et al., 2023; Levis et al., 2021; Machado et al., 2013; L. Taniguchi et al., 2026). Human neuroimaging and rodent behavioral data thus converge on reward circuit dysregulation as a consistent, replicable outcome of ELA (Birnie et al., 2020; Bolton et al., 2018; Kangas et al., 2022; Pizzagalli et al., 2005).

Sex Differences in Outcomes of ELA

ELA does not uniformly elevate psychiatric risk across biological sexes. In humans, women with childhood adversity histories show disproportionate susceptibility to comfort-food craving and to the development of eating and opioid use disorders (Evans et al., 2017; J. G. Johnson et al., 2002), while men with comparable adversity histories are more prone to alcohol use disorders (Colman et al., 2013; Evans et al., 2017). These divergent profiles likely reflect sex-specific characteristics of reward circuitry operations, potentially compounded by sex-biased developmental vulnerabilities to ELA (Bale & Epperson, 2015; Bath, 2020; Becker & Chartoff, 2019; Hodes & Epperson, 2019). Nevertheless, the precise nature of sex differences in ELA outcomes remains incompletely characterized, with findings that are not fully consistent across populations, and establishing direct causal relationships between ELA and sex-specific reward pathology in humans is inherently difficult given the correlational nature of these studies. Animal experimentation is therefore essential for isolating the neurobiological mechanisms that underlie these sex-specific vulnerabilities. Consistent with this approach, a recent study using chemogenetic circuit manipulation in mice identified a sex-specific amygdalo-striatal pathway as a driver of sex-divergent alcohol-

related behaviors, demonstrating that the BLA→NAc projection contributes to binge drinking specifically in females (Maddern et al., 2026).

Rodent ELA models reproduce sex-specific behavioral divergence with experimental precision. Adult males reared in LBN ELA conditions display reduced appetitive and consummatory reward behaviors consistent with anhedonia, whereas ELA females show augmented reward motivation without altered consummatory pleasure (Birnie et al., 2023; Bolton et al., 2018; Levis et al., 2021, 2022; Machado et al., 2013; Molet, Heins, et al., 2016; Molet, Maras, et al., 2016). At the molecular level, early-life adversity produces sex-specific transcriptional reprogramming across the reward circuitry including the NAc (Peña et al., 2019), and interactions between ELA and ovarian hormones generate distinct NAc gene expression profiles that influence sex-specific responses to cocaine (Rocks et al., 2023). Sex-specific roles for long non-coding RNAs in stress-induced transcriptional changes have further been documented (Issler et al., 2020), and the epigenetic mechanisms governing sex-specific brain organization are now being systematically characterized more broadly (Kundakovic & Tickerhoof, 2024). Both human prospective studies and rodent experiments demonstrate that early-life unpredictability produces sex-specific changes in brain circuit connectivity (Birnie et al., 2023; Bolton et al., 2018; Davis et al., 2025; Granger et al., 2021; L. Taniguchi et al., 2026), providing a structural framework for understanding how the same early experience generates opposite behavioral outcomes depending on biological sex.

Animal Models of ELA: Limited Bedding and Nesting Model

As mentioned above, human studies of ELA generate important epidemiological and clinical insights, but they cannot establish causality or access the cellular and circuit-level mechanisms through which early adversity reprograms the developing brain (Birnie & Baram, 2025). Dissociating genetic from environmental contributions is impossible when the same caregiver provides both the adverse behavioral environment and 50% of the child's genome. Animal models directly address this limitation, enabling controlled isolation of neurotransmitter and neuromodulator contributions, identification of stress-sensitive circuits, mechanistic testing via genetic and pharmacological manipulation, and separation of genetic from environmental factors in controlled laboratory conditions (Birnie & Baram, 2025).

Early rodent models relied on maternal separation, in which pups are removed from the dam daily during the first one to two postnatal weeks for periods ranging from 15 minutes to several hours (Champagne et al., 2008; Gildawie et al., 2024; Huot et al., 2002; Oomen et al., 2010, 2011; Plotsky & Meaney, 1993). Short separations (~15 minutes) typically improved long-term pup outcomes through a compensatory surge of augmented maternal care following reunion (Fenoglio et al., 2006; Korosi et al., 2010), while prolonged separations of 3–4 hours per day reduced cognitive function and disrupted reward behaviors (Champagne et al., 2008; Gildawie et al., 2024; Huot et al., 2002; Oomen et al., 2010, 2011; Plotsky & Meaney, 1993).

The limited bedding and nesting (LBN) paradigm was developed to model the chronic stress of poverty and resource scarcity while maintaining continuous maternal presence, thereby eliminating the confounds of caloric deprivation and predictable daily

separation inherent to separation-based models (Ivy et al., 2008; Molet et al., 2014; Rice et al., 2008). In this model, beginning on postnatal day 2 through day 9, bedding and nesting materials are limited in the dam's home cage by placing a mesh platform over the bedding and providing only half the normal amount of nesting material. The biological indicators of stress in LBN-exposed pups included: plasma corticosterone was elevated, adrenal gland weights were increased, and CRH mRNA in the hypothalamic paraventricular nucleus was reduced by the end of the one-week exposure period (Ivy et al., 2008; Molet et al., 2014; Rice et al., 2008); these changes persisted to adulthood (Rice et al., 2008). Critically, the overall quantity of measured maternal caring behaviors was similar to control dams, but the temporal pattern of care was profoundly disrupted: individual licking-and-grooming bouts were shorter (fragmented), and their sequences were no longer recurrent (unpredictable), as quantified by entropy rate (Demaestri et al., 2022; Ivy et al., 2008; Molet, Heins, et al., 2016; Vegetabile et al., 2019). Demaestri et al. (2022) confirmed the mechanistic specificity of this disruption, demonstrating that resource scarcity, but not maternal separation, provokes unpredictable maternal care sequences and upregulates CRH-associated gene expression in the amygdala. This model has been adopted by research groups worldwide as a reproducible, translatable paradigm for chronic early-life adversity (Walker et al., 2017) and produces robust, sex-dependent disruptions in memory, reward behaviors, and vulnerability to addiction-like behaviors in adult rodents (Birnie et al., 2023; Bolton et al., 2018; Levis et al., 2021, 2022; Molet, Heins, et al., 2016; Molet, Maras, et al., 2016; L. Taniguchi et al., 2026).

For LBN findings to translate meaningfully to human early development, the P2–P9 exposure window must correspond to a genuinely sensitive period in human brain maturation. Comparative analysis of reward circuitry developmental milestones across species, encompassing the timing of NAc appearance, striatal D1 receptor detectability, BLA identifiability, and peak prefrontal synaptic density, indicates that reward circuitry development during the first postnatal week in the rodent approximates that of a full-term human newborn (Birnie et al., 2020). The sensitive period for emotional circuit vulnerability spans approximately the first two postnatal weeks in rodents and the first two years of human life, supported by studies of internationally adopted children demonstrating cognitive recovery contingent on the timing of caregiving normalization and by rodent work linking ELA during this window to enduring cognitive and emotional deficits (Birnie & Baram, 2022; Cohen et al., 2008; C. A. Nelson et al., 2007; Van Den Dries et al., 2010). Within this window, the principal sensory environment consists of the caregiver, and it is the patterning, not merely the quantity, of parental signals that governs circuit maturation: predictable sequences support the network oscillations required for synaptic refinement, while unpredictable sequences disrupt them (Davis et al., 2019; Molet, Heins, et al., 2016). This principle accounts for why a seven-day LBN manipulation during P2–P9 produces lasting changes in adult reward circuit architecture and behavior.

Transducing ELA into Enduring Phenotypes

How does a temporary episode of ELA produce permanent changes in brain circuit architecture and adult behavior? At the molecular level, ELA drives large-scale,

enduring changes in neuronal gene expression across discrete brain regions that persist into adulthood in humans (Arcego et al., 2024; Burns et al., 2018; Turecki et al., 2014) and experimental animals (Maccari et al., 2014; Ochi & Dwivedi, 2023; Peña et al., 2019; Torres-Berrío et al., 2019; Winter et al., 2023). The epigenetic machinery responsible encompasses modifications to DNA methylation (Weaver et al., 2004), histone modifications (Burns et al., 2018; Torres-Berrío et al., 2019), microRNA (L. Allen & Dwivedi, 2020), and long non-coding RNAs (Issler et al., 2020), all of which reorganize chromatin architecture to govern transcriptional access. These mechanisms produce two mechanistically distinct outcomes. The first involves persistent constitutive alterations in expressed genes within specific brain regions and cell types. The second, transcriptional priming, is arguably more behaviorally consequential: ELA renders the chromatin hypersensitive to subsequent experiences by establishing permissive or repressive configurations at specific genomic enhancers, generating pathological gene expression in response to later salient stimuli. A canonical example is ELA-driven priming of ventral tegmental area gene programs via the transcription factor OTX2, which renders animals disproportionately vulnerable to adult stress (Peña et al., 2017). The altered activity of OTX2, DeltaFosB (Nestler, 2015), NRSF (Bolton et al., 2020), and the glucocorticoid receptor (Bolton et al., 2020) reflects chromatin state changes that bias specific sites toward permissive or repressive gene expression upon future challenges (Griffith et al., 2024). Sex, timing, cell type, and genetic background each modulate this epigenomic response, such that identical early exposures can produce divergent molecular outcomes across individuals (Birnie & Baram, 2025).

At the circuit level, a parallel mechanism operates through ELA's disruption of the activity-dependent processes that sculpt developing synaptic architecture. Throughout the postnatal brain, spontaneous network oscillations, including hippocampal sharp waves, thalamocortical rhythms, and sensorimotor spindle bursts, translate patterns of pre- and postsynaptic activity into lasting changes in synaptic strength, converting the over-connected neonatal circuit into a refined adult architecture (Birnie & Baram, 2025). These oscillations are sensitive to circuit-specific sensory inputs: patterned caregiver signals, such as touch from a dam or voice from a parent, directly modulate organizing rhythms in the developing thalamus, cortex, and hippocampus (Birnie & Baram, 2022). When those signals become fragmented and unpredictable, as they are in the LBN model, circuit-organizing activity is disrupted during the emotional circuit sensitive period, initiating cascades of aberrant synaptic strengthening and pruning that produce lasting functional abnormalities (Birnie & Baram, 2022).

Microglia are positioned at the cellular intersection of these structural consequences. Abundant and functional in the neonatal brain, microglia execute the activity-driven synapse pruning that refines developing circuits into their mature form (Block et al., 2022; Bolton et al., 2022; Garvin & Bolton, 2022). ELA disrupts this pruning process in a cell-type-specific manner directly relevant to this dissertation: following resource-scarcity adversity, the density of excitatory synapses onto CRH-expressing neurons in the hypothalamic paraventricular nucleus is augmented in adult mice, generating lasting aberrations in hormonal and behavioral stress responses (Bolton et al., 2022). This structural excess results from ELA-induced microglial dysfunction that impairs the capacity of microglia adjacent to CRH-expressing cells to eliminate surplus

excitatory inputs during the critical developmental window (Bolton et al., 2022). Notably, sex differences in microglial activity are well established (Block et al., 2022; Bolton et al., 2022; Garvin & Bolton, 2022; Lenz et al., 2013), providing a cellular basis for why males and females might show divergent structural reorganization of CRH-expressing projections following ELA. At other circuit nodes, ELA produces structurally opposite outcomes: in the hippocampus, adversity generates selective deficits in neuronal arborization within specific layers (Brunson et al., 2005; Ivy et al., 2010), while observations of increased axonal labeling in the prefrontal cortex of adolescent rats exposed to ELA are consistent with augmented axon sprouting or impaired developmental pruning (Honeycutt et al., 2020). Together, these findings identify ELA-driven dysregulation of structural circuit maturation as a common mechanistic theme across multiple brain regions.

The molecular and structural mechanisms described above are coupled rather than parallel. Neuronal activity drives transcription, and the gene expression programs activated through activity-dependent cascades directly govern axonal and dendritic growth, synapse maturation, and connection strength, feeding back to compound the structural consequences of the initial adversity (Birnie & Baram, 2025). Among the stress-sensitive molecular actors that execute these lasting changes, corticotropin-releasing hormone occupies a privileged position, operating at multiple levels of these mechanisms to translate early adversity into lasting disruption of reward and threat circuits.

Chapter 2 – Role of the CRH/GABA BLA→NAc projection in male mice

Introduction

Corticotropin-Releasing Hormone in Early-Life Stress

Among the molecular mediators linking early-life experience to lasting changes in brain circuit operations, neuropeptides occupy a distinctive functional niche, bridging the rapid effects of classical neurotransmitters with the prolonged genomic actions of steroid hormones (Joëls & Baram, 2009). Corticotropin-releasing hormone (CRH) is the most studied of these, distinguished by its evolutionary conservation across species from fruit flies to humans (Francés et al., 2024; E. C. Johnson et al., 2005) and by the direct implication of its signaling in stress-related psychiatric disorders through genome-wide association studies (Gelernter et al., 2019; Gupta et al., 2024).

Beyond its canonical role in hypothalamic-pituitary-adrenal axis regulation, CRH is synthesized and released at other brain regions, including the hippocampus, central and basolateral amygdala (BLA), extended amygdala, nucleus accumbens (NAc), and many cortical regions, where it modulates synaptic transmission and behavioral state locally (Birnie & Baram, 2025). In accord with its evolutionary function as a threat-responsive suppressor of resource-demanding behaviors, CRH broadly inhibits actions that are energetically costly or reproductively risky during stressful periods (Chrousos et al., 1998; Rivest, 1995). ELA augments CRH expression in the hippocampus and amygdala (Dubé et al., 2015; Ivy et al., 2010), and the functional relevance of this upregulation has been established causally: partial silencing of CRH within the central amygdala of adult ELA-exposed rats reversed anhedonia across multiple behavioral

measures, identifying the amygdala as a locus of CRH-driven maladaptive circuit plasticity following early adversity.

The context-dependence of CRH in the NAc is mechanistically instructive for understanding how ELA produces anhedonia. Under baseline conditions, CRH in the NAc promotes appetitive behavior and increases dopamine release via CRF receptors expressed in both rodent and primate NAc (Y. Chen et al., 2000; Millan et al., 1986). However, following severe prior stress, this valence reverses: CRH-mediated dopamine release is abolished and NAc CRH signaling switches from appetitive to aversive (Hupalo et al., 2019; Lemos et al., 2012). A stress-sensitive peptide that normally facilitates reward thus becomes, in a circuit sensitized by early-life adversity, a driver of anhedonia. CRH-expressing neurons additionally influence neighboring microglia and their synapse-pruning function (Bolton et al., 2022), directly linking these cell populations to the structural remodeling of the circuits they inhabit. These properties collectively position CRH, and the specific projections that express it, as a mechanistically defined target for understanding how ELA produces lasting disruption of reward circuit function.

CRH/GABA BLA→NAc Projection: Rationale and Current Findings

The NAc is a major integrative hub of the reward circuit, receiving convergent excitatory and inhibitory input from cortical, limbic, and subcortical regions to modulate the salience and motivational value of rewarding stimuli (Floresco, 2015; Nestler & Carlezon, 2006; Stuber, 2023). Its primary function is to encode deviations between expected and actual reward outcomes, executed through connections with the

amygdala, thalamic nuclei, and prefrontal cortex (Hurley et al., 2019; Leung & Balleine, 2015; Lichtenberg & Wassum, 2017). This position renders the NAc both a locus of reward computation and a site of vulnerability when the circuits converging upon it are altered by early-life adversity.

The anatomical case for a CRH-expressing amygdaloid input to the NAc was established by Itoga and colleagues, who used viral-genetic mapping alongside anterograde and retrograde tracing in CRH-ires-Cre mice to identify an enrichment of CRH-expressing inputs to the NAc from brain regions involved in sensing, processing, and memory of emotionally salient events (Itoga et al., 2019). These include the paraventricular nucleus of the thalamus, bed nucleus of the stria terminalis, BLA, and medial prefrontal cortex (Itoga et al., 2019). This work demonstrated that the central nucleus of the amygdala, the classically studied CRH-rich structure, does not project directly to the NAc, positioning the BLA as the underappreciated source of CRH-mediated amygdaloid input to the reward hub (Itoga et al., 2019).

The BLA is a principal limbic afferent to the NAc and plays a well-established role in reward learning and addiction (Wassum & Izquierdo, 2015). BLA cell populations are organized by their downstream projection target, with distinct molecular identities and opposing valence-encoding properties characterizing projection-defined subpopulations (Beyeler et al., 2018). The canonical BLA→NAc projection is glutamatergic: BLA neurons activated during reward anticipation facilitate reward-seeking behavior by exciting NAc neurons (Ambroggi et al., 2008; Stuber et al., 2011). However, the novel BLA→NAc CRH pathway's function was unknown at the time of its discovery.

The first functional characterization of this pathway was provided by Birnie et al. (2023). Using chemogenetic and optogenetic approaches, here we characterize the role of this pathway in reward behavior and establish that it mediates the reward-seeking deficits that ELA produces in adult male mice.

Adult male mice raised in early-life adversity conditions have reward deficits

The LBN model, in which poverty is simulated via a resource-scarce environment during postnatal days 2–10 in mice, leads to clear reward circuit disruptions in male mice. To determine whether the CRH/GABA BLA→NAc projection contributes to this, we first identified the reward behaviors affected after ELA. In adult males raised in ELA conditions (Figure 2.1A), we found significantly reduced consumption of palatable food, specifically Cocoa Pebbles, compared to typically reared controls (CTL), while regular chow consumption was unchanged (Figure 2.1B). We also found that ELA males spent significantly less time investigating a sex cue, the scent of a female mouse in estrus (Figure 2.1C). Finally, preference for sucrose solution was also significantly lower in ELA males (Figure 2.1D). Together, these findings establish that ELA produces broad reward deficits in male mice.

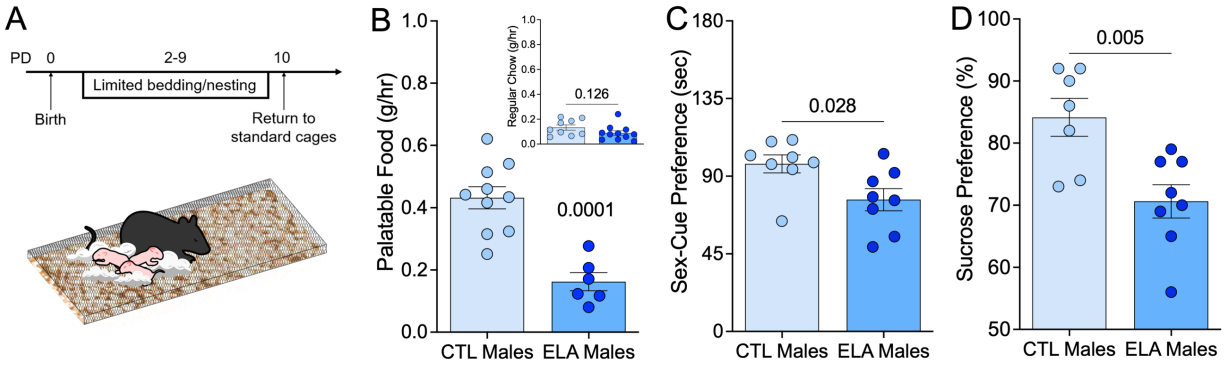

Figure 2.1: Adult male mice raised in early-life adversity conditions have reward deficits

(A) Timeline and environment (limited bedding and nesting) of ELA. (B) ELA reduced palatable food consumption in male mice (n = 16 mice; CTL = 10, ELA = 6) yet did not alter regular chow consumption (n = 20 mice; CTL = 9, ELA = 11). (C) ELA reduced preference for a sex-cue (n = 16 mice; CTL = 8, ELA = 8) and (D) preference for sucrose (n = 15 mice; CTL = 7, ELA = 8). In B–D, bars represent mean ± SEM. Two-sided unpaired t-tests (B,D), two-sided unpaired U-test (C). B, CTL vs. ELA main: p = 0.0001, inset: p = 0.126; C, CTL vs. ELA: p = 0.028. Lighter blue, typical-reared control (CTL). Darker blue, early-life adversity (ELA).

Exciting the CRH/GABA BLA→NAc projection in typically reared (control) male mice reduces reward behaviors

To investigate the function of the CRH/GABA BLA→NAc projection, we targeted it during two different reward behaviors, palatable food consumption and sex cues, using chemogenetic and optogenetic strategies. In adult male control CRH-ires-Cre mice, we injected Cre-dependent AAV2-hM3D(Gq) excitatory DREADD virus or Cre-dependent channelrhodopsin bilaterally into the basolateral amygdala. We then implanted bilateral guide cannulas or optic fibers into the medial shell of the NAc, allowing us to infuse CNO (1 mM) or deliver light (blue light 473 nm at 10 Hz) directly to the projection terminals, enabling pathway-specific manipulation. When we excited the CRH/GABA BLA→NAc projection in typically reared CTL males, we observed significant suppression of both palatable food consumption and sex-cue investigation (Figure 2.2A–D), recapitulating the reward deficits we observed in ELA mice. In contrast, inhibiting the same projection using Cre-dependent AAV2-hM4D(Gi) inhibitory DREADD virus in control males produced no change in reward behavior in either palatable food or sex-cue preference (Figure 2.2E–F). These findings show an unexpected reward-suppressing role for the CRH/GABA BLA→NAc projection in control males, and differ from the well-established, reward-enhancing glutamatergic projection connecting the BLA and NAc (Ambroggi et al., 2008; Stuber et al., 2011). Given that CRH expression and function are often modulated by stress (Y. Chen et al., 2016;

Lemos et al., 2012; Walsh et al., 2014), these data support the possibility that this projection, acting via GABA, CRH, or both neuromodulators, might mediate suppressed reward behaviors which are often observed after adult or developmental stresses.

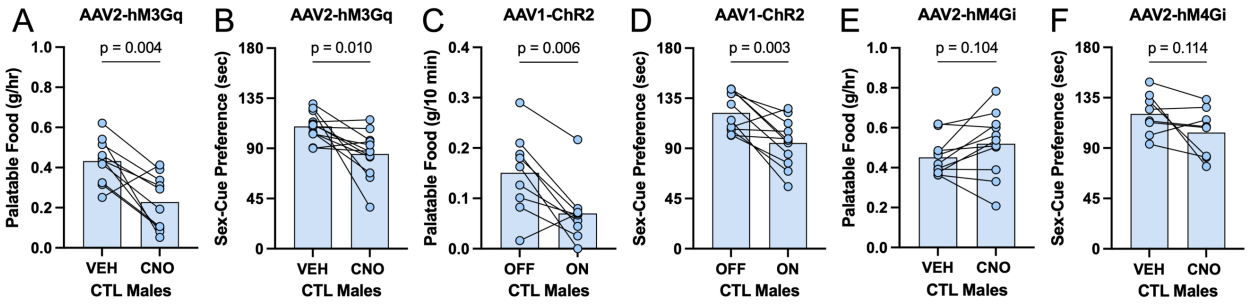

Figure 2.2: Exciting the CRH/GABA BLA→NAc projection in typically reared (control) male mice reduces reward behaviors

(A–B) Chemogenetically stimulating the CRH/GABA BLA→NAc projection with microinfusion of CNO in the medial NAc shell suppressed (A) palatable food consumption (n = 10 mice) and (B) preference for a sex-cue (n = 12 mice). (C–D) Stimulating the CRH/GABA ChR2-expressing BLA→NAc projection decreased (C) palatable food consumption (n = 9 mice) and (D) approach time to a sex-cue (n = 11 mice). (E–F) Inhibiting the CRH/GABA BLA→NAc projection in CTL male mice did not increase (E) palatable food consumption (n = 11 mice) or (F) preference for a sex-cue (n = 8 mice). In A–F, bars represent mean. Two-sided paired t-tests (A–F). A, hM3D(Gq) BLA→NAc: p = 0.004; B, hM3D(Gq) BLA→NAc: p = 0.010. C, ChR2 BLA→NAc: p = 0.006; D, ChR2 BLA→NAc: p = 0.003. E, hM4D(Gi) BLA→NAc: p = 0.104; F, hM4D(Gi) BLA→NAc: p = 0.114. VEH, vehicle. CNO, clozapine-N-oxide. CTL, control.

Inhibiting the CRH/GABA BLA→NAc projection in male mice raised in early-life adversity conditions rescues reward deficits

Given that chemogenetic and optogenetic stimulation of the CRH/GABA BLA→NAc projection in CTL male mice recapitulated the reward deficits seen in adult ELA male mice, we speculated that the projection may have a role in these ELA-induced reward deficits. To test the role of the projection in ELA male mice, we inhibited the projection by injecting a Cre-dependent AAV2-hM4D(Gi) inhibitory DREADD virus bilaterally into the basolateral amygdala of CRH-ires-Cre males raised in ELA conditions using the LBN model, and infused CNO bilaterally in the NAc. When the CRH/GABA

BLA→NAc projection was inhibited, palatable food consumption was restored (Figure 2.3A) as well as sex-cue preference (Figure 2.3B). When we excited the pathway using Cre-dependent AAV2-hM3D(Gq) excitatory DREADD in ELA males, there was no significant effect on reward behavior in either measure and it did not further decrease palatable food consumption or the preference for a sex cue (Figure 2.3C–D). Because excitation of the CRH/GABA BLA→NAc projection suppresses reward in control mice, while inhibition of the projection rescues reward in ELA mice, this suggests a selective ELA-induced maladaptive plasticity of this reward-circuit pathway.

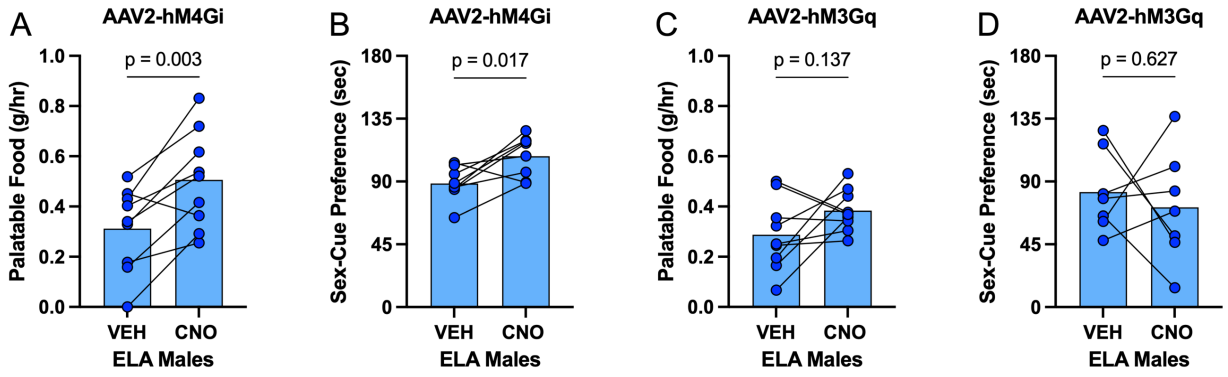

Figure 2.3: Inhibiting the CRH/GABA BLA→NAc projection in male mice raised in early-life adversity conditions rescues reward deficits

(A) Inhibiting the hM4D(Gi) CRH/GABA BLA→NAc projection with microinfusion of CNO in the medial NAc shell increased palatable food consumption (n = 9 mice) and (B) preference for a sex-cue (n = 8 mice). However, stimulating the hM3D(Gq) CRH/GABA BLA→NAc projection did not influence (C) palatable food consumption (n = 9 mice) or (D) the preference for a sex-cue (n = 7 mice). In A–D, bars represent mean. Two-sided paired t-tests (A–D). A, ELA hM4D(Gi) BLA→NAc: p = 0.003; B, ELA hM4D(Gi) BLA→NAc: p = 0.017; C, ELA hM3D(Gq) BLA→NAc: p = 0.137; D, ELA hM3D(Gq) BLA→NAc: p = 0.627. VEH, vehicle. CNO, clozapine-N-oxide. ELA, early-life adversity.

Discussion and Conclusion

We found that exciting the CRH/GABA BLA→NAc projection in CTL male mice recapitulated the reward deficits we saw in male mice that experienced ELA. These outcomes were not the result of off-target effects of CNO (Figure 2.4A), as non-reward

behaviors were unaffected. We also confirmed the activation of hM3D(Gq)-expressing CRH neurons by CNO via quantification of selective Fos expression in the BLA 90 min after CNO microinfusion (Figure 2.4D).

On the other hand, inhibiting the projection in ELA male mice rescued their reward deficits. Again, non-reward behaviors were not influenced by CNO (Figure 2.4B–C). We have thus delineated a population of CRH/GABA neurons in the BLA which project to the NAc to influence reward behavior in male mice. Importantly, the function of this pathway is impacted by ELA, promoting pathological deficits in these reward behaviors in adult male mice that were raised in ELA conditions.

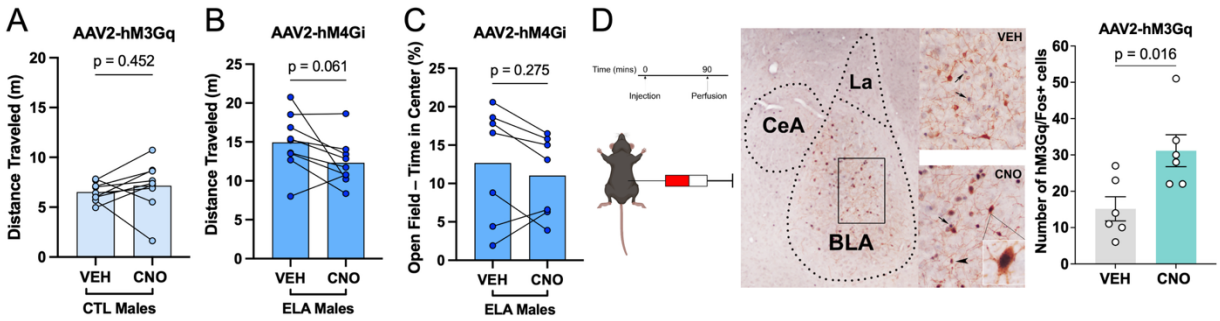

Figure 2.4: CNO activates hM3D(Gq)-expressing neurons and has no off-target effects

(A) Microinjections of CNO in the medial NAc shell of mice to stimulate the hM3D(Gq) expressing CRH BLA-origin projection did not affect distance traveled during the sex-cue task (*n* = 9 mice). (B) Inhibiting the CRH/GABA BLA→NAc projection did not affect distance traveled during the sex-cue task (n = 9 mice) or (C) time spent in the center in an open field task (n = 7 mice). (D) Experimental timeline, example Fos expression in hM3D(Gq) expressing CRH/GABA BLA neurons 90 minutes post injection of vehicle or CNO shows increased hM3D(Gq)/Fos reactivity with CNO treatment compared to vehicle (n = 12 mice; vehicle = 6, CNO = 6). In A–D, bars represent mean. Two-sided paired *t*-tests (A–C), two-sided unpaired *t*-test (D). A, hM3D(Gq) BLA→NAc: p = 0.452; B, hM4D(Gi) BLA→NAc: p = 0.061; C, hM4D(Gi) BLA→NAc: p = 0.275; D, hM3D(Gq) BLA Fos: p = 0.016. VEH, vehicle. CNO, clozapine-N-oxide. CTL, control. ELA, early-life adversity.

Severe or chronic adversity experienced during sensitive developmental windows can produce persistent, detrimental changes to brain circuit operations, increasing vulnerability to mental illness in adulthood (Green et al., 2010; Malter Cohen et al.,

2013). The majority of the world's adults carry a history of some form of early-life adversity, which frequently precedes and likely contributes to the emergence of affective disorders, including depression, substance use disorders, and compulsive risk-taking (Dennison et al., 2019; Koob & Le Moal, 2005; Luby et al., 2020; Lüthi & Lüscher, 2014; Nestler & Carlezon, 2006), all conditions defined in part by disrupted reward processing (Volkow et al., 2010; Whitton et al., 2016). Despite the strength of these clinical associations, the specific cell types, projections, and circuit mechanisms that mediate ELA-induced reward disruption had remained poorly resolved (Luby et al., 2020). The present work identifies an inhibitory BLA→NAc projection as responsible for ELA-provoked deficits in reward behavior. This pathway is molecularly distinguished from the well-characterized glutamatergic BLA→NAc projection that promotes reward-seeking (Ambroggi et al., 2008; Stuber et al., 2011): it co-expresses CRH and GABA and suppresses reward behaviors in typically reared male mice. Whether GABA, CRH, or an interaction between both neuromodulators executes these behavioral effects remains an open question for future investigation.

The present findings also establish the BLA as a source of CRH-expressing projection neurons that target the reward circuitry. This is notable because the vast majority of prior work on amygdalar CRH has centered on the central nucleus, a region densely populated by CRH-expressing cells (De Guglielmo et al., 2019; Jo et al., 2020; McCullough et al., 2020; Roberto et al., 2010) that does not, however, send direct projections to the NAc (Itoga et al., 2019). CRH is a peptide released in multiple brain regions during stress and is an established modulator of circuit function across the stress and memory systems (Baumgartner et al., 2021; Y. Chen et al., 2016; Gunn et

al., 2017; Lemos et al., 2012). Its actions within the NAc are context-dependent: under baseline conditions, locally infused CRH promotes appetitive motivation and sucrose-seeking (Peciña et al., 2006), yet following severe prior stress, the same signaling axis reverses its valence, shifting from reward-promoting to aversion-promoting (Lemos et al., 2012; Lemos & Alvarez, 2020).

These findings provide a circuit-level mechanism through which ELA generates maladaptive changes in reward function and identifies the CRH/GABA BLA→NAc projection as a potential intervention target for stress-related affective disorders characterized by dysregulated reward processing.

Methods and Materials

Experimental animals

Male and female B6(Cg)-Crhtm1(cre)Zjh/J (CRH-ires-Cre) mice were used in experimental procedures. Food and water were available ad libitum. Mice were bred in house from Jackson Laboratories stock (Stock no: 012704). All mice were housed in standard conditions at 72 °F and 42% humidity and on a 12-h light–dark cycle (lights on: 0600; lights off: 1800). All mice were single housed following surgical procedures for experimental purposes. All experimental procedures were approved by the University of California-Irvine Institutional Animal Care and Use Committee (AUP 21-128 and 18-183) and were in accordance with the guidelines from the National Institute of Health.

Limited bedding and nesting paradigm

Early-life adversity was induced on postnatal day (PN) 2 to 9 using our laboratory's standard protocol (Molet, Heins, et al., 2016; Walker et al., 2017). Briefly, routine plastic mouse cages (L37 x W20 x H17 cm) were fitted with an aluminum mesh (cat # 4700313244, McNichols, US) platform sitting ~2.5 cm above the cage floor. Bedding was reduced to cover the cage floor sparsely, and one-half of a single nestlet (5 × 2.5 cm) was provided for nesting material. Typically reared (CTL) dams and pups resided in standard bedding cages but were moved to new cages on P2 to control for handling during the LBN setup. CTL and LBN cages were undisturbed from P2–P9 and housed in a quiet room. On P10, both CTL and ELA (LBN) groups were transferred to fresh, routine cages.

Animal surgery

Mice (PN 60) were anesthetized with either ketamine/xylazine (100/10 mg/kg body weight) or isoflurane (1–1.5%) for stereotaxic surgery. For in vivo chemogenetic excitation during behavior testing, mice were injected with the AAV2-hM3D(Gq)-mCherry virus or the same viral vectors carrying mCherry alone (5 × 1012 vector genomes/mL) bilaterally into the BLA (AP: −1.76, ML: ± 4.19 at 15° oblique, DV: 3.92). For in vivo chemogenetic inhibition during behavior testing, mice were injected with the AAV2-hM4D(Gi)-mCherry bilaterally into the BLA (AP: −1.76, ML: ± 4.19 at 15° oblique, DV: 3.92). For intra-NAc drug infusion, guide cannulae were implanted over the medial NAc shell (AP: 1.18, ML: ± 0.6, DV: 4.2). For in vivo optogenetic excitation during behavior, and in vitro electrophysiology experiments, mice were injected with the AAV1-

EF1a-DIO-hChR2(h134R)-EYFP virus or the same viral vector carrying EYFP alone, bilaterally into the BLA. For projection specific targeting during behavior testing, optic fibers (0.22 NA, 100 µm diameter) were placed dorsal to EYFP-expressing axonal terminals in the medial NAc shell (AP:1.18, ML: ± 0.6, DV:4.4).

Chemogenetic studies

For excitatory (AAV2-hM3D(Gq)-mCherry) and inhibitory (AAV2-hM4D(Gi)-mCherry) DREADD experiments: Intraperitoneal injection of 1 mg/kg clozapine-N-oxide (CNO) (NIMH, # MH-929, Batch #14073-1), CNO was dissolved in 1% dimethyl sulfoxide (DMSO) in phosphate buffer saline (PBS). For microinfusion of CNO (CNO dihydrochloride, cat #HB6149, Batch #E1169-1-2, Hello Bio, UK) into the medial NAc shell, 1 mM CNO (0.2 µl/side) in artificial cerebrospinal fluid (in mM: 124 NaCl, 3 KCl, 26 NaHCO3, 1.4 NaH2PO4, 1 MgSO4, 10 d-Glucose, 2 CaCl2).

Optogenetic studies

For in vivo experiments, <5 mW of blue light (95–159 mW/mm2 at the tip) was generated by 473-nm µLED (Prizmatix, US) and bilaterally delivered through two fiber optic patch cords (0.22 NA, 200 µm diameter, Prizmatix, US). Light delivery was controlled using a pulse generator (PulserPlus, Prizmatix, US) to deliver 5 ms light pulse trains at 10 Hz (Stuber et al., 2011) during behavior testing.

Behavioral assays

All training and testing took place in standard housing mouse cages (34 × 18 cm) (home cage), apart from open field (45 × 45 cm) and swim stress. All behavior was

carried out in low light (<15 lux) and during the animal's active period. Prior to testing start, all mice were placed in the behavior room for at least 1 h to acclimatize to their surroundings.

Sucrose preference task

Single-housed mice were habituated to the presence of two drinking bottles (both containing water) in their home cage for 3 days. Following acclimatization, one of the bottles was replaced with 1% sucrose solution and intake was measured 4 h after IP CNO injection for 3 consecutive days during the early active period. The bottles switched sides daily to prevent side bias. Total consumption of water and sucrose solution was measured at the end of each time session by weighing the bottles. Sucrose preference was defined as the ratio of the consumption of sucrose solution versus the consumption of both water and sucrose solution combined. Testing was performed over 3 consecutive days. For chemogenetic experiments, mice were injected 1 h prior to the start of the 4 h test session.

Sex-cue approach

For studies in male mice, urine was collected from females in the estrus phase of the estrous cycle. For assessing interest and preference of sex cues in female mice, male urine was collected. For both sexes, urine was collected on the day of the test and stored in 0.2 ml PCR tubes and capped until used. 60 µl of urine and 60 µl of a non-reward scent (Almond; Pure Almond extract, Target) were pipetted onto cotton tip applicators and fixed to the home cage of single-housed mice at either end. The mouse

was given free access to both tips for 3 min. For chemogenetic experiments, IP CNO or intra NAc CNO was administered to the mice prior to test start (>1 h and <5 min, respectively). For optogenetic experiments, mice were habituated to cable attachment prior to testing (>15 min). 3-point animal tracking was used to measure preference for scent with Ethovision XT15 (Noldus, US) software.

Palatable food consumption

Single-housed mice were habituated to ~1 g of Cocoa Pebbles cereal (Post, USA) in their home cage for 3 days prior to testing, also conducted in their home cage. Pre-weighed Cocoa Pebbles (~1 g) were placed in their cage, and intake was measured following 1 h (chemogenetic manipulation) or 10 min (optogenetic manipulation). For chemogenetic experiments, IP CNO or intra NAc CNO was administered to the mice prior to start (>1 h and <5 min, respectively). For optogenetic experiments, the mice were habituated to cable attachment prior to test start (>15 min).

Statistical analysis

All experiments and data analyses were conducted blind to experimental groups. The number of replicates (n) is indicated in figures as lines/dots and in figure legends and refers to the total number of experimental subjects independently treated in each experimental condition. Data are presented as mean values, and where applicable, accompanied by SEM. Statistical comparisons were performed using Prism 9 software (GraphPad, USA). Unpaired t-tests, paired t-tests, unpaired U-tests, and two-way ANOVA with repeated measures were used to test for statistical significance when

appropriate. No statistical methods were used to pre-determine sample sizes. Statistical significance was set at $\alpha = 0.05$. P-values are provided in all figures and legends. Experiments were replicated in at least two independent batches, and from at least four different litters that yielded consistent results.

Chapter 3 – Role of the CRH/GABA BLA→NAc projection in female mice

Introduction

Early-life adversity (ELA) arising from poverty, trauma, and chaotic environments affects millions of children worldwide (Merrick et al., 2018). Studies link ELA to adverse cognitive and emotional outcomes (Hailes et al., 2019; McKay et al., 2022; Short & Baram, 2019), including disruptions in reward circuitry function (Birnie et al., 2020; Bolton et al., 2018; Kangas et al., 2022; Pizzagalli et al., 2005) and impaired development of associated brain regions (Brieant et al., 2023; Callaghan & Tottenham, 2016; Gee et al., 2013). Mental health disorders characterized by disruptions in the brain's reward circuits often include anhedonia, a construct denoting decreased pleasure or desire for rewards (Pizzagalli, 2014). In humans, the relationship between ELA and dysregulated reward behaviors differs by sex (Bale & Epperson, 2015; Becker & Chartoff, 2019), with women more susceptible to craving comfort food and developing eating and opioid use disorders (Evans et al., 2017; J. G. Johnson et al., 2002), whereas men are more prone to alcohol use disorders (Colman et al., 2013; Evans et al., 2017). These differences may derive from sex-dependent characteristics of reward circuitry operations (Bale & Epperson, 2015; Becker & Chartoff, 2019) which may be coupled with sex-biased developmental vulnerabilities to ELA (Bale & Epperson, 2015; Bath, 2020; Hodes & Epperson, 2019; Luby et al., 2020; Parel & Peña, 2022). However, establishing a direct causal link between ELA and anhedonia and aberrantly augmented reward motivation in humans while also accounting for sex differences is challenging. Conversely, our rodent model of ELA consistently induces sex-specific disturbances in

reward circuits, including anhedonia in males and augmented motivation for reward cues in females (Birnie et al., 2023; Bolton et al., 2018; Levis et al., 2021, 2022; Machado et al., 2013; Molet, Heins, et al., 2016; Molet, Maras, et al., 2016), providing a framework for addressing the mechanisms underlying these sex differences.

The brain is organized in circuits that execute complex behaviors, including those involved in reward. We hypothesized that circuits expressing stress-sensitive molecules such as the peptide corticotropin-releasing hormone (CRH), which is often involved in stress responses and adaptation (Hupalo et al., 2019; Joëls & Baram, 2009; Roozendaal et al., 2002), might be poised to be influenced by ELA. We initially mapped CRH projections to a key reward center in the brain, the nucleus accumbens (NAc), and identified a CRH-expressing GABAergic projection from the basolateral amygdala (BLA) to NAc shell (Itoga et al., 2019). This was significant because CRH modulates reward-related behaviors in the NAc, and its actions there are context-dependent, influenced by prior or ongoing stress (Lemos et al., 2012; Peciña et al., 2006). We then established that activating the CRH/GABA BLA→NAc projection reduced reward behavior in adult control male mice, and silencing it in “anhedonic” ELA male mice restored reward behaviors to control levels (Birnie et al., 2023). This discovery is significant because it provides a mechanistic link between ELA and mood disorders (Birnie & Baram, 2025; Y. Chen & Baram, 2016; Molet, Heins, et al., 2016).

Here, we investigate this novel, cell type-specific projection's role in modulating motivated reward behaviors in female mice and the fundamental sex- and ELA-dependent differences in the projection's structure and function. Does the CRH/GABA BLA→NAc have the same functional role in female mice as it does in male mice?

Adult female mice raised in early-life adversity conditions have augmented reward behaviors

As adults, male and female mice exposed to ELA (Figure 3.1A) exhibited profound sex-dependent changes in reward behaviors. Male ELA mice consumed less palatable food (Figure 3.1B) and explored the scent of a female in heat in the SoaM task (scent of a mouse, otherwise known as a sex cue preference) less than control male mice (Figure 3.1C). In contrast, adult female mice that were reared in ELA conditions showed augmented reward behaviors compared with control females, evidenced by increased consumption of Cocoa Pebbles (Figure 3.1B) and increased number of approaches toward the scent of urine from a male mouse (Figure 3.1C). Of note, in males there was a significant difference between ELA and controls in both the number of approaches to this sex cue (Figure 3.1C) and the duration of sniffing (Figure 3.1D). In females, in contrast, the ELA and control groups did not differ in the duration of sniffing (Figure 3.1D), a measure of consummatory pleasure. Rather, ELA females approached the male scent more frequently (Figure 3.1C), a measure of motivation for reward. This suggests potential sex-specific reward behavior disruptions induced by ELA in male and female mice.

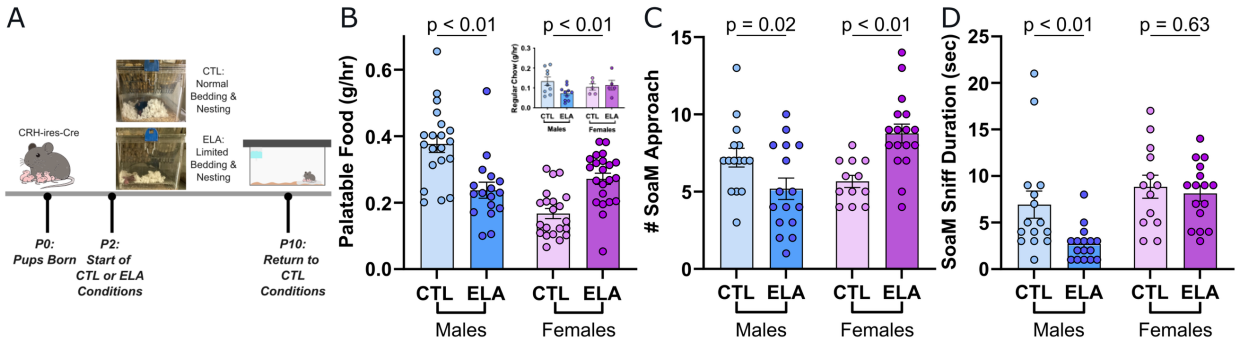

Figure 3.1: Adult female mice raised in early-life adversity conditions have augmented reward behaviors

Sex differences in the impact of ELA on adult reward behaviors. (A) Schematic of the LBN model of ELA. Adult male mice raised in ELA cages exhibited “anhedonia-like” reward behaviors compared with typically reared mice (CTL) in (B) palatable food consumption, (C) number of approaches toward the SoaM of the opposite sex, and (D) duration spent sniffing this sex cue. In contrast, adult ELA female mice had augmented motivated reward behaviors compared with control females, with increased (B) palatable food consumption and (C) number of approaches toward the scent of a male mouse but not increased duration of sniffing (D), a measure of consummatory pleasure. The cycle phase or litter had no influence on data (Figure 3.5). In B–D, dots represent individual mice, error bars represent mean ± SEM. Two-way ANOVA (B, $F_{rearing \times sex}(1,76) = 35.2$; $p < 0.01$; $F_{sex}(1,76) = 18.14$; $p < 0.01$; $F_{rearing}(1,76) = 0.712$; $p = 0.40$; n, CTL male = 20 mice/7 litters; ELA male = 17 mice/7 litters; CTL female = 21 mice/5 litters; ELA female = 22 mice/7 litters; C, $F_{rearing \times sex}(1,56) = 17.1$; $p < 0.001$; $F_{sex}(1,56) = 2.74$; $p = 0.103$; $F_{rearing}(1,56) = 0.773$; $p = 0.383$; n, CTL male = 15 mice/5 litters; ELA male = 16 mice/9 litters; CTL female = 12 mice/5 litters; ELA female = 17 mice/6 litters; D, $F_{rearing \times sex}(1,56) = 2.88$; $p = 0.095$; $F_{sex}(1,56) = 12.5$; $p < 0.001$; $F_{rearing}(1,56) = 5.72$; $p = 0.020$; n, CTL male = 15 mice/5 litters; ELA male = 16 mice/9 litters, CTL female = 13 mice/5 litters; ELA female = 16 mice/6 litters). CTL, control. ELA, early-life adversity. LBN, limited bedding and nesting. SoaM, scent of a mouse.

The CRH-expressing GABAergic BLA→NAc projection mediates reward behaviors in male but not female mice

In a recent paper, we discovered a CRH/GABA BLA→NAc pathway which inhibits reward-seeking behaviors and mediates the effects of ELA on reward behaviors in male mice (Birnie et al., 2023). When the pathway was chemogenetically- or optogenetically stimulated in control male mice, it suppressed reward behaviors. Here, we recapitulated these findings (Figure 3.2A,B). Importantly, we report here the results of systematic manipulation of the projection in female mice, demonstrating profound sex differences. Chemogenetic activation of the CRH/GABA BLA→NAc pathway in control female mice did not affect palatable food consumption in contrast to control males (Figure 3.2C). Similarly, exciting the projection in ELA females had little effect (Figure 3.2C). Chemogenetic inhibition of the CRH/GABA BLA→NAc pathway in female control and ELA mice failed to significantly alter palatable food consumption (Figure 3.2D), in stark contrast to its effect in rescuing reward deficits in ELA males (Birnie et al., 2023).

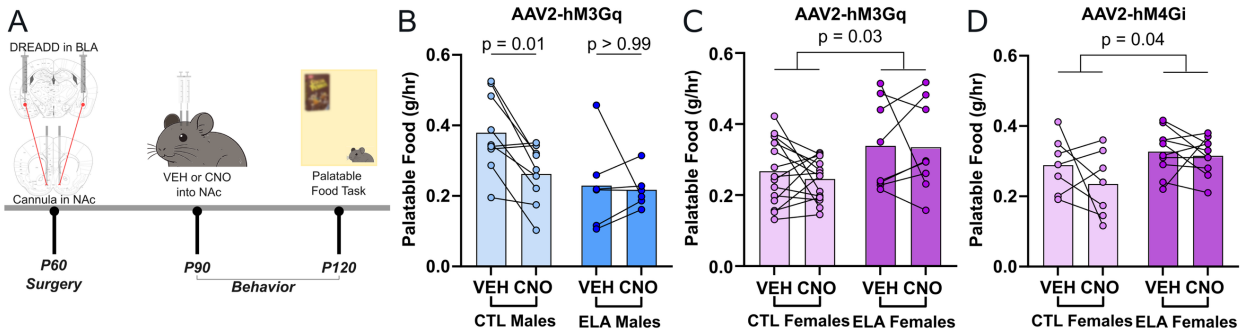

Figure 3.2: The CRH-expressing GABAergic BLA→NAc projection mediates reward behaviors in male but not female mice

Chemogenetic manipulation of the CRH/GABA BLA→NAc projection in vivo influences reward behavior in male but not female control and ELA-exposed adult mice. (A) Viral strategy to chemogenetically target the CRH/GABA BLA→NAc projection neurons. DREADD (Gq) excitation of CRH/GABA BLA-origin axon terminals in the NAc with 1 mM CNO reduced (B) palatable food consumption in control male mice but not in ELA male mice, in which the pathway is overactive (Birnie et al., 2023). (C) Excitation of the projection in control and ELA females had no effect. (D) Chemogenetic (Gi) inhibition of CRH/GABA BLA-origin axon terminals in the NAc with 1 mM CNO did not alter palatable food consumption in control or ELA female mice. In B–D, lines indicate individual mice, bars indicate mean. Two-way RM-ANOVA (B, $F_{rearing \times CNO}(1,13) = 3.372$; $p = 0.09$; $F_{rearing}(1,13) = 5.182$; $p = 0.04$; $F_{CNO}(1,13) = 5.083$; $p = 0.04$; n, CTL male = 9 mice/4 litters; ELA male = 6 mice/3 litters; C, $F_{rearing \times CNO}(1,21) = 0.144$; $p = 0.71$; $F_{rearing}(1,21) = 5.187$; $p = 0.03$; $F_{CNO}(1,21) = 0.298$; $p = 0.59$; n, CTL female = 15 mice/5 litters; ELA female = 8 mice/6 litters; D, $F_{rearing \times CNO}(1,15) = 0.734$; $p = 0.40$; $F_{rearing}(1,15) = 5.275$; $p = 0.04$; $F_{CNO}(1,15) = 1.851$; $p = 0.19$; n, CTL female = 7 mice/3 litters; ELA female = 10 mice/5 litters). VEH, vehicle. CNO, clozapine-N-oxide. CTL, control. ELA, early-life adversity.

Early-life adversity does not influence threat response behavior in females

Given that the CRH/GABA BLA→NAc projection originates in the amygdala, a region associated with fear and threat processing, and expresses CRH, a stress-sensitive neuropeptide, we hypothesized that it may regulate threat response or defensive behaviors in females. The looming disk task, which presents a rapidly expanding overhead visual stimulus that mimics a predator threat (X. Yang et al., 2020) and elicits defensive behaviors such as flight, freezing, and rearing in rodents (De Franceschi et al., 2016; Wallace et al., 2013; Yilmaz & Meister, 2013) allows us to test this hypothesis directly. Previously, our lab had shown that ELA causes an impairment in threat response behavior in male mice (Bolton et al., 2022), and thus first

looked at if there were any differences in this task at baseline in CTL and ELA females. All mice experienced 5 trials of a 15 sec looming shadow stimulus, and behavior was scored as either freezing, escape (to the shelter) or no response (Figure 3.3A). At baseline, we found no significant differences between CTL and ELA females in latency to freeze, latency to escape, percentage of freeze trials, or percentage of escape trials (Figure 3.3B–D).

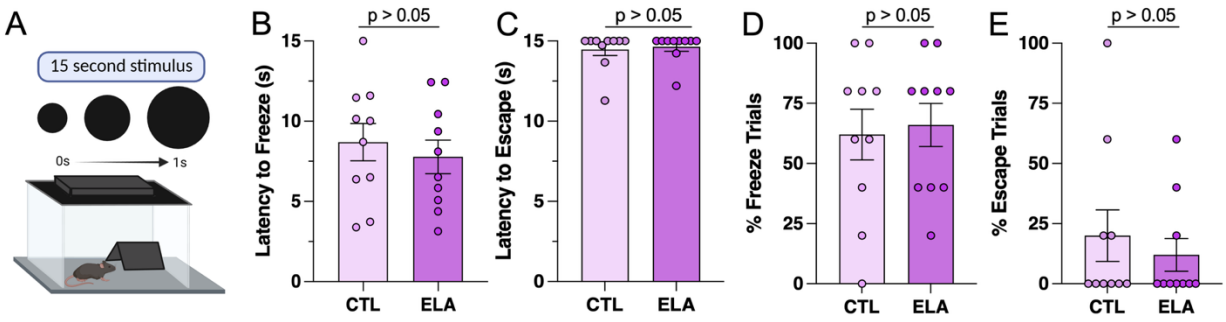

Figure 3.3: Early-life adversity does not influence threat response behavior in females

(A) Schematic of the looming disk task. (B–D) Over the five consecutive trials of a 15 sec looming shadow per mouse, CTL female and ELA female mice did not differ in: latency to freeze, latency to escape to the shelter, percentage of trials out of total trials that resulted in freezing, or escape. In B–D, dots indicate individual mice, error bars represent mean ± SEM. Two-sided unpaired t-tests (B, $p = 0.566$; C, $p = 0.714$; D, $p = 0.776$; E, $p = 0.537$; n = 10 CTL females, 10 ELA females). CTL, control. ELA, early-life adversity.

Chemogenetic excitation of the CRH/GABA BLA→NAc projection does not affect threat response behavior in females

While we did not see an effect of ELA on looming disk threat response behavior in female mice, previous studies have demonstrated the involvement of CRH paraventricular nucleus neurons in this task in male mice (Bolton et al., 2022; Daviu et al., 2020), therefore we speculated that this CRH-specific projection also may have a role in affecting threat response behaviors in this task. When we chemogenetically excited the CRH/GABA BLA→NAc projection immediately before the looming disk task, there was no change in escape or freezing behavior in either CTL or ELA females

(Figure 3.4 A–D). Therefore, this projection does not appear to regulate threat-defense behaviors in females in addition to the reward behaviors already tested.

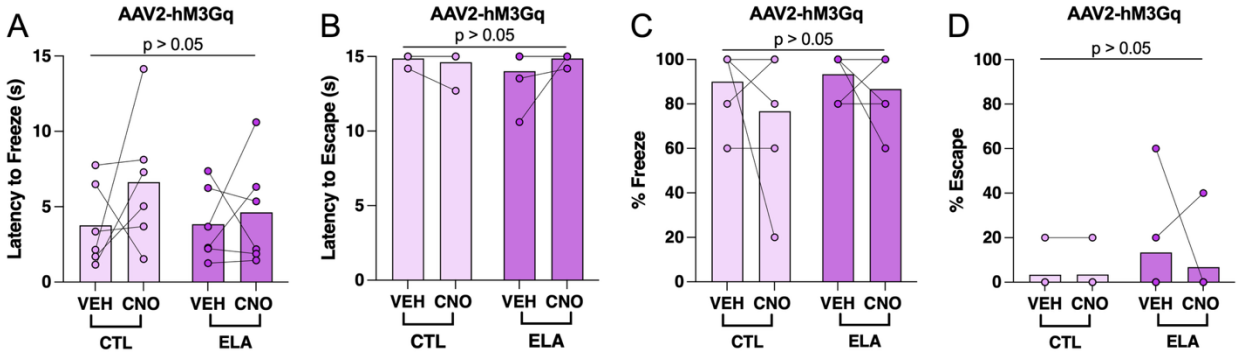

Figure 3.4: Chemogenetic excitation of the CRH/GABA BLA→NAc projection does not affect threat response behavior in females

(A–D) Following chemogenetic excitation of the CRH/GABA BLA→NAc projection preceding the looming disk task, there was no change in freezing or escape behavior in either CTL or ELA female mice. In A–D, lines indicate individual mice, bars represent mean. Two-way RM-ANOVA (A, $F_{rearing \times CNO}(1,10) = 0.508$; $p = 0.492$; $F_{rearing}(1,10) = 0.568$; $p = 0.468$; $F_{CNO}(1,10) = 1.57$; $p = 0.239$; B, $F_{rearing \times CNO}(1,10) = 2.06$; $p = 0.182$; $F_{rearing}(1,10) = 0.424$; $p = 0.530$; $F_{CNO}(1,10) = 0.610$; $p = 0.453$; C, $F_{rearing \times CNO}(1,10) = 0.161$; $p = 0.696$; $F_{rearing}(1,10) = 0.625$; $p = 0.448$; $F_{CNO}(1,10) = 1.45$; $p = 0.256$; D, $F_{rearing \times CNO}(1,10) = 0.357$; $p = 0.563$; $F_{rearing}(1,10) = 0.870$; $p = 0.373$; $F_{CNO}(1,10) = 0.357$; $p = 0.563$; n, CTL female = 10 mice; ELA female = 10 mice). VEH, vehicle. CNO, clozapine-N-oxide. CTL, control. ELA, early-life adversity.

Discussion and Conclusion

Unlike in males, chemogenetic manipulations of the CRH/GABA BLA→NAc projection in females do not influence reward or threat response behaviors. In male mice, we previously discovered that the CRH/GABA BLA→NAc projection mediates the anhedonic-like effects of ELA on reward behaviors (Birnie et al., 2023). Here we recapitulated these results, finding that chemogenetic excitation of the projection in typically reared adult male mice reduced palatable food consumption, while in contrast, a similar manipulation in females did not affect consumption in either control or ELA groups. Furthermore, while inhibiting the projection in ELA males rescued reward deficits (Birnie et al., 2023), this manipulation in control or ELA-adult females failed to influence palatable food consumption. Excitation of the projection in a looming disk task

also failed to identify any function of the projection in threat response behaviors. Importantly, these results were not due to litter or estrus cycle effects (Figure 3.5A–E). These surprising results indicate profound, sex-specific differences in the functional roles of the projection in male and female mice.

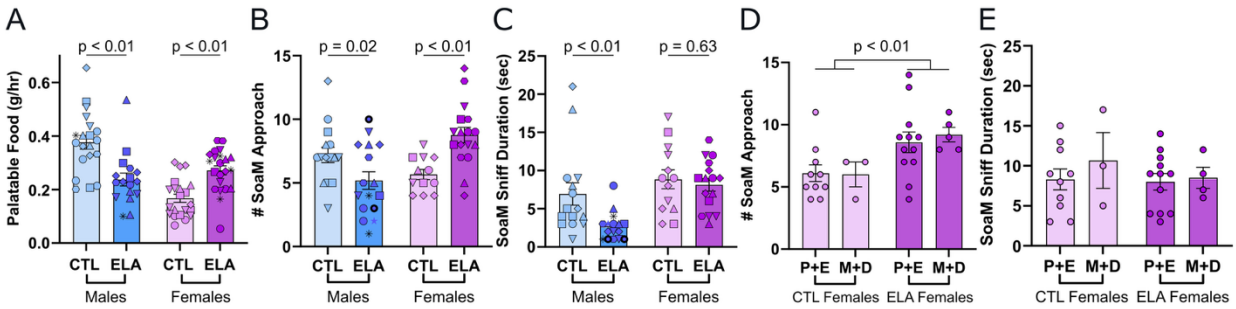

Figure 3.5: Effects of litter and estrus cycle on palatable food and SoaM behavior

(A–C) To look for effects of litter on behavior, different symbols on the bar graphs represent individual mice from different litters for each group, showing that behaviors can vary within the litter, yet the effects of ELA for the palatable food task and SoaM task remain robust. (D–E) Female mice were stratified into a 'receptive' (in proestrus or estrus) or 'non-receptive' (in metestrus or diestrus) phase based on a vaginal swab sample taken immediately after the behavioral test. Estrus cycle stage did not affect their behavior and ELA effects of augmented reward behavior in SoaM approach remained consistent. In A–E, symbols represent individual mice, error bars represent mean ± SEM. Two-way ANOVA (A: $F_{rearing \times sex}(1,76) = 35.2$, $p < 0.01$; $F_{sex}(1,76) = 18.14$, $p < 0.01$; $F_{rearing}(1,76) = 0.712$, $p = 0.40$; *n*, CTL male = 20 mice/7 litters, ELA male = 17 mice/7 litters, CTL female = 21 mice/5 litters, ELA female = 22 mice/7 litters; B: $F_{rearing \times sex}(1,56) = 17.1$, $p < 0.001$; $F_{sex}(1,56) = 2.74$, $p = 0.103$; $F_{rearing}(1,56) = 0.773$, $p = 0.383$; *n*, CTL male = 15 mice/5 litters, ELA male = 16 mice/9 litters, CTL female = 12 mice/5 litters, ELA female = 17 mice/6 litters; C: $F_{rearing \times sex}(1,56) = 2.88$, $p = 0.095$; $F_{sex}(1,56) = 12.5$, $p < 0.001$; $F_{rearing}(1,56) = 5.72$, $p = 0.020$; *n*, CTL male = 15 mice/5 litters, ELA male = 16 mice/9 litters, CTL female = 13 mice/5 litters, ELA female = 16 mice/6 litters; D: $F_{rearing \times cycle}(1,26) = 0.129$, $p = 0.72$; $F_{rearing}(1,26) = 8.10$, $p < 0.01$; $F_{cycle}(1,26) = 0.067$, $p = 0.80$; *n*, CTL female = 13 mice/5 litters, ELA female = 17 mice/6 litters; E: $F_{rearing \times cycle}(1,25) = 0.292$, $p = 0.59$; $F_{rearing}(1,25) = 0.509$, $p = 0.48$; $F_{cycle}(1,25) = 0.688$, $p = 0.41$; *n*, CTL female = 13 mice/5 litters, ELA female = 16 mice/6 litters). CTL, control. ELA, early-life adversity. LBN, limited bedding and nesting. P = proestrus. E = estrus. M = metestrus. D = diestrus.

In conclusion, we discovered that the CRH/GABA BLA→NAc projection does not function the same way in females as in males. The mechanisms underlying this apparent functional silence in female mice remain unclear. Several possible explanations are considered in the following chapters.

Methods and Materials

Mice

B6(Cg)-Crhtm1(cre)Zjh/J (CRH-ires-Cre, Jackson 012704; Taniguchi et al., 2011; Chen et al., 2015) mice were bred in-house and weaned and group-housed by sex on a 12 h light/dark cycle (lights on 0700). Post surgery, single-housed males and group-housed females were moved to a reverse light/dark cycle (lights on 2400). Mice used in each figure were separate cohorts, and all were a CRH-ires-Cre strain (Y. Chen et al., 2015). Procedures were approved by University of California–Irvine's IACUC (AUP 24-104, 21-128) and adhered to NIH guidelines.

The limited bedding and nesting ELA model

To study ELA, we used a model of resource scarcity developed by our group and adopted worldwide, the limited bedding and nesting (LBN) protocol (Ivy et al., 2008; Molet, Heins, et al., 2016; Rice et al., 2008). Multiparous dams and pups (minimum 4–maximum 8; sex balanced) were randomly assigned to cages with either customary or LBN materials. LBN cages had a plastic-coated mesh platform (McNichols 4700313244) ~2.5 cm above the floor and reduced bedding (150 ml) and nesting material (0.5 vs. 1 nestlet). Cages were undisturbed during postnatal day (P)2–P9 in a ventilated, quiet area. All mice returned to typical cages on P10 and weaned on P21.

Surgical procedures

The 2–3-month-old CRH-ires-Cre mice were anesthetized with 5% isoflurane and maintained at 1–1.5% on a stereotaxic apparatus with a heating pad. The crown fur was

shaved, the skin was sanitized (betadine and 70% ethanol), and the skull was exposed. Injection sites were drilled, and viral vectors were delivered via pulled pipettes (Drummond 2-000-010) at 100 nl/min, leaving the pipette in place for 5 min to minimize backflow. Post surgery, mice received buprenorphine (Patterson Vet 07-894-9214) and were monitored for 2 d. To allow viral expression in axonal processes (Itoga et al., 2019), we waited 6 weeks prior to chemogenetics and 8 weeks prior to electrophysiology, optogenetics, and brain clearing. For the latter, AAV1-EF1a-DIO-hChR2(H134R)-EYFP (Addgene 20298-AAV1) was injected into the medial BLA bilaterally (0.2 µl/side; A/P −1.4 mm, M/L ± 4.25 mm, D/V −4.60 mm, 15° angle). For chemogenetic experiments, AAV2-hM3D(Gq)-mCherry (excitatory, Addgene 44361-AAV2) or AAV2-hM4D(Gi)-mCherry (inhibitory, Addgene 44362-AAV2) was bilaterally injected into the medial BLA (0.2 µl/side). Guide cannulas were implanted bilaterally into the medial NAc shell (A/P + 1.2 mm, M/L ± 1.5 mm, D/V −3.5 mm, 12° angle). A dental cement headcap (Patterson Dental Orthojet Liquid 74594412; Powder 74598371) secured the cannulas with skull screws (Antrin AMS1201BINDSS).

Behavioral and chemogenetic experiments

Behavior tests were performed at ages 3–5 months. Experiments assessing the impact of rearing alone involved naive mice. Chemogenetic experiments were performed on mice that underwent surgery for virus-mediated DREADDs and cannulas as described above. Experiments were initiated within the first 2 h of the active, dark phase (R. J. Nelson et al., 2021; Robins et al., 2020) in a dimly lit room. All experiments were conducted in standard mouse cages (34 × 18 cm), either the home cage (males) or

individual cages following habituation (females). For chemogenetic experiments, 0.2 µl clozapine-N-oxide (CNO; 1 mM, Hello Bio HB6149; (Mahler et al., 2014, 2019)) dissolved in saline (VetOne V1510223) was bilaterally infused into the medial NAc shell via an indwelling cannula.

Palatable food task

This test determines palatable food consumption (Cocoa Pebbles, Post^{R}) over 1 h in non-food-restricted mice, providing a measure of reward (Birnie et al., 2023). Mice were habituated to Cocoa Pebbles for 3 d to minimize novelty effects (Greiner & Petrovich, 2020) as follows: On Day 0, ~1 g of Cocoa Pebbles was placed in the home cage overnight; consumption was visually confirmed but not measured. On Days 1–3, mice were placed in individual cages in the testing room for 1 h and provided with 1 g of Cocoa Pebbles. Consumption was measured after 1 h. For baseline behavioral measurements, Day 4 (Test Day) followed the same procedure as Days 1–3. For chemogenetic manipulations, male mice, on Day 4 (Test Day 1), received counterbalanced infusions of CNO or saline into the NAc, then were placed in individual cages in the behavior room with 1 g Cocoa Pebbles, and consumption was measured after 1 h. Following 2 d of rest and 3 additional days of habituation, the same procedure was repeated on Day 11 (Test Day 2) with the opposite treatment. For females, Day 4 (Test Day 1) followed the same infusion and testing procedure as males, but Test Day 2 occurred after a 1 d rest (Day 6), without additional habituation, to minimize observed increases in average consumption with repeated exposure. Intertest intervals (1 d for

females, 1 week for males) allowed sufficient washout of CNO or vehicle (Smith et al., 2016) and counterbalancing controlled for infusion order effects.

Scent of a mouse (SoaM) task (also known as the sex cue or urine sniff test)

This task measures the active approach and duration of interest of mice toward a cotton tip applicator scented with urine of a member of the opposite sex (SoaM) versus one scented with almond (neutral scent). Female subjects were exposed to cotton tip applicators scented with male urine (Roberts et al., 2010); male subjects were exposed to cotton tip applicators scented with estrous female urine (Birnie et al., 2023). Urine was collected on the test day or stored, capped, at 4°C for <3 d. Frequency of approaches toward the urine- or almond-scented cotton tip applicator and the durations of sniffing were recorded. On Day 1, mice received CNO or saline (counterbalanced) into the NAc and then moved to cages with cotton tip applicators (60 µl each of urine and almond scents) placed at opposite corners. Exploration of the SoaM (number of approaches to each cotton tip applicator and total duration spent sniffing each cotton tip applicator) was assessed manually over 3 min. After one rest day, the procedure was repeated with counterbalanced infusions (CNO or saline). While typically performed in receptive (estrous or proestrus) females (Cheetham et al., 2007; Miller et al., 2025; Ramm et al., 2008; Roberts et al., 2010), we conducted this test throughout the estrous cycle, based on our prior experience (Figure 3.5).

Looming disk task

The task was performed in the dark, active phase as described (Daviu et al., 2020). Adult mice were habituated to an arena containing a shelter for 15 min. Following habituation, a stimulus was presented to the mouse from above, consisting of an expanding disk (growing from small to expanded in 1 sec and repeating for a total of 15 sec), which was repeated 5 times with at least 1 minute between each trial. The mouse's response to the looming stimulus was scored as no response, freezing, or escape (to the shelter), both live and on recording by an experimenter watching through a webcam. The latency to respond with either freezing or escape during the 15 sec stimulus was measured (the latency was recorded as 15 sec if no response was observed during the stimulus).

Sex considerations

To consider the possible effects of the estrous cycle and associated hormonal fluctuations on the function of the projection and female reward behaviors (McCarthy et al., 2012; Shansky & Woolley, 2016), females were swabbed on the test day for a vaginal smear (<5 s).

Quantitative approaches and statistical analyses

All statistical comparisons and analyses were performed in GraphPad Prism V10 or MATLAB 2022a. The specific experimental design and statistical analyses can be found in the figure legends.

Chapter 4 – Investigation of the absence of detectable effects of the CRH/GABA BLA→NAc projection on behavior in female mice

Introduction

Thus far we have discovered a novel projection from the BLA to the NAc that expresses CRH, is GABAergic, and inhibits reward-seeking behaviors in male mice. We also targeted and manipulated this projection in females by utilizing viral genetic techniques; however, we did not find a functional role. Given that CRH may be present in either GABAergic or glutamatergic neurons (Y. Chen et al., 2015; Gunn et al., 2017, 2019), it is essential to ascertain the molecular characteristics of this projection in females. There is the possibility that the molecular identity of this projection may be different between males and females to explain these functional differences, such as the CRH BLA cells expressing glutamate markers in females. There is also the possibility of heterogeneous CRH populations in the BLA projecting to the NAc, where some express GABA markers and some express glutamate markers. These are possible hypotheses to explore to explain our failure to detect any effects of the projection in female mice.

Here, we will verify that the CRH BLA→NAc projection cells are long-range GABAergic neurons in female mice like the male mice using viral genetic tracing techniques and subsequently investigate whether they establish GABAergic synapses on their target cells using optogenetic-paired electrophysiology and neuro-anatomical markers. We will also use whole brain tissue clearing techniques to compare the quantity and location of the CRH BLA→NAc projection innervations brain wide between females and males and to also look at differences between control and ELA mice.

In both males and females, NAc-projecting CRH BLA neurons are GABAergic, evident by both electrophysiological and neurochemical markers

In male mice, CRH/GABA BLA→NAc neurons inhibited reward behaviors, whereas in females, activating the projection had no detectable effects on reward behaviors. Therefore, we tested if the projections might differ across sexes in terms of cell identity or electrophysiological properties. Specifically, we tested whether, in females, the projection also made GABAergic synapses onto target NAc cells, as found in males. We injected CRH-ires-Cre mice with DIO-ChR2 in the BLA and obtained whole-cell patch-clamp recordings from target neurons in the NAc medial shell. IPSCs were optically evoked (oIPSCs) with a 2 ms light pulse in the NAc (Figure 4.1). Representative oIPSCs traces are shown in Figure 4.1, A and E. After 5 min, the $GABA_A$ receptor antagonist picrotoxin was washed on, blocking oIPSCs in both males and female slices across all groups as apparent in the time-course data of normalized oIPSCs amplitudes (Figure 4.1B,F) and timepoint analysis (Figure 4.1C,G). Raw oIPSCs amplitudes pre- and post-picrotoxin are shown in Figure 4.1, D and H. These data indicate that in both sexes, optically evoked currents from CRH BLA-origin axons in NAc are inhibitory and are mediated by $GABA_A$ receptors. In further support of the GABAergic nature of the CRH BLA projection, all CRH cells in the BLA expressed the GABAergic markers GAD 65/67 (Figure 4.1I–K), including those projecting to the NAc (Figure 4.1L,M).

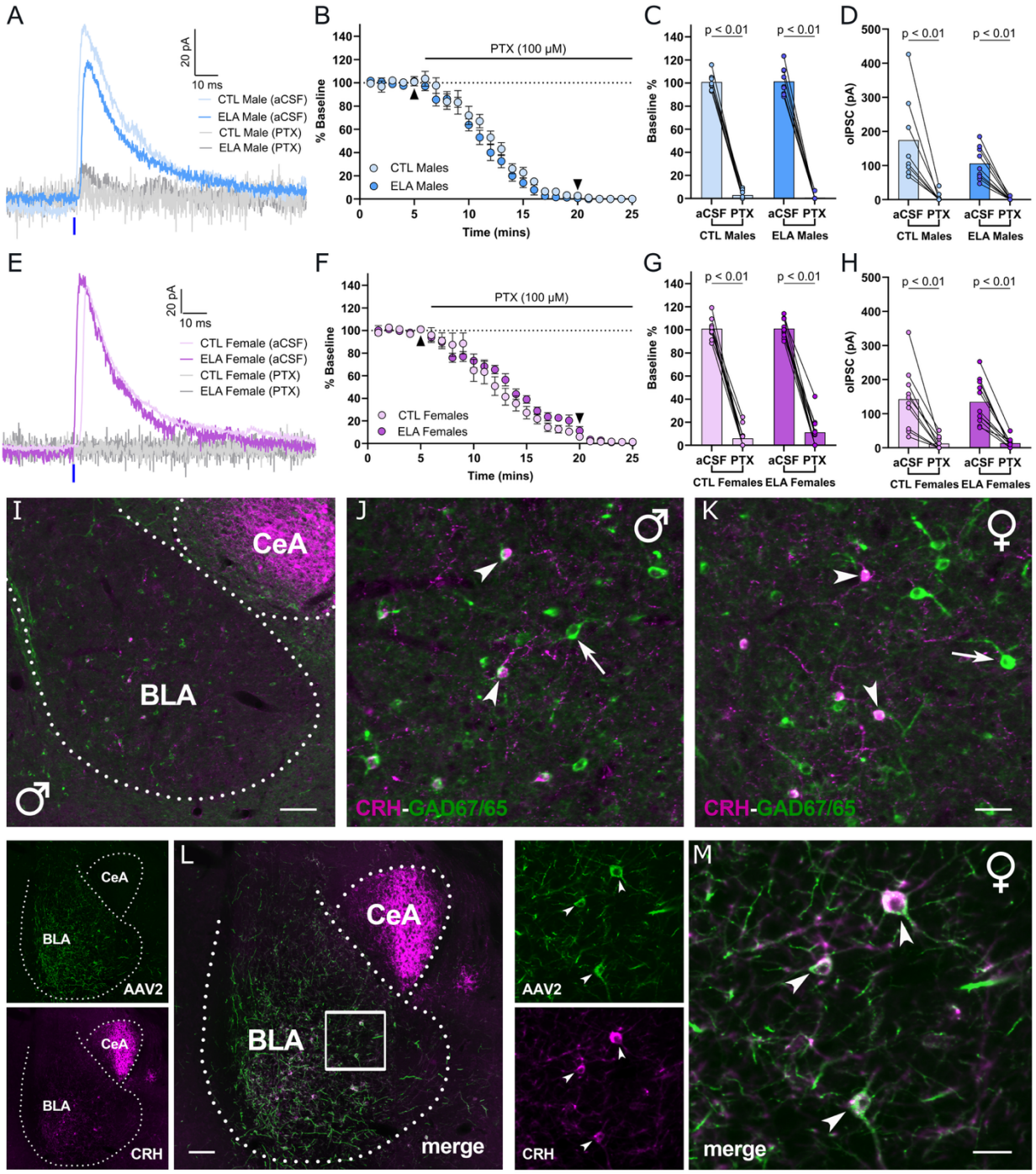

Figure 4.1: NAc-projecting CRH BLA neurons are GABAergic in both males and females, evident by both electrophysiological and neurochemical markers

NAc-projecting CRH BLA neurons are GABAergic in both males and females, evident by both electrophysiological and neurochemical markers. Whole-cell patch-clamp recordings were obtained from NAc medial shell neurons, while IPSCs were optically evoked from CRH BLA neurons with a 2 ms light pulse at 488 nm in the NAc. Representative traces of oIPSCs in males (A) and females (E). Time-course plot of normalized oIPSCs amplitudes before and after

application of picrotoxin in (B) males and (F) females. Timepoint analysis of normalized oIPSC amplitudes at 5 min after start of recording compared with 15 min after picrotoxin application for (C) males and (G) females. D,H, oIPSCs amplitudes pre- and post-picrotoxin. In B and F, dots and error bars indicate mean ± SEM. In C–D and G–H, dots represent individual cells, error bars indicate mean. Two-way RM-ANOVA (C, $F_{rearing \times PTX}(1,15) = 0.266$; $p = 0.614$; $F_{rearing}(1,15) = 0.107$; $p = 0.748$; $F_{PTX}(1,15) = 1408$; $p < 0.001$; D, $F_{rearing \times PTX}(1,15) = 2.25$; $p = 0.154$; $F_{rearing}(1,15) = 2.31$; $p = 0.149$; $F_{PTX}(1,15) = 43.1$; $p < 0.001$; B–D, n, CTL male = 8 cells/4 mice/2 litters; ELA male = 9 cells/4 mice/2 litters; G, $F_{rearing \times PTX}(1,19) = 0.721$; $p = 0.406$; $F_{rearing}(1,19) = 0.758$; $p = 0.395$; $F_{PTX}(1,19) = 939$; $p < 0.001$; H, $F_{rearing \times PTX}(1,19) = 0.0844$; $p = 0.775$; $F_{rearing}(1,19) = 0.0328$; $p = 0.858$; $F_{PTX}(1,19) = 65.0$; $p < 0.001$; F–H, n, CTL female = 10 cells/4 mice/2 litters; ELA female = 11 cells/4 mice/2 litters). I–K, Concurrent immunolabeling of CRH and both isoforms of GAD (65 and 67) in the BLA of a CTL male (J) and CTL female (K). High-magnification photomicrographs indicate that all CRH cells (magenta) also express GAD (arrowheads), whereas numerous GABAergic cells are devoid of CRH expression (arrows). In I, scale bars, 100 µm. In J–K, scale bars, 35 µm; arrows, GAD 65/67 only (green); arrowheads, colocalization of CRH and GAD 65/67. L–M, AAV2-infected cells in the BLA co-express endogenous CRH. Representative images (L) indicating that AAV2 injection is limited to the BLA. Cells in the CeA are not virus infected. Boxed area in the BLA was magnified in the right panel (M) to show the colocalization between AAV2 and CRH expressions. In L, scale bars, 100 µm. In M, scale bars, 25 µm; arrowheads, AAV2-infected cells in the BLA co-expressing CRH. aCSF, artificial cerebrospinal fluid. PTX, picrotoxin. CTL, control. ELA, early-life adversity.

Sex- and rearing-dependent axonal innervation patterns of BLA-origin CRH/GABA cells within the NAc

The results above indicate that there are sex-dependent differences in the function of the CRH/GABA BLA→NAc projection that are not explained by neurotransmitter identity or by the electrophysiology of the originating cells. To investigate if structural differences in this pathway underlie the distinct sex-specific behaviors, we utilized a whole-brain imaging approach to determine if sex or rearing alters the innervation of CRH/GABA BLA axonal projections within the NAc. Using a viral approach, we fluorescently labeled CRH/GABA BLA axons in adult male and female CRH-Cre mice that experienced typical (control) or ELA rearing (Figure 4.2A). We then cleared the brains, imaged them using LSFM, and quantified the brain-wide axonal projections of CRH/GABA BLA neurons (Figure 4.2B).

Given the surprising differences in the functional role of the CRH/GABA BLA→NAc pathway in reward behavior, we first focused our analysis on the NAc, a well-established reward circuit hub. In this region, both sex and rearing influenced the density of CRH/GABA BLA axonal innervation (Figure 4.2C–E). Overall, ELA reduced labeling of axons in the NAc of male mice, with no effect on females (Figure 4.2C,D). Notably, when comparing innervation of the NAc along the anterior–posterior axis, we found that this reduction in ELA males was most notable in the anterior NAc, with negligible changes in the posterior NAc (Figure 4.2E). These changes were not a result of differences in the numbers of CRH/GABA neurons in the BLA of the four groups studied (Figure 4.3) and are in line with the sex-dependent functional role of the CRH/GABA BLA→NAc pathway in motivated behavior.

The significant reduction in density of CRH/GABA axon terminals emanating from the BLA in ELA males, in whom the projection exerts a strong anhedonic effect, was surprising. Therefore, we tested the possibility that inputs of the projection target both medium spiny neurons (MSNs) and inhibitory interneurons. A selective loss in ELA males of innervation by the CRH/GABA projection of interneurons could augment their effect on NAc function. Indeed, concurrent labeling for the projection (channelrhodopsin) and dopamine receptor 1 (D1) or parvalbumin (PV) suggests that both MSNs and PV-expressing interneurons are targeted by the CRH/GABA BLA→NAc projection (Figure 4.2F–I).

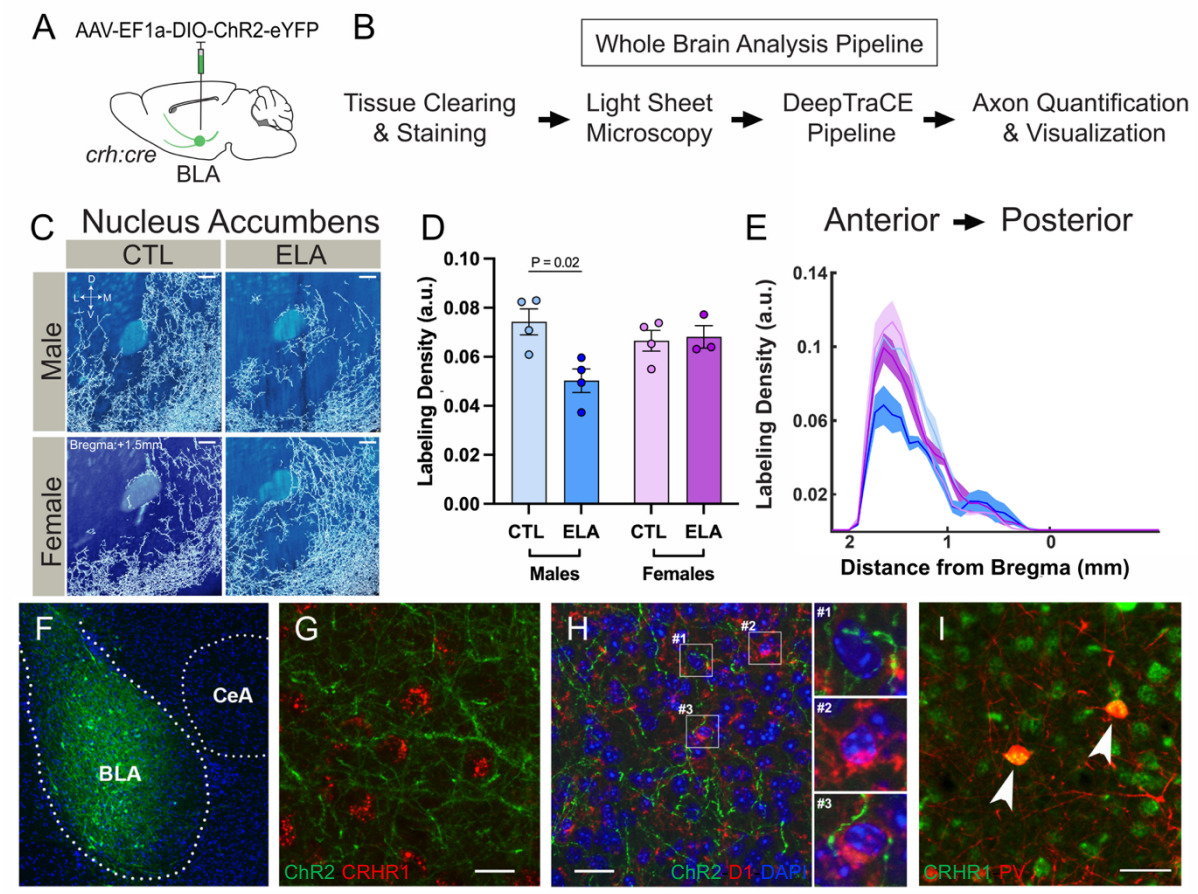

Figure 4.2: Axonal innervation patterns of the BLA-origin CRH/GABA projection in the NAc

(A) Viral strategy for labeling axonal projections of CRH/GABA BLA neurons and (B) whole-brain analysis pipeline. (C) Coronal view of 80 μm z-projections of skeletonized axons determined by DeepTraCE (axons, white) from example brains. In C, scale bars, 200 μm. (D) Differences in sex and rearing-specific innervation patterns in the NAc and quantification of differences in axonal innervation patterns among all groups. Results were not due to differences in the numbers of CRH/GABA neurons in the BLA (Figure 4.3) and considered the possibility that regions with low axonal density might be more likely to show more significant effects (Figure 4.4). In D, error bars indicate mean ± SEM. (E) Quantification of axonal innervation density along the anterior–posterior axis of the NAc. Two-way ANOVA (D, $F_{rearing}(1,11) = 5.365$; $p = 0.04$; $F_{sex}(1,11) = 1.088$; $p = 0.32$; $F_{rearing \times sex}(1,11) = 6.942$; $p = 0.02$; n, CTL male = 4 mice/2 litters; ELA male = 4 mice/1 litter; CTL female = 4 mice/1 litter; ELA female = 3 mice/1 litter). CTL, control. ELA, early-life adversity. (F–K) The BLA-origin CRH/GABA projection targets both medium spiny neurons (MSNs) and interneurons in the NAc. (F) A low-magnification micrograph showing GFP, indicating channelrhodopsin expression at the site of injection, the BLA, but not the central amygdala nucleus (CeA). (G) Channelrhodopsin-expressing fibers in the NAc (green) and CRH receptor type 1-expressing neurons (red, CRHR1). (H) High-resolution confocal image showing the BLA-origin projection terminals (green) abutting dopamine receptor type 1 (D1) expressing, presumed MSNs (red) in the NAc. The frames in the main panel delineate the more detailed images on the right. Section counterstained with DAPI (blue). (I) Dual immunohistochemistry of CRHR1 (green) and parvalbumin (red, PV) in the NAc suggests

targeting of PV-expressing NAc interneurons by the projection. Scale bars, 20 μm in G and H and 40 μm in I.

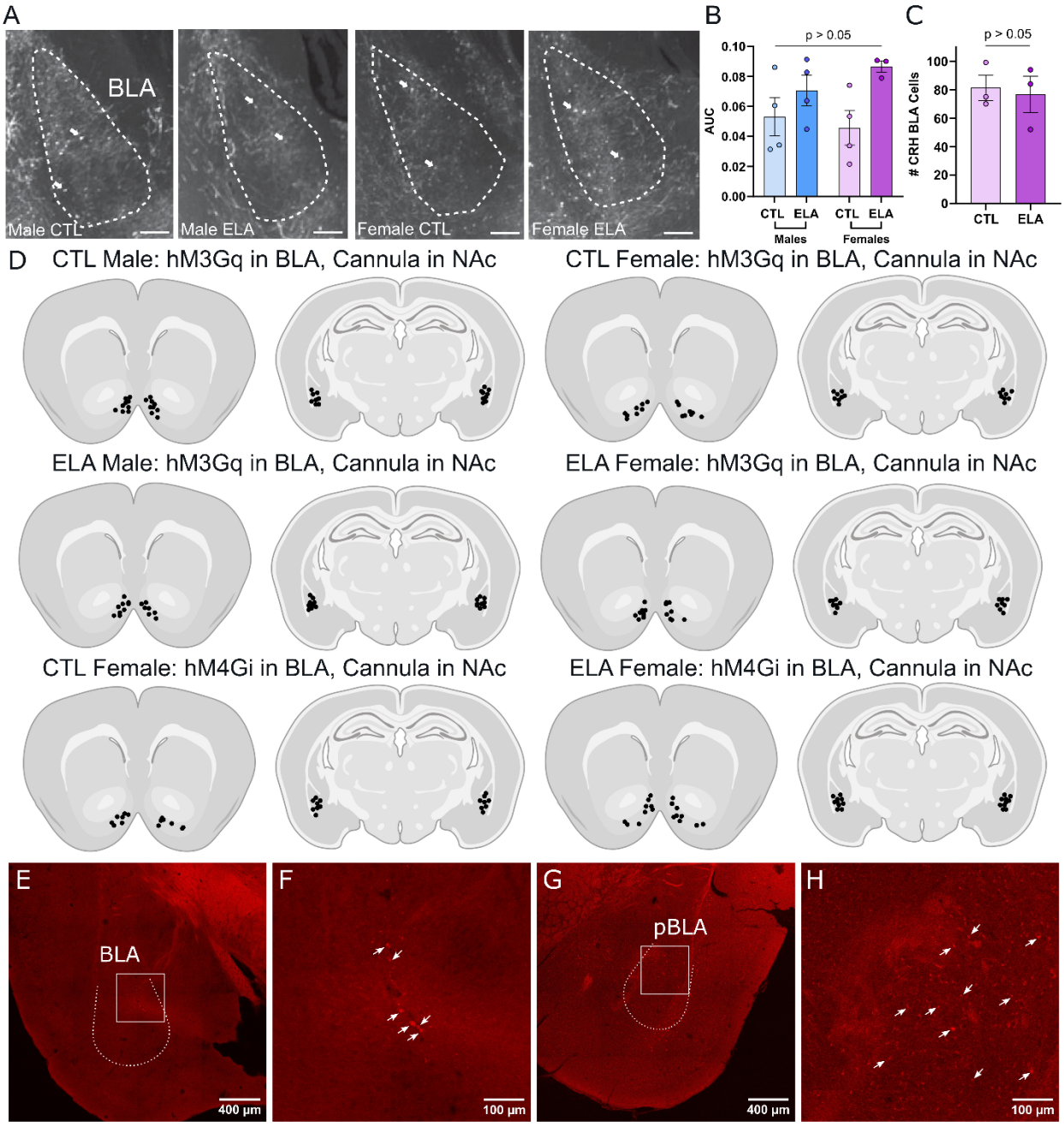

Figure 4.3: Viral labeling of CRH/GABA neurons in the BLA and viral injection and cannula fiber locations in the BLA and NAc

(A) Example 80 μm z-projections from raw images of posterior BLA in representative brains from each group. (B) Quantification of labeling as area under the curve (AUC). White arrows point to example labeling of CRH cell bodies. Two-way ANOVA (B: $F_{rearing \times sex}(1,11) = 1.116$, p =

0.31; $F_{sex}(1,11) = 0.1473$, $p = 0.71$; $F_{rearing}(1,11) = 7.033$, $p = 0.02$; n, CTL male = 4 mice/2 litters, ELA male = 4 mice/1 litter; CTL female = 4 mice/1 litter, ELA female = 3 mice/1 litter). (C) Quantification of endogenous CRH/GABA cells in the BLA of CTL females and ELA females in 25 µm coronal sections, sampling from 4 sections per mouse. Unpaired t-test (C: n, CTL female = 3 mice/3 litters, ELA female = 3 mice/2 litters). (D) Schematic representations of bilateral viral injection sites and cannula locations of experiments in Chapter 3. (E–H) Example images of hM3D(Gq) viral spread in 40 µm coronal sections of the BLA in two different mice, one with low spread in the BLA (E) and one with higher spread in the posterior BLA (G). Dotted lines outline the BLA, squares indicate area magnified in F and H, white arrows point to example CRH cells expressing hM3D(Gq) tagged with mCherry. Scale bars = 400 µm in E,G; scale bars = 100 µm in F,H. CTL, control. ELA, early-life adversity.

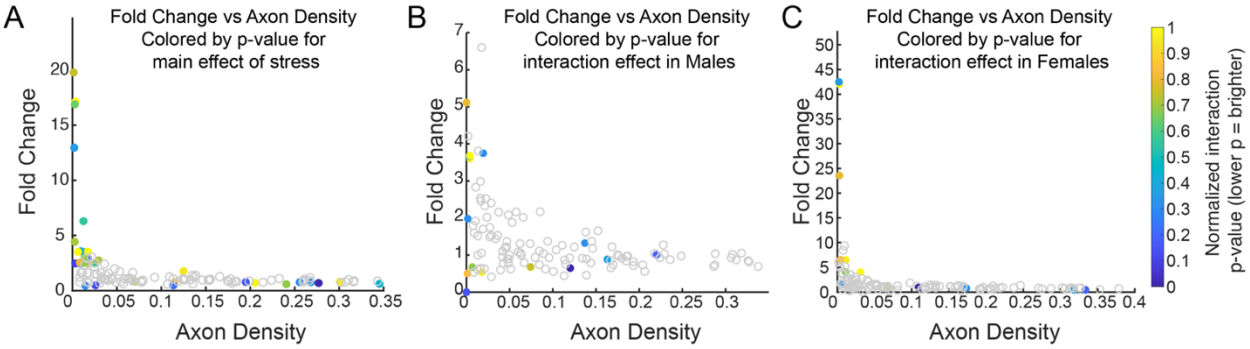

Figure 4.4: Fold change vs. axon density for the main effect of early-life adversity (ELA, stress)

Each point represents a brain region, with the x-axis showing axon density and the y-axis showing fold change. (A) Fold change of pooled ELA male and female axon density compared to pooled CTL mice. Points are colored according to the normalized resampled p-value for the main effect of stress, with lower p-values represented by brighter colors. (B) Fold change in axon density comparing ELA males to CTL males and (C) ELA and CTL females. Points are colored according to the normalized resampled p-value for the interaction effect, with lower p-values represented by brighter colors. CTL, control. ELA, early-life adversity.

Sex and ELA influence brain-wide projection patterns of CRH/GABA BLA cells

Our results above, showing a rearing effect in males but not in females, on axonal innervation of CRH/GABA BLA neurons within the NAc correlate with, and potentially contribute to, the reduction in reward behaviors in males who experience ELA compared with typically reared males. As no differences in axon labeling was observed in the NAc of female mice reared in ELA compared with controls, we speculated whether ELA might induce anatomical changes in CRH/GABA BLA neuronal innervation in other downstream (target) regions. To investigate this, we expanded our

analysis to compare brain-wide projection patterns of CRH/GABA neurons in the BLA in typically reared and ELA mice of both sexes.

The axonal projection patterns of the CRH/GABA BLA neurons were consistent with previous reports of BLA connectivity (Figure 4.5A,B). For example, we found that these neurons project to the temporal association area, the hippocampal formation, including the entorhinal cortex, CA1, and CA3 (Hintiryan et al., 2021; Wahlstrom et al., 2018; Y. Yang & Wang, 2017), the nucleus of the solitary tract, the piriform cortex, and the zona incerta (ZI; (Arena et al., 2024; East et al., 2021)). Unlike the overall BLA cell population, CRH/GABA cells also robustly innervated hypothalamic areas, including the paraventricular nucleus, anterior hypothalamic nucleus, ventral mammillary nucleus, and the medial preoptic area.

We next performed quantitative comparisons of axonal innervation density in each individual brain region and identified several regions in which CRH/GABA BLA axonal density was selectively altered in females that experienced ELA. Salient examples include the ZI, superior colliculus, auditory cortex, and retrosplenial cortex. All these regions are involved in various forms of sensory processing and memory formation (Cheng et al., 2024; Letzkus et al., 2011; X. Wang et al., 2020; Z. Wang et al., 2020; Ye et al., 2023). Within the ZI and superior colliculus, ELA females displayed greater axonal innervation than control females and both male groups (Figure 4.5C,D). In the auditory cortex, males who experienced ELA displayed greater labeling compared with control males and both female groups (Figure 4.5E). Lastly, within the retrosplenial cortex, both the effect of ELA and increased axon density are apparent in both males

and females. However, only in males are these increases significant, compared with controls and both female groups (Figure 4.5F).

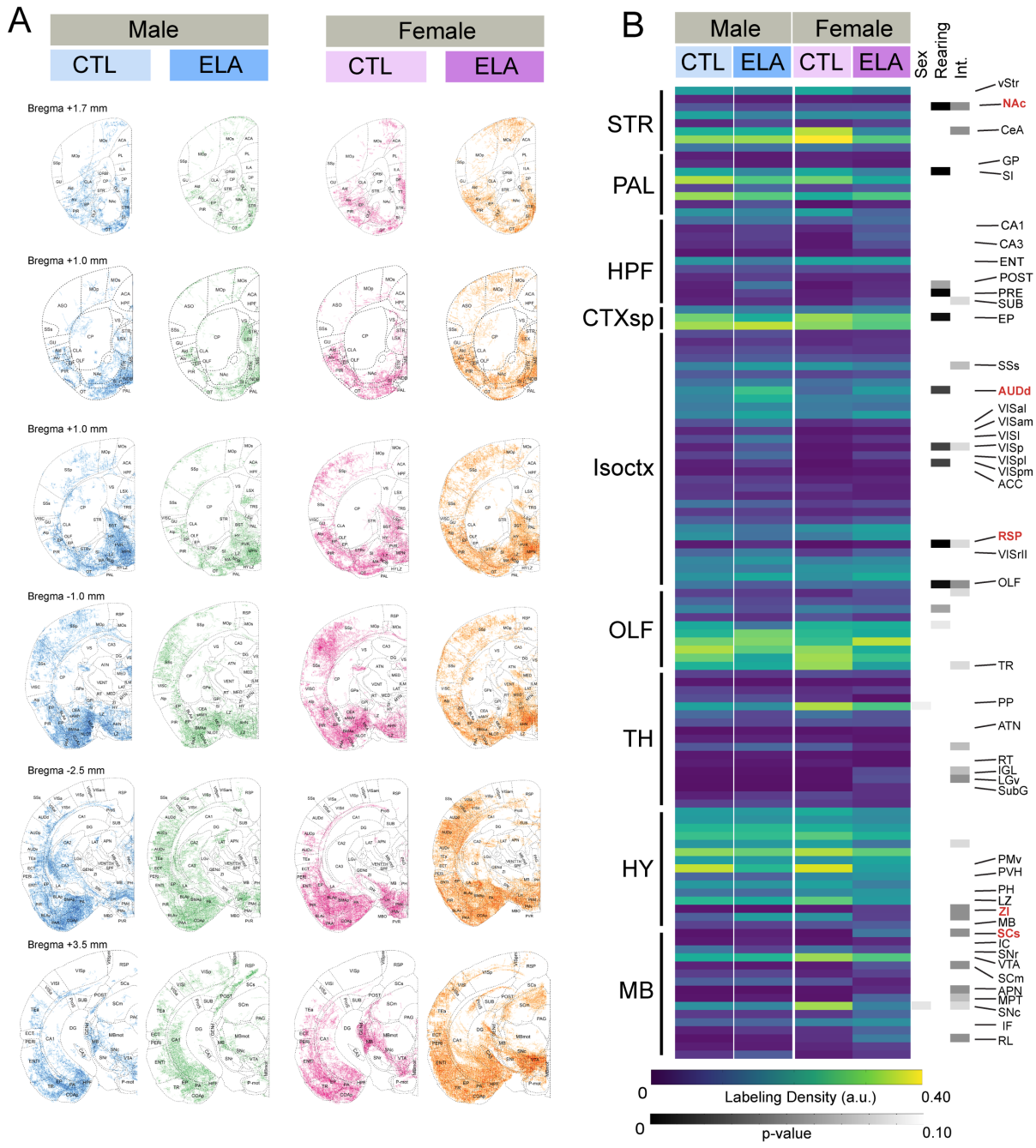

Figure 4.5: Visualization and quantification of brain-wide projection patterns of CRH/GABA BLA cells

(A) The 80 µm coronal optical sections showing CRH/GABA BLA axons registered to the standardized brain atlas. Each image represents one example brain from each group.

Innervation of CRH/GABA BLA cells in CTL males, ELA males, CTL females, and ELA females are shown in blue, green, pink, and orange, respectively. (B) Heatmap on the left shows the relative labeling density averaged across conditions (normalized to region volume and total labeling) of 120 regions defined by the Allen Brain Atlas. Right heatmap, p values from aligned rank transform of axon innervation density comparing the effect of sex, rearing, and their interaction for each individual brain region. (C–F) Sex and rearing effect on labeling density of axons in specific regions, (C) zona incerta, (D) superior colliculus, (E) auditory cortex, (F) retrosplenial cortex. Two-way ANOVA (C, $F_{rearing}(1,11) = 4.866$; $p = 0.05$; $F_{sex}(1,11) = 9.672$; $p < 0.01$; $F_{rearing \times sex}(1,11) = 6.324$; $p = 0.03$; D, $F_{rearing}(1,11) = 12.90$; $p < 0.01$; $F_{sex}(1,11) = 9.853$; $p < 0.01$; $F_{rearing \times sex}(1,11) = 10.27$; $p < 0.01$; E, $F_{rearing}(1,11) = 11.62$; $p < 0.01$; $F_{sex}(1,11) = 5.515$; $p = 0.04$; $F_{rearing \times sex}(1,11) = 0.099$; $p = 0.76$; F, $F_{rearing}(1,11) = 22.76$; $p < 0.01$; $F_{sex}(1,11) = 21.97$; $p < 0.01$; $F_{rearing \times sex}(1,11) = 3.022$; $p = 0.11$; n, CTL male = 4 mice/2 litters; ELA male = 4 mice/1 litter; CTL female = 4 mice/1 litter; ELA female = 3 mice/1 litter). See Table 4.1 and 4.2 for full abbreviations and statistical analyses and tests. CTL, control. ELA, early-life adversity.

Table 4.1: Abbreviations of brain regions analyzed in Figure 4.5

Abbreviation	Brain Region
vStr	ventral striatum
NAc	nucleus accumbens
OT	olfactory tubercle
CeA	central amygdala
MeA	medial amygdala
SI	substantia innominata
MA	magnocellular nucleus
MS	medial septal nucleus
CA1	field CA1
CA2	field CA2
CA3	field CA3
DG	dentate gyrus
ENTl	entorhinal cortex
POST	postsubiculum
Pre	presubiculum
SUB	subiculum
EP	endopiriform cortex
SSs	somatosensory cortex, secondary

AUDd	auditory cortex, dorsal
VISal	anterolateral visual area
VISam	anteromedial visual area
VISl	lateral visual area
VISp	primary visual area
VISpl	posterolateral visual area
ACC	anterior cingulate cortex
AIp	Agranular insular area, posterior part
RSP	retrosplenial cortex
VISrll	Rostrolateral lateral visual area
ECT	ectorhinal cortex
OLF	olfactory areas
TT	taenia tecta
PIR	piriform cortex
NLOT	nucleus of the solitary tract
COA	cortical amygdalar area
PAA	piriform-amygdalar area
TR	postpiriform transition area
PP	peripeduncular cortex
GENd	geniculate group, dorsal thalamus
IGL	intergeniculate leaflet of the lateral geniculate complex
LGv	ventral part of the lateral geniculate complex
Subg	subgeiniculate nucleus
LH	lateral habenula
LZ	hypothalamic lateral zone
ZI	zona incerta
MB	mammillary body
SCs	superior colliculus, sensory related
IC	inferior colliculus
SNr	substantia nigra, reticular part
VTA	ventral tegmental area

APN	anterior pretectal nucleus
MPT	medial pretectal area
SNc	substantia nigra, compact part
IF	interfascicular nucleus raphe
IPN	interpeduncular nucleus
RL	rostral linear nucleus raphe
CLI	central linear nucleus raphe

Table 4.2: ANOVA tables of F-values and P-values for all brain regions analyzed in Figure 4.5

df = 11 for all	**F values**			**Benjamini–Hochberg False Discovery Rate Corrected P value**		
Area	**Sex**	**Rearing**	**Interaction**	**Sex**	**Rearing**	**Interaction**
Frontal pole, cerebral cortex	0.639	1.375	1.368	0.524	0.835	0.458
Primary motor area	3.566	5.839	2.855	0.170	0.425	0.260
Secondary motor area	1.702	39.000	12.103	0.001	0.678	0.049
Primary somatosensory area	4.216	8.058	6.544	0.099	0.425	0.102
Supplemental somatosensory area	0.464	4.967	0.019	0.221	0.846	0.914
Gustatory areas	9.486	0.202	12.103	0.817	0.132	0.049
Visceral area	2.077	0.012	5.353	0.928	0.611	0.129
Dorsal auditory area	0.012	0.319	0.502	0.776	0.928	0.647
Primary auditory area	0.012	0.319	1.022	0.776	0.928	0.529
Posterior auditory area	0.848	5.839	1.782	0.170	0.816	0.384
Ventral auditory area	0.012	39.000	0.736	0.001	0.928	0.610

Anterolateral visual area	0.319	2.077	0.000	0.416	0.891	1.000
Anteromedial visual area	0.012	3.566	0.317	0.316	0.928	0.693
Lateral visual area	3.000	1.702	2.273	0.460	0.493	0.316
Primary visual area	0.113	4.967	1.022	0.221	0.909	0.529
Posterolateral visual area	0.319	0.319	2.273	0.776	0.891	0.316
Posteromedial visual area	0.639	1.092	0.317	0.591	0.835	0.693
Anterior cingulate area	0.639	2.507	2.273	0.383	0.835	0.316
Prelimbic area	0.202	0.848	5.353	0.641	0.891	0.129
Infralimbic area	0.202	0.639	5.353	0.683	0.891	0.129
Orbital area, lateral part	0.202	3.000	0.502	0.338	0.891	0.647
Orbital area, medial part	0.848	3.566	1.368	0.316	0.816	0.458
Orbital area, ventrolateral part	0.202	0.113	0.000	0.873	0.891	1.000
Agranular insular area, dorsal part	0.050	3.566	3.545	0.316	0.927	0.206
Agranular insular area, posterior part	1.702	11.209	6.544	0.057	0.678	0.102
Agranular insular area, ventral part	0.848	29.959	4.368	0.003	0.816	0.166
Retrosplenial area	0.012	0.319	8.000	0.776	0.928	0.081

Rostrolateral visual area	0.113	0.113	1.022	0.873	0.909	0.529
Temporal association areas	3.000	23.794	4.368	0.006	0.493	0.166
Perirhinal area	0.000	0.050	0.176	0.910	1.000	0.764
Ectorhinal area	0.464	0.012	0.176	0.928	0.846	0.764
Olfactory areas	0.113	2.077	0.176	0.416	0.909	0.764
Accessory olfactory bulb	0.202	2.077	2.273	0.416	0.891	0.316
Anterior olfactory nucleus	0.202	3.000	4.368	0.338	0.891	0.166
Taenia tecta	3.566	4.216	9.809	0.270	0.425	0.068
Dorsal peduncular area	1.092	0.639	0.502	0.683	0.804	0.647
Piriform area	0.012	0.319	0.019	0.776	0.928	0.914
Nucleus of the lateral olfactory tract	5.839	15.955	0.736	0.020	0.339	0.610
Cortical amygdalar area, anterior part	0.319	6.858	5.353	0.134	0.891	0.129
Cortical amygdalar area, posterior part	0.113	0.639	0.502	0.683	0.909	0.647
Piriform-amygdalar area	0.464	3.000	0.078	0.338	0.846	0.848
Postpiriform transition area	2.507	8.058	5.353	0.099	0.532	0.129
Hippocampal formation	3.566	8.058	6.544	0.099	0.425	0.102

Field CA1	4.967	8.058	3.545	0.099	0.378	0.206
Field CA2	5.839	15.955	8.000	0.020	0.339	0.081
Field CA3	3.566	8.058	0.317	0.099	0.425	0.693
Dentate gyrus	0.848	15.955	2.855	0.020	0.816	0.260
Entorhinal area, lateral part	3.566	3.000	0.317	0.338	0.425	0.693
Entorhinal area, medial part, dorsal zone	0.464	0.464	0.736	0.734	0.846	0.610
Parasubiculum	0.319	1.702	6.544	0.460	0.891	0.102
Postsubiculum	2.507	3.000	1.782	0.338	0.532	0.384
Presubiculum	13.319	2.507	4.368	0.383	0.118	0.166
Subiculum	0.050	0.000	0.502	1.000	0.927	0.647
Claustrum	1.092	0.848	2.855	0.641	0.804	0.260
Endopiriform nucleus	0.464	1.702	3.545	0.460	0.846	0.206
Posterior amygdalar nucleus	1.375	3.000	6.544	0.338	0.767	0.102
Striatum	11.209	39.000	8.000	0.001	0.132	0.081
Caudoputamen	4.967	1.702	0.078	0.460	0.378	0.848
Nucleus accumbens	1.375	2.077	0.078	0.416	0.767	0.848
Olfactory tubercle	0.848	0.639	0.317	0.683	0.816	0.693
Lateral septal complex	0.113	2.507	0.317	0.383	0.909	0.693
Central amygdalar nucleus	1.092	23.794	12.103	0.006	0.804	0.049
Medial amygdalar nucleus	3.566	0.202	8.000	0.817	0.425	0.081

Pallidum	1.375	4.216	3.545	0.270	0.767	0.206
Globus pallidus, external segment	0.050	11.209	2.855	0.057	0.927	0.260
Globus pallidus, internal segment	1.092	0.113	1.368	0.873	0.804	0.458
Substantia innominata	0.202	9.486	6.544	0.088	0.891	0.102
Magnocellular nucleus	2.077	0.202	1.782	0.817	0.611	0.384
Medial septal nucleus	0.050	0.050	0.736	0.910	0.927	0.610
Diagonal band nucleus	0.012	1.092	0.019	0.591	0.928	0.914
Triangular nucleus of septum	0.639	2.077	0.176	0.416	0.835	0.764
Bed nuclei of the stria terminalis	9.486	0.202	8.000	0.817	0.132	0.081
Thalamus	1.092	0.464	0.078	0.734	0.804	0.848
Ventral group of the dorsal thalamus	0.012	0.848	1.368	0.641	0.928	0.458
Subparafascicular nucleus	2.507	1.702	3.545	0.460	0.532	0.206
Subparafascicular area	0.464	0.848	1.782	0.641	0.846	0.384
Peripeduncular nucleus	15.955	0.319	0.502	0.776	0.092	0.647
Geniculate group, dorsal thalamus	0.050	2.077	0.019	0.416	0.927	0.914

Lateral group of the dorsal thalamus	0.113	1.092	0.317	0.591	0.909	0.693
Anterior group of the dorsal thalamus	2.077	6.858	0.502	0.134	0.611	0.647
Medial group of the dorsal thalamus	0.012	0.012	0.502	0.928	0.928	0.647
Midline group of the dorsal thalamus	0.464	0.464	9.809	0.734	0.846	0.068
Intralaminar nuclei of the dorsal thalamus	0.012	0.639	4.368	0.683	0.928	0.166
Reticular nucleus of the thalamus	0.639	1.375	1.368	0.524	0.835	0.458
Intergeniculate leaflet of the lateral geniculate complex	0.000	0.013	9.902	0.928	1.000	0.068
Ventral part of the lateral geniculate complex	0.204	0.204	12.145	0.817	0.891	0.049
Subgeniculate nucleus	0.528	0.000	0.771	1.000	0.846	0.610
Medial habenula	6.858	2.077	6.544	0.416	0.283	0.102
Lateral habenula	0.319	0.202	0.176	0.817	0.891	0.764
Hypothalamus	1.702	0.113	4.368	0.873	0.678	0.166
Periventricular zone	0.639	0.639	0.019	0.683	0.835	0.914
Periventricular region	0.202	0.050	1.022	0.910	0.891	0.529
Anterior hypothalamic nucleus	0.464	0.848	0.502	0.641	0.846	0.647

Mammillary body	0.202	0.050	8.000	0.910	0.891	0.081
Medial preoptic nucleus	0.113	0.012	0.000	0.928	0.909	1.000
Dorsal premammillary nucleus	0.113	0.050	0.502	0.910	0.909	0.647
Ventral premammillary nucleus	0.202	3.566	0.176	0.316	0.891	0.764
Paraventricular hypothalamic nucleus, descending division	3.000	0.113	0.317	0.873	0.493	0.693
Ventromedial hypothalamic nucleus	0.848	0.319	3.545	0.776	0.816	0.206
Posterior hypothalamic nucleus	3.566	1.375	2.273	0.524	0.425	0.316
Hypothalamic lateral zone	0.639	1.092	5.353	0.591	0.835	0.129
Zona incerta	0.050	1.375	12.103	0.524	0.927	0.049
Median eminence	4.226	0.465	12.145	0.734	0.425	0.049
Midbrain	4.967	0.639	2.273	0.683	0.378	0.316
Superior colliculus, sensory related	0.050	2.507	12.103	0.383	0.927	0.049
Inferior colliculus	0.848	4.216	1.022	0.270	0.816	0.529
Substantia nigra, reticular part	0.050	5.839	0.019	0.170	0.927	0.914

Ventral tegmental area	9.486	0.050	2.855	0.910	0.132	0.260
Superior colliculus, motor related	2.507	3.000	12.103	0.338	0.532	0.049
Periaqueductal gray	1.702	0.012	1.782	0.928	0.678	0.384
Precommissural nucleus	0.012	0.848	1.022	0.641	0.928	0.529
Anterior pretectal nucleus	0.848	0.202	12.103	0.817	0.816	0.049
Medial pretectal area	0.165	0.013	10.094	0.928	0.909	0.068
Substantia nigra, compact part	19.330	0.464	8.000	0.734	0.087	0.081
Pedunculopontine nucleus	0.050	0.012	5.353	0.928	0.927	0.129
Interfascicular nucleus raphe	2.507	0.012	0.317	0.928	0.532	0.693
Interpeduncular nucleus	1.092	0.464	0.502	0.734	0.804	0.647
Rostral linear nucleus raphe	9.486	2.507	12.103	0.383	0.132	0.049
Central linear nucleus raphe	0.257	0.078	3.545	0.910	0.891	0.206
Dorsal nucleus raphe	0.641	1.705	0.318	0.460	0.835	0.693

Discussion and Conclusion

In the aggregate, 1. Optical stimulation and immunohistochemistry indicate that the basic cell types and synaptic functions of the CRH/GABA BLA→NAc projection are similar in males and females. 2. The structural organization of the projection is sex-specific and is further modulated by early-life rearing conditions. 3. Beyond projections to the NAc, the innervation patterns of CRH/GABA BLA neurons suggest global sex-dependent differences in their brain-wide organization, which might account for both fundamental differences in their operations as well as sex-dependent differences in the outcomes of ELA.

In females, we found no sex or rearing effects on the basic functional properties of NAc-projecting CRH/GABA cells. Using optogenetics paired with electrophysiology, we found that activating CRH/GABA cells in the BLA triggered inhibitory currents in the medial shell of the NAc across all groups, regardless of sex or rearing conditions. All CRH BLA cells were GABAergic, indicating that the fundamental cell type and function of the projection are common across sexes and rearing. We then reasoned that the sex-dependent differences in the behavioral functions of the projection result from neuroanatomical differences in the organization and target innervation of CRH/GABA BLA cells.

We first determined the qualitative and quantitative aspects of the CRH/GABA BLA→NAc projection within the NAc. As blocking terminals in the NAc restored typical reward responses to a palatable food cue in ELA males (Birnie et al., 2023), we hypothesized that in ELA mice, CRH/GABA BLA neurons may have increased NAc axonal innervation, thus leading to increased synaptic activity that influences NAc

operations. To our surprise, we observed a “decrease” in axon labeling in the NAc of ELA male mice. The NAc contains both MSNs, the main output population, and GABAergic interneurons that regulate MSN activity. We found that CRH/GABA BLA→NAc axons innervate both MSNs and interneurons. This complexity allows reconciling of the observed data in which activating this pathway in control males mimics the effects of ELA despite reduced axon density in the latter. Target-specific circuit reorganization, e.g., preferential loss of inputs onto inhibitory interneurons, may be at play. In that scenario, stimulating the GABAergic pathway in control males could inhibit MSNs, enhancing NAc inhibition thereby suppressing reward behaviors. In contrast, ELA males already exhibit reduced NAc activity, through reduced disinhibition (or heightened activity of the GABAergic pathway), which could occlude the effects of stimulating this pathway. In females we found no differences in axonal innervation in the NAc. As for males, we excluded the possibility that any differences in signal density might result from differences in the number of CRH/GABA BLA cells (Figure 4.3). We also considered potential influence of the estrous cycle stage and established that the cycle phase had no influence on the data and there was no litter effect (Figure 3.5). We also excluded misplacement of virus or cannulae as a potential explanation of this observation (Figure 4.3).

Because ELA impacted reward behaviors in females and because NAc innervation by the BLA-origin CRH/GABA cells did not differ in ELA and control females, we speculated that other projections of the same, apparently ELA-sensitive, cells might contribute to the observed behavioral effects of ELA. Indeed, our brain-wide analysis uncovers other projection targets of CRH/GABA BLA cells that exhibit female-specific

changes in ELA mice. One of these regions, the ZI, exhibited female-specific increases in CRH/GABA BLA axons following ELA. The ZI, an extension of the reticular formation of the thalamus, is a largely inhibitory nucleus containing genetically heterogeneous cell populations (Arena et al., 2024). Recent studies have found the ZI to be involved in integrating multisensory inputs, controlling motor behavior and importantly, driving motivational and appetitive behaviors (X. Wang et al., 2020; Ye et al., 2023). Altered ZI activity contributes to anxiety-related and coping behaviors following chronic stress (Ge et al., 2024; Zhou et al., 2021), but the effects of ELA on ZI functions in the context of reward are poorly understood. This analysis paves the way for future studies elucidating the role of the CRH/GABA BLA→ZI pathway in reward behaviors and the effects of ELA.

Beyond the ZI, our brain-wide analysis revealed extensive target and sex specificity in the effects of ELA on CRH/GABA BLA innervation patterns. Notably, the retrosplenial cortex exhibits increased axon density in the ELA group, with significantly greater increases in males compared with females. The retrosplenial cortex is critically involved in spatial and contextual learning and memory (Cheng et al., 2024; Vann et al., 2009), and one study has reported male-specific impairments in the novel object placement task, a paradigm that depends on spatial learning, following ELA (Bath et al., 2017).

We also find male-specific increases in axon density within the auditory cortex, which supports the perception, interpretation, and memory of auditory cues (Letzkus et al., 2011; Rothschild et al., 2010), and aligns with findings of male-specific deficits in auditory learning in adult rodents exposed to ELA (Hardy et al., 2023; Mazi et al., 2025).

In contrast, a different sensory processing region, the superior colliculus, shows female-specific increases in CRH/GABA BLA innervation in ELA mice compared with controls. The superior colliculus integrates multisensory information, enabling the detection and prioritization of environmental stimuli (Perrault et al., 2005; Stein et al., 1989). Multisensory processing can be influenced by experience (Z. Wang et al., 2020) and altered sensitivity to external stimuli is a hallmark of several psychiatric conditions (Harrold et al., 2024; Liss et al., 2005). Whether these changes in sensory processing are sex-dependent and the neural mechanisms underlying these changes remain unclear, but they present a compelling direction for future investigation. Together these findings suggest that ELA, and perhaps the aspect of fragmented maternal care observed in our LBN ELA model, may alter sensory processing circuitry in a sex-specific manner. This may lead to enduring differences in how males and females process environmental cues, governing their reward behaviors.

Our observations of region-specific increases in axon labeling are consistent with previous studies that observed elevated BLA axon density in the prefrontal cortex of adolescent rats that experienced ELA (Honeycutt et al., 2020). We also considered the possibility that regions with low axonal density might be more likely to show more significant effects. To that end, we generated density plots and established that while numerous regions with low density indeed show significant effects, more than a third of the significantly altered regions have high axon densities (Figure 4.4).

Several mechanisms may contribute to the increased axon labeling we observed. The increased density may result from augmented axon sprouting or a failure of developmental pruning mechanisms. The latter mechanism is supported by our prior

work on the failure of synaptic pruning onto CRH cells in the hypothalamic paraventricular nucleus (Bolton et al., 2022).The deficient synaptic pruning was a result of ELA-induced microglial dysfunction. In contrast, in the hippocampus, ELA has led to selective deficits of neuronal arborization in specific hippocampal layers (Brunson et al., 2005; Ivy et al., 2010). Thus, ELA-induced dysregulation of structural brain circuit maturation is a plausible common theme for the altered innervation observed here and for the behavioral consequences (Birnie & Baram, 2022, 2025).

These studies reveal that ELA causes sex-specific changes in adult reward behaviors which in males are mediated, at least in part, by a CRH/GABA BLA→NAc projection. In contrast, this projection's function or innervation does not explain female-specific ELA-induced behavioral changes. Importantly, we find sex- and rearing-related plasticity of brain-wide projections of CRH/GABA BLA neurons, suggesting that ELA can exert potent, lasting effects on brain organization of stress-sensitive cells and projections (Birnie & Baram, 2025). Our brain-wide datasets and the effects of sex and rearing will enable future investigations of how sex-specific BLA circuit alterations contribute to behavioral outcomes following ELA.

Notably, the above comprehensive studies did not solve the conundrum of an apparent lack of any effect of manipulating the projection in females, a topic addressed in the next chapter.

Methods and Materials

Electrophysiology slice preparation

Mice were deeply anesthetized with isoflurane and quickly decapitated. Acute horizontal slices (300 μm) encompassing the NAc and BLA were obtained using a vibratome (Leica V1200S) in an ice-cold sucrose cutting solution containing the following (in mM): 228 sucrose, 11 glucose, 26 $NaHCO_3$, 1.2 NaH_2PO_4, 2.5 KCl, 5 Na-ascorbate, 3 Na-pyruvate, 10 $MgSO_4 \cdot 7H_2O$, and 0.5 $CaCl_2$ (305–310 mOsm), pH 7.4. Slices equilibrated in a homemade chamber for 25–30 min (34°C) and then 45 min in room-temperature aCSF containing the following (in mM): 119 NaCl, 26 $NaHCO_3$, 1 NaH_2PO_4, 2.5 KCl, 11 glucose, 10 sucrose, 1.3 $MgSO_4 \cdot 7H_2O$, and 2.5 $CaCl_2$ (290–300 mOsm), pH 7.4, before being transferred to a recording chamber. Solutions were continuously bubbled with 95% O_2/5% CO_2.

Whole-cell patch clamp

Recordings were performed in the medial NAc shell using a Multiclamp 700B, Digidata 1550B, and Clampex 11 (Molecular Devices). Recordings were conducted in a voltage-clamp mode at 31°C, low-pass filtered at 2 kHz, and digitized at 10 kHz. Borosilicate glass pipettes (3–4 MΩ, Molecular Devices) filled with internal solution (295–305 mOsm, adjusted with CsOH), pH 7.4, contained the following (in mM): 135 $CsMeSO_4$, 8 CsCl, 10 HEPES, 0.25 EGTA, 5 phosphocreatine, 4 MgATP, 0.3 NaGTP, and 1 mg/ml NeuroBiotin (295–305 mOsm), pH 7.4 with CsOH. Access resistance (Ra) was monitored, and recordings with Ra changes >20% were excluded. Cells were visualized with infrared DIC microscopy (Olympus BX51WI). Neurons were held at 0 mV

to record optically evoked inhibitory postsynaptic currents (oIPSCs) using 488 nm LED light. After 5 min of stable oIPSCs, picrotoxin (100 μM) was superfused until oIPSCs were blocked. Neurons were then held at −60 mV to record optically evoked excitatory postsynaptic currents (oEPSCs). Stable oEPSCs were followed by the superfusion of CNQX (10 μM) and AP5 (50 μM). Slices were fixed in 4% PFA at 4°C overnight and then stored in 0.1 M PBS for histological processing.

Immunohistochemistry

Concurrent immunolabeling of CRH and GAD was performed as described previously (Y. Chen et al., 2015; Yan et al., 1998), and concurrent immunolabeling of CRH and virus-expressed fluorophore followed (Birnie et al., 2023). Briefly, sections were first incubated with a rabbit anti-CRH antiserum (PBL rC68, courtesy of Dr. Paul Sawchenko, Salk Institute for Biological Studies; 1:20,000, 7 d, 4°C), and then treated with HRP-conjugated anti-rabbit IgG (1:1,000, PerkinElmer) for 1.5 h. Cyanine 3-conjugated tyramide (1:150, Akoya) was applied in the dark for 5–6 min. After CRH detection, sections were exposed to a mixture of mouse anti-GAD67 (1:250, Santa Cruz Biotechnology sc-28376) and anti-GAD65 (1:1,000, Boehringer Mannheim #1522 825; 3 d, 4°C) or to a mouse monoclonal anti-RFP (1:2,000, Rockland #200-301-379) to detect AAV2-mCherry–infected neurons and visualized using anti-mouse IgG conjugated to Alexa Fluor 488 (1:400, Invitrogen). The ChR2-EGFP signal was detected using a rabbit anti-GFP antibody (1:2,000, Sigma G1544; 2 d, 4°C) and visualized using an anti-rabbit IgG conjugated to Alexa Fluor 488 (1:200, Invitrogen A-11034). For dual labeling, the sections were first subjected to GFP immunostaining and then incubated for 2 d (4°C)

with a goat anti-CRHR1 antibody (1:2,000, Everest Biotech EB08035, Lot P1 E090910), mouse anti-dopamine D1R (1:1,000, Novus NB110-6001 7SS), or mouse anti-parvalbumin antibody (1:10,000, Chemicon MAB1572). Fluorescence signals were visualized using cyanine 3-conjugated tyramide as described above or with anti-mouse IgG conjugated to Alexa Fluor 568 (1:400, Invitrogen).

Brain clearing

Brains were processed using the Adipo-Clear protocol (Chi et al., 2018) with slight modifications. Mice were transcardially perfused and brains hemisected ~1 mm past the midline and postfixed overnight in 4% paraformaldehyde (Sigma-Aldrich 30525-89-4) at 4°C. The following day, samples were dehydrated with a gradient of methanol (MeOH; Thermo Fisher Scientific 67-56-1)/B1n buffer (1:1,000 Triton X-100, 2% w/v glycine, 1:10,000 NaOH 10N, 0.02% sodium azide) for 1 h for each step (20, 40, 60, 80%) on a nutator. Samples were then washed with 100% MeOH 2× for 1 h each and then incubated in 2:1 dichloromethane (DCM):MeOH solution overnight. The following day, the samples were washed 2× for 1 h in 100% DCM, followed by three washes of 100% MeOH (30 min, 45 min, 1 h). Samples were bleached for 4 h in 5:1 H2O2/MeOH buffer. A cascade of MeOH/B1n washes (80, 60, 40, 20%; 30 min each) rehydrated the samples, followed by a 1 h wash in B1n buffer. The tissue was permeabilized in 5% DMSO/0.3 M glycine/PTxwH (1 h then 2 h). Samples were washed with PTxwH for 30 min and incubated in fresh PTxwH overnight. The following day, we performed two PTxwH washes (1 h, then 2 h). Samples were incubated in primary GFP antibody (GFP-1020, AVES Labs NC9510598) at 1:2,000 in PTxwH shaking at 37°C for 11 d, washed

in PTxwH (2× for 1 h, 2× for 2 h and then once per day for 2 d). Samples were then incubated in a secondary antibody (Alexa Fluor 647, Thermo Fisher Scientific A78952) for 8 d shaken at 37°C. Samples were washed in PTxwH (same as after primary antibody). Samples were then washed in 1× PBS twice (1 h, 2 × 2 h, overnight). Samples were dehydrated in a gradient of MeOH:H2O (20, 40, 60, and 80%; 30 min each and then 100% 30 min, 1 h, 1.5 h). Samples were incubated overnight in 2:1 DCM:MeOH on a nutator, washed in 100% DCM (2× for 1 h). Samples were cleared in 100% DBE. DBE was changed after 4 h. Samples were stored in DBE in a dark location at room temperature. Imaging took place at least 24 h after clearing.

Whole-brain imaging

Brain samples were imaged on a light sheet microscope (Ultramicroscope II, LaVision Biotec) equipped with a sCMOS camera (Andor Neo) and a 2×/0.5 NA objective lens (MVPLAPO 2×) with a 6 mm working distance dipping cap. Image stacks were acquired at 0.8× optical zoom using Inspector Microscope v285 controller software. We imaged using 488 nm (laser power 20%) and 640 nm (laser power 50%) lasers. The samples were scanned with a step size of 3 µm using the continuous light sheet scanning method with the included contrast adaptive algorithm for the 640 nm channel (20 acquisitions per plane) and without horizontal scanning for the 488 nm channel.

DeepTraCE pipeline

Whole-brain image stacks were analyzed using a Python based DeepTraCE GUI (https://github.com/jcouto/DeepTraCE). Briefly, image stacks in the 640 nm channel were segmented using the 3D U-net-based machine learning pipeline TrailMap (Friedmann et al., 2020) with a model trained to recognize clearly delineated axons (Model 1) described in Gongwer et al. (2023). Following segmentation, the 488 nm autofluorescence channel and axon segmentation were converted to 8 bit, scaled to 10 µm resolution, and rotated to match the reference atlas. The autofluorescence channel was registered using elastix to the Gubra Lab light sheet fluorescence microscopy (LSFM) atlas average template, which has annotations that match the Allen CCF (Klein et al., 2010; Perens et al., 2021; Q. Wang et al., 2020). The same transformation was applied to the segmented brain using transformix and converted to 8 bit .tif format. Axons were then skeletonized (reduced to a single pixel thickness) for quantification, as described previously (Friedmann et al., 2020; Gongwer et al., 2023).

To account for variability in BLA viral expression across animals, we normalized all axon counts to the total number of labeled pixels across the whole brain (Figure 4.3). Regional axon innervation was quantified by counting the number of skeletonized pixels in each brain region above a threshold, then dividing this pixel count by the total number of pixels in a region. Regions were defined by a collapsed version of the Gubra Lab LSFM atlas. The atlas was cropped on the anterior and posterior ends to match the amount of tissue visible in our data. Fiber tracts, ventricular systems, cerebellum, pons, medulla, and olfactory bulb were excluded from analysis.

Axon quantification

Medial–lateral axon distributions within regions were calculated in MATLAB by binning the whole-brain image into 100 μm voxels, calculating the percentage of segmented pixels within each voxel normalizing for total fluorescence as above. The averaged summation of axon counts from each group was then averaged and plotted along with the SEM.

Axon visualization

To visualize axons in the NAc of representative brains (Figure 4.2), z-projections of raw light sheet data were created in FIJI by scaling images to a 4.0625 μm space, virtually re-slicing images in the coronal plane and performing maximum intensity z-projections of 30 μm depth followed by local contrast enhancement. To visualize axons at various coronal levels (Figure 4.5), representative brains from each group were resliced in the coronal plane, and then 80 μm-thick z-projections of the skeletonized and registered axons were produced from the resliced brains.

Quantitative approaches and statistical analyses

All statistical comparisons and analyses were performed in GraphPad Prism V10 or MATLAB 2022a. The specific experimental design and statistical analyses can be found in the figure legends.

Chapter 5 – Ipsilateral vs. contralateral CRH/GABA BLA→NAc projections may mediate different functions in female mice

Introduction

We had previously implemented bilateral chemogenetic manipulations of the CRH/GABA BLA→NAc projection in mice. However, excitation or inhibition of the projection in female mice resulted in no change in reward behavior (L. Taniguchi et al., 2026). The absence of a behavioral effect in females, compared to males, could not be attributed to the absence of the projection or to differences in its molecular or electrophysiological properties.

One possibility is that the ipsilateral CRH/GABA BLA→NAc projection and the contralateral CRH/GABA BLA→NAc projection may have opposing valences and antagonizing functions. Therefore, when bilaterally chemogenetically manipulating these projections, the effects would cancel out. A recent study by Tian and colleagues demonstrated that it is possible to have the same projection with different functions depending on the interhemispheric connections. The authors found that glutamatergic ipsilateral BLA→NAc projections were associated with positive valence and drive reward-seeking, while contralateral glutamatergic BLA→NAc projections traversing the anterior commissure were associated with negative valence and drive avoidance behavior (Tian et al., 2024). Thus, this led us to the question: could the CRH/GABA BLA→NAc ipsilateral and contralateral projections have opposing functions, differences in structural properties, or different downstream targets, leading to processing of opposite valences or coordination of entirely different functions?

Ipsilateral excitation of the CRH/GABA BLA→NAc projection reduces motivated reward behavior in control female mice

For these studies, we used Feeding Experimentation Device version 3 (FED3) operant devices (Matikainen-Ankney et al., 2021) placed in the animals' home cages. We used a progressive ratio schedule (Richardson & Roberts, 1996), where the mouse nose-pokes into the left active port to earn sucrose pellets, and the number of required pokes scales up with each successive reward according to an established formula. This measures motivation and how hard the animal is willing to work for a reward. We used the same chemogenetic approach as before but this time injecting the excitatory Cre-dependent DREADD only unilaterally in the BLA and infusing CNO into the NAc on the same hemisphere. Over the cumulative nose-poke data from the 4-hour progressive ratio sessions, we show that, as expected, ELA females nose-poke more frequently to obtain palatable food versus control females, even when the effort is high (Figure 5.1B). Notably, in control females, chemogenetically exciting the ipsilateral CRH/GABA BLA→NAc projection reduced active nose pokes. However, in ELA females, exciting the ipsilateral projection had no effect on motivated behavior in ELA females. These data are of particular interest, because they begin to clarify the major enigma described in Chapter 3: the apparent lack of effect of manipulating the projection in females. It shows that our conventional experimental approach, bilateral stimulation, may mask the effects of an ipsilateral projection.

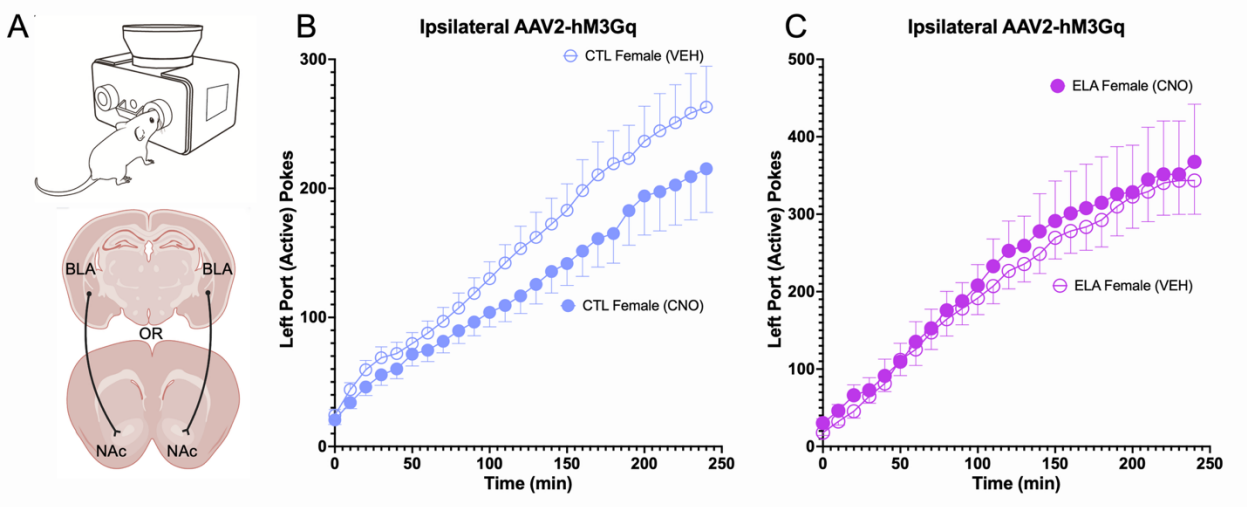

Figure 5.1: Ipsilateral excitation of the CRH/GABA BLA→NAc projection reduces motivated reward behavior in control female mice

(A) Schematic of the FED3 operant device (Matikainen-Ankney et al., 2021). (B) Cumulative number of nose pokes in the left active port over four hours of a progressive ratio task in CTL females (n = 13) and (C) ELA females (n = 7) immediately following ipsilateral chemogenetic excitation of the CRH/GABA BLA→NAc projection. Symbols and error bars represent mean and SEM. CTL, control. ELA, early-life adversity. VEH, vehicle. CNO, clozapine-N-oxide.

Left vs. right ipsilateral projections may have different effects on motivation

Whereas the brain on the exterior appears to be symmetric, there is evidence in humans and rodents of internal laterality in which neuropeptides modulate hemispheric function (Kolber et al., 2026). In this review the authors provide evidence for three different patterns in studies thus far in lateralized neuropeptide regulation including: 1. Neuropeptides exerting opposite effects on each side (e.g. CGRP suppresses pain through the left amygdala but facilitates pain through the right amygdala (H. N. Allen et al., 2023), 2. Neuropeptides exerting effects preferentially on one hemisphere (e.g. oxytocin modulates rodent auditory cortex activity and subsequently dam-pup behavior on the left side (Marlin et al., 2015; Mitre et al., 2016), cholecystokinin modulates vagus nerve stimulation effect on reward in the right nodose ganglia (Han et al., 2018; Lansbury et al., 2025), and 3. Functionally symmetric responses on both sides may be

modulated differently through neuropeptide receptors that are lateralized depending on the side (e.g. KOR agonists elicit left hindlimb flexion while vasopressin elicits right hindlimb flexion (Watanabe et al., 2020, 2024).

Given the evidence for many neuropeptides' roles in lateralized functions, we queried whether the CRH/GABA BLA→NAc may differ in function between the left BLA→left NAc and right BLA→right NAc. To do this, we stratified the data in Figure 5.1 by hemisphere and found a striking pattern. In CTL females, suppression of motivation appears to be driven more by the CRH/GABA right BLA→right NAc, while excitation of the left hemisphere may increase motivated reward seeking (Figure 5.2A,B). Similarly in ELA females, suppression of motivation is also driven by the CRH/GABA right BLA→right NAc, while there may also be an increase in reward motivation driven by the CRH/GABA left BLA→left NAc (Figure 5.2C,D). These findings are noteworthy given that bilateral manipulations consistently failed to reveal effects in females. By examining the projection unilaterally and stratifying by hemisphere, we have begun to uncover promising functional differences that merit further investigation.

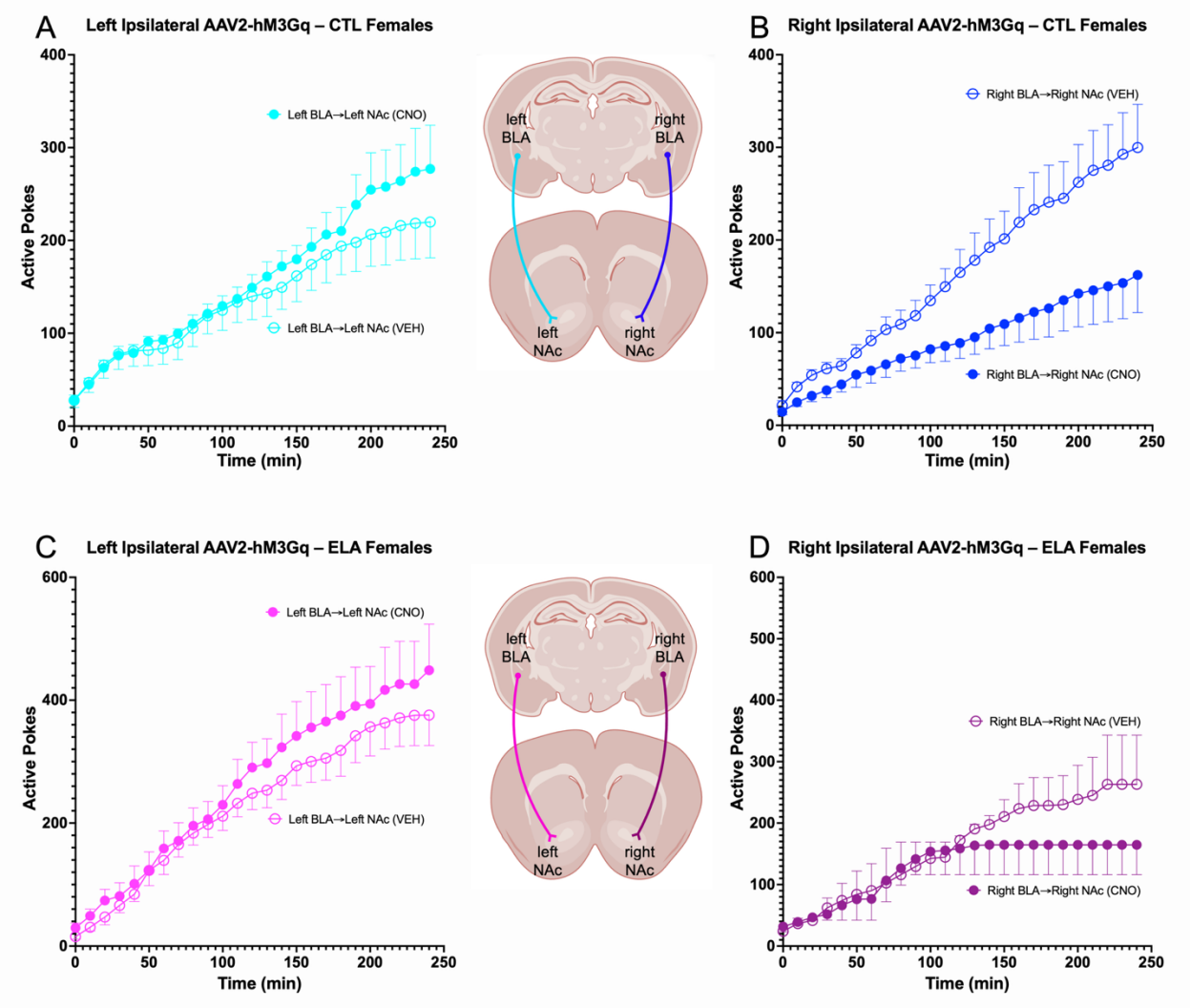

Figure 5.2: Left vs. right ipsilateral projections may have different effects on motivation

(A–D) Comparing the CRH/GABA left BLA→left NAc vs. right BLA→right NAc ipsilateral projection function in female mice. Cumulative number of nose pokes in the left active port over four hours of a progressive ratio task in (A) left BLA→left NAc CTL females (n = 6); (B) right BLA→right NAc CTL females (n = 7); (C) left BLA→left NAc ELA females (n = 5); (D) right BLA→right NAc ELA females (n = 2) immediately following ipsilateral chemogenetic excitation of the CRH/GABA BLA→NAc projection. Symbols and error bars represent mean and SEM. CTL, control. ELA, early-life adversity. VEH, vehicle. CNO, clozapine-N-oxide.

Discussion and Conclusion

To summarize the results: the apparent functional silence we observed in females during bilateral manipulations is likely a result of potential opposing, lateralized functions of the projections canceling each other out. When we manipulate unilaterally,

we can resolve robust effect of the projection on reward behaviors. Specifically, we find that the right ipsilateral CRH/GABA BLA→NAc projection suppresses motivation in CTL females as well as in ELA females. In contrast, the left ipsilateral CRH/GABA BLA→NAc projection may increase motivation. These ongoing studies do not yet have sufficient statistical power, but the results represent a promising initial step toward elucidating the functional role of the CRH/GABA BLA→NAc projection in female mice.

Methods and Materials

Mice

CRH-ires-Cre mice (B6(Cg)-Crhtm1(cre)Zjh/J, Jackson 012704; (Y. Chen et al., 2015; H. Taniguchi et al., 2011) were bred in-house, weaned at P21, and group-housed by sex on a 12 h light/dark cycle (lights on 0700). Following surgery, females were transferred to a reverse cycle (lights on 2400). Mice used in each figure were separate cohorts. All procedures were approved by the UC Irvine IACUC (AUP 24-104) and adhered to NIH guidelines.

The limited bedding and nesting ELA model

ELA was induced using the limited bedding and nesting (LBN) paradigm (Ivy et al., 2008; Molet, Heins, et al., 2016; Rice et al., 2008). Multiparous dams and litters (4–8 pups; sex-balanced) were randomly assigned to control or LBN conditions. LBN cages contained a plastic-coated mesh platform (McNichols 4700313244) approximately 2.5 cm above the cage floor, with reduced bedding (150 ml) and nesting material (0.5 nestlet vs. 1 standard nestlet). Cages were left undisturbed from postnatal day (P) 2–9

in a ventilated, low-traffic area. All pups were returned to standard caging on P10 and weaned on P21.

Surgical procedures

At 2–3 months, mice were anesthetized with isoflurane (5% induction, 1–1.5% maintenance) and secured in a stereotaxic frame with a heating pad. The scalp was shaved, cleaned with betadine and 70% ethanol, and the skull was exposed. Craniotomies were made at injection and implant sites. Viral vectors were delivered at 100 nl/min through pulled glass pipettes (Drummond 2-000-010), with the pipette left in place for 5 min post-injection to minimize backflow. Mice received buprenorphine postoperatively (Patterson Vet 07-894-9214) and were monitored for 2 days.
For chemogenetic experiments, AAV2-hM3D(Gq)-mCherry (excitatory DREADD; Addgene 44361-AAV2) was unilaterally injected into the medial BLA (0.2 µl) on either the left or right side (counterbalanced across subjects). Bilateral guide cannulas were implanted into the medial NAc shell (A/P +1.2, M/L ±1.5, D/V −3.5 mm, 12° angle) and secured with dental cement (Patterson Dental Orthojet; Liquid 74594412, Powder 74598371) and skull screws (Antrin AMS1201BINDSS). Viral expression in axonal processes was allowed to develop over 6 weeks prior to behavioral testing (Itoga et al., 2019).

Behavioral and chemogenetic testing

All behavioral experiments were conducted at ages 3–5 months, within the first 2 h of the active dark phase (R. J. Nelson et al., 2021; Robins et al., 2020) in a dimly lit

room. Testing took place in individual standard home cages (34 × 18 cm) following habituation. For all chemogenetic experiments, clozapine-N-oxide (CNO; 0.2 µl, 1 mM, Hello Bio HB6149; (Mahler et al., 2014, 2019)) or saline vehicle (VetOne V1510223) was infused unilaterally into the medial NAc shell via indwelling cannula immediately prior to behavioral testing. Intertest intervals allowed sufficient CNO washout and rest (K. S. Smith et al., 2016). Counterbalancing across test days controlled for infusion order effects.

FED3 progressive ratio task

Reward motivation was assessed using a home-cage operant device (FED3.1, Open Ephys OEPS-7510) that delivers 20 mg sucrose pellets (TestDiet 5TUT 1811149) to non-food-restricted mice (Matikainen-Ankney et al., 2021). Mice underwent a 3-day habituation and training sequence to minimize novelty effects (Greiner and Petrovich, 2020) prior to testing.

Habituation and Training (Days 0–2): On Day 0, the FED3 was placed in the home cage on a free feeding program, in which pellets are continuously available upon removal from the well. On Day 1, the program was switched to fixed ratio 1 (FR1), in which one left nose-poke dispenses one pellet; both pokes remain inactive until the pellet is retrieved. Timestamps of nose-pokes, pellet retrieval, and retrieval latency were recorded. Mice that did not achieve ≥60% left-poke accuracy by Day 2 received an additional 6 h FR1 session.

Progressive Ratio Testing (Days 3–11): The PR program required an exponentially increasing number of nose-pokes per pellet, following: Nose Pokes

Required = [5 × e^(0.2 × Pellet Count)] − 5 (yielding a sequence of 1, 2, 4, 9, 12, 15, 20, 25… pokes per successive pellet).

Testing followed a within-subject 2 × 2 design across four test days, with one rest day between each session. On Test Days 1 and 2, mice received CNO or saline (counterbalanced) infused into one side of the NAc (left or right, counterbalanced across subjects), then completed a 6 h PR session. On Test Days 3 and 4 (after 3 days of rest), the same procedure was repeated with infusions into the opposite NAc. Active port nose-pokes and total sucrose pellets obtained were the primary outcome measures. Any mouse that did not reach at least 50 active nose pokes on any of the test days by 120 min was excluded from the final analysis.

Chapter 6 – Discussion and Future Directions

Taken together, the findings presented in this dissertation support a model in which ELA recruits the CRH/GABA BLA→NAc projection in a sex-dependent manner with divergent consequences for reward-related behavior. Specifically: (1) ELA produces reward deficits in male mice, and the CRH/GABA BLA→NAc projection mediates these effects (Chapter 2); (2) ELA augments reward behaviors in female mice, yet bilateral chemogenetic activation of the CRH/GABA BLA→NAc projection does not recapitulate this phenotype, suggesting that the projection's functional role in females may be lateralized, behavior-specific, or dependent on circuit dynamics not fully captured by bilateral manipulations (Chapter 3); (3) the electrophysiological and neurochemical properties of the CRH/GABA BLA→NAc projection are conserved across sexes, yet subtle but potentially important sex- and ELA-dependent differences emerge in the projection's innervation patterns and quantification within the NAc and across the broader brain (Chapter 4); and (4) ipsilateral and contralateral CRH/GABA BLA→NAc projections may serve distinct and potentially opposing functions in female mice (Chapter 5).

These findings do not indicate a lack of function of the CRH/GABA BLA→NAc projection in females. Rather, they suggest that the projection may operate through distinct circuit mechanisms in males and females. In males, the contralateral and ipsilateral projections have the same function, while in the females, they likely do not. The sex-dependent behavioral outcomes (reward deficits in males and reward augmentation in females) coupled with preliminary evidence for lateralized projection function, suggest that the CRH/GABA BLA→NAc system is not a uniform circuit, but its

contribution to behavior depends on sex, early-life experience, and the lateralized architecture. The following future directions are designed to systematically test these possibilities.

Future Directions

Characterizing ipsilateral vs. contralateral and left vs. right effects of the CRH/GABA BLA→NAc projections

The most immediately compelling future direction to emerge from this work concerns the lateralized organization and function of the CRH/GABA BLA→NAc projection. The results presented in Chapter 5 revealed that isolating and activating the ipsilateral CRH/GABA BLA→NAc projection in female mice differentially affected motivational behavior depending on which hemisphere was manipulated, a pattern that was not apparent when the projection was activated bilaterally. This hemisphere-dependent effect motivates an investigation of ipsilateral versus contralateral projection function, as well as potential left versus right asymmetries within each. Adequate statistical power will require substantially increased sample sizes, and the contralateral projection in females remains to be tested.

To organize this line of investigation, we draw on the theoretical framework proposed by Kolber et al. (2026), which identifies four models through which neuropeptides may exert lateralized effects within neural circuits. Applied to the CRH/GABA BLA→NAc system, these models generate the following specific, testable hypotheses:

Model 1 proposes that symmetrically located left and right circuits differ in the number of neuropeptide-expressing neurons. In our system, this would predict quantitative asymmetries in the number of CRH/GABA co-expressing BLA neurons projecting to the left versus right NAc. This hypothesis can be directly tested using viral vector-based circuit tracing combined with whole-brain clearing and axon quantification, or through systematic serial sectioning across both hemispheres.

Model 2 proposes that structurally asymmetric circuits with lateralized connectivity and function are regulated by symmetric neuropeptide systems. In our context, this would predict that ipsilateral and contralateral CRH/GABA BLA→NAc projections innervate different NAc target cells expressing different CRH receptor subtypes, producing functionally distinct postsynaptic effects despite equivalent neuropeptide release. Future experiments should incorporate CRH receptor agonists and antagonists to determine whether receptor-level differences underlie the observed functional asymmetries, while simultaneous recording of postsynaptic currents in NAc target cells will characterize the synaptic consequences of such receptor differences.

Model 3 proposes that structurally symmetric circuits with symmetric connectivity are differentially modulated by lateralized neuropeptide release. Distinguishing this model from Model 2 will require not only CRH receptor pharmacology, but also examination of other neuropeptides or neuromodulators co-expressed within this population that may contribute to hemisphere-specific signaling.

Model 4 proposes that a neuropeptide operates exclusively on one side within an otherwise structurally symmetric circuit. Testing this in our system would require unilateral CRH receptor blockade combined with hemisphere-specific chemogenetic

activation, to determine whether CRH release is necessary for the behavioral effects observed in one hemisphere but not the other.

Alongside these functional experiments, it will be critical to revisit our brain clearing approach to enable direct comparison of ipsilateral and contralateral projections. The brain clearing experiments in Chapter 4 were performed using only one hemisphere, which precluded comparisons across the hemispheres. Future experiments should employ whole-brain clearing protocols to quantify projection density bilaterally, directly linking anatomical organization to the functional asymmetries observed behaviorally. These anatomical and functional analyses should be conducted in both male and female mice and in both control and ELA conditions, as Chapter 4 already identified differences in axon innervation density along the anterior-posterior axis of the NAc between control and ELA males. Establishing the full ipsilateral versus contralateral organization across sexes and rearing conditions will be essential for interpreting the functional results.

Dissociating the functional contributions of CRH and GABA signaling

Importantly, although the CRH/GABA BLA→NAc projection co-expresses both CRH and GABA, the functional contribution of each to the projection's behavioral effects remains to be determined. This represents an interpretive caveat for the findings presented across all chapters, as the chemogenetic manipulations used throughout this dissertation activated the co-expressing population without dissociating CRH from GABA-mediated components.

Endogenous CRH co-expressed in GABAergic neurons has been reported to produce an overall excitatory net effect in several reward circuit regions (Hahn et al., 2009; Silberman & Winder, 2013), while other studies have reported an overall inhibitory effect (Hartley et al., 2019; Yarur et al., 2020). Resolving this in the context of the BLA→NAc projection will require targeted pharmacological experiments. Ex vivo slice electrophysiology with bath application of CRH receptor antagonists, while recording spontaneous and evoked postsynaptic currents in NAc target cells, will isolate the CRH-specific component of synaptic transmission at this synapse. Complementary in vivo experiments combining intra-NAc CRH receptor blockade with simultaneous chemogenetic activation of the CRH/GABA BLA→NAc projection will determine whether CRH signaling is necessary for the behavioral outcomes mediated by this projection, and whether its contribution differs as a function of sex or rearing condition.

In addition, fiber photometry recordings of CRH/GABA BLA→NAc axon terminal calcium dynamics during reward behavioral tasks (performed separately for ipsilateral and contralateral projections in both left and right hemispheres) would allow us to directly test whether endogenous projection activity is lateralized during motivated behavior. This approach would provide evidence linking any structural asymmetries identified through anatomical methods to functional differences observed behaviorally, and would help us bridge the electrophysiology, chemogenetics, and behavioral findings across chapters.

Identifying the target cell population of the CRH/GABA BLA→NAc projection

Understanding which NAc cell types receive direct synaptic input from the CRH/GABA BLA→NAc projection is essential for establishing the circuit-level mechanism through which this projection influences behavior. Over 90% of neurons in the NAc are GABAergic medium spiny neurons (MSNs), classified into D1-expressing MSNs of the direct pathway, which promote reward-associated behaviors, and D2-expressing MSNs of the indirect pathway, which suppress them (Floresco, 2015; Francis & Lobo, 2017; Kupchik et al., 2015). A subset of MSNs in the medial NAc shell co-expresses both D1 and D2 receptors (R. Chen et al., 2021; Surmeier et al., 1996), the precise sub-region in which the majority of BLA-originating CRH terminals are concentrated (Birnie et al., 2023; Itoga et al., 2019). Beyond MSNs, the NAc contains several interneuron populations relevant to this circuit, including cholinergic interneurons previously identified as targets of specific CRH-expressing neurons (Lemos et al., 2019) and parvalbumin-expressing interneurons (Sohal et al., 2009). Preliminary data presented in Chapter 4 (Figure 4.2) suggest that the CRH/GABA BLA→NAc projection may contact both MSNs and interneuron populations.

Identifying the precise postsynaptic targets of this projection will require combining serial sectioning with electrophysiology and cell-type-specific immunohistochemistry. If the CRH/GABA BLA→NAc projection differentially targets D1 versus D2 MSNs in a sex- or ELA-dependent manner, this would provide a direct mechanistic basis for the divergent motivational phenotypes observed across sexes.

Expanding behavioral testing in female mice

A final and important consideration is whether the behavioral paradigms employed in this dissertation were suited to reveal the functional contribution of the CRH/GABA BLA→NAc projection in females specifically. The behavioral paradigms used throughout were selected based on established functions of the BLA→NAc pathway in reward processing; however, the sex-dependent findings suggest that the projection's functional contribution in females may be more behaviorally specific or context-dependent than initially hypothesized, motivating a more targeted interrogation.

Reward-related behavior encompasses both motivational ("wanting") and consummatory ("liking") components, which are supported by partially dissociable anatomical substrates (Berridge & Robinson, 2016). In the sex cue preference task, ELA reduced both consummatory behavior (sniff durations) and motivation (approaches to the scent-bearing stimulus) in males, while in females ELA selectively augmented motivational approaches with little change in consummatory sniff durations (Figure 3.1). Similarly, in the FED3 tasks, ELA augmented motivation under high-effort conditions (progressive ratio) without affecting consumption under low-effort conditions (fixed ratio 1). These dissociations suggest that ELA may preferentially alter the motivational rather than consummatory dimension of reward in females, and that the CRH/GABA BLA→NAc projection's apparent functional silence under bilateral activation may reflect selectivity for high-effort or context-dependent motivational demands rather than a true absence of function. Future studies should employ paradigms that more precisely isolate motivational and consummatory components of reward in females across varied

effort, context, and rewards, also within the ipsilateral versus contralateral and left versus right framework established earlier.

Closing remarks

Collectively, the future directions outlined above are designed to help answer three core questions raised by this dissertation: 1. What is the functional role of the CRH/GABA BLA→NAc projection in female mice, and why does it appear to be organized differently than in males? 2. How does the lateralized structure of this projection contribute to the sex- and ELA-dependent reward behaviors? What are the contributions of CRH and GABA signaling, and which NAc cell populations modulate the projection's effects to produce behavioral change?

Addressing these questions will contribute to a broader understanding of how early-life adversity shapes reward circuitry in a sex-dependent manner and hopefully lead to direct translational relevance to the differential vulnerability to stress-related psychiatric conditions observed across sexes in the human population.

REFERENCES

Allen, H. N., Chaudhry, S., Hong, V. M., Lewter, L. A., Sinha, G. P., Carrasquillo, Y., Taylor, B. K., & Kolber, B. J. (2023). A Parabrachial-to-Amygdala Circuit That Determines Hemispheric Lateralization of Somatosensory Processing. *Biological Psychiatry*, *93*(4), 370–381. https://doi.org/10.1016/j.biopsych.2022.09.010

Allen, L., & Dwivedi, Y. (2020). MicroRNA mediators of early life stress vulnerability to depression and suicidal behavior. *Molecular Psychiatry*, *25*(2), 308–320. https://doi.org/10.1038/s41380-019-0597-8

Ambroggi, F., Ishikawa, A., Fields, H. L., & Nicola, S. M. (2008). Basolateral Amygdala Neurons Facilitate Reward-Seeking Behavior by Exciting Nucleus Accumbens Neurons. *Neuron*, *59*(4), 648–661. https://doi.org/10.1016/j.neuron.2008.07.004

Anda, R. F., Felitti, V. J., Bremner, J. D., Walker, J. D., Whitfield, Ch., Perry, B. D., Dube, Sh. R., & Giles, W. H. (2006). The enduring effects of abuse and related adverse experiences in childhood: A convergence of evidence from neurobiology and epidemiology. *European Archives of Psychiatry and Clinical Neuroscience*, *256*(3), 174–186. https://doi.org/10.1007/s00406-005-0624-4

Arcego, D. M., Buschdorf, J.-P., O'Toole, N., Wang, Z., Barth, B., Pokhvisneva, I., Rayan, N. A., Patel, S., De Mendonça Filho, E. J., Lee, P., Tan, J., Koh, M. X., Sim, C. M., Parent, C., De Lima, R. M. S., Clappison, A., O'Donnell, K. J., Dalmaz, C., Arloth, J., … Meaney, M. J. (2024). A Glucocorticoid-Sensitive Hippocampal Gene Network Moderates the Impact of Early-Life Adversity on Mental Health Outcomes. *Biological Psychiatry*, *95*(1), 48–61. https://doi.org/10.1016/j.biopsych.2023.06.028

Arena, G., Londei, F., Ceccarelli, F., Ferrucci, L., Borra, E., & Genovesio, A. (2024). Disentangling the identity of the zona incerta: A review of the known connections and latest implications. *Ageing Research Reviews*, *93*, 102140. https://doi.org/10.1016/j.arr.2023.102140

Auerbach, R. P., Pisoni, A., Bondy, E., Kumar, P., Stewart, J. G., Yendiki, A., & Pizzagalli, D. A. (2017). Neuroanatomical Prediction of Anhedonia in Adolescents. *Neuropsychopharmacology*, *42*(10), 2087–2095. https://doi.org/10.1038/npp.2017.28

Baldwin, J. R., Caspi, A., Meehan, A. J., Ambler, A., Arseneault, L., Fisher, H. L., Harrington, H., Matthews, T., Odgers, C. L., Poulton, R., Ramrakha, S., Moffitt, T. E., & Danese, A. (2021). Population vs Individual Prediction of Poor Health From Results of Adverse Childhood Experiences Screening. *JAMA Pediatrics*, *175*(4), 385. https://doi.org/10.1001/jamapediatrics.2020.5602

Bale, T. L., & Epperson, C. N. (2015). Sex differences and stress across the lifespan. *Nature Neuroscience*, *18*(10), 1413–1420. https://doi.org/10.1038/nn.4112

Bath, K. G. (2020). Synthesizing Views to Understand Sex Differences in Response to Early Life Adversity. *Trends in Neurosciences*, *43*(5), 300–310. https://doi.org/10.1016/j.tins.2020.02.004

Bath, K. G., Nitenson, A. S., Lichtman, E., Lopez, C., Chen, W., Gallo, M., Goodwill, H., & Manzano-Nieves, G. (2017). Early life stress leads to developmental and sex selective effects on performance in a novel object placement task. *Neurobiology of Stress*, *7*, 57–67. https://doi.org/10.1016/j.ynstr.2017.04.001

Baumgartner, H. M., Schulkin, J., & Berridge, K. C. (2021). Activating Corticotropin-Releasing Factor Systems in the Nucleus Accumbens, Amygdala, and Bed Nucleus of Stria Terminalis: Incentive Motivation or Aversive Motivation? *Biological Psychiatry*, *89*(12), 1162–1175. https://doi.org/10.1016/j.biopsych.2021.01.007

Becker, J. B., & Chartoff, E. (2019). Sex differences in neural mechanisms mediating reward and addiction. *Neuropsychopharmacology*, *44*(1), 166–183. https://doi.org/10.1038/s41386-018-0125-6

Berridge, K. C., & Robinson, T. E. (2016). Liking, wanting, and the incentive-sensitization theory of addiction. *American Psychologist*, *71*(8), 670–679. https://doi.org/10.1037/amp0000059

Beyeler, A., Chang, C.-J., Silvestre, M., Lévêque, C., Namburi, P., Wildes, C. P., & Tye, K. M. (2018). Organization of Valence-Encoding and Projection-Defined Neurons in the Basolateral Amygdala. *Cell Reports*, *22*(4), 905–918. https://doi.org/10.1016/j.celrep.2017.12.097

Birnie, M. T., & Baram, T. Z. (2022). Principles of emotional brain circuit maturation. *Science*, *376*(6597), 1055–1056. https://doi.org/10.1126/science.abn4016

Birnie, M. T., & Baram, T. Z. (2025). The evolving neurobiology of early-life stress. *Neuron*, *113*(10), 1474–1490. https://doi.org/10.1016/j.neuron.2025.02.016

Birnie, M. T., Kooiker, C. L., Short, A. K., Bolton, J. L., Chen, Y., & Baram, T. Z. (2020). Plasticity of the Reward Circuitry After Early-Life Adversity: Mechanisms and Significance. *Biological Psychiatry*, *87*(10), 875–884. https://doi.org/10.1016/j.biopsych.2019.12.018

Birnie, M. T., Short, A. K., De Carvalho, G. B., Taniguchi, L., Gunn, B. G., Pham, A. L., Itoga, C. A., Xu, X., Chen, L. Y., Mahler, S. V., Chen, Y., & Baram, T. Z. (2023). Stress-induced plasticity of a CRH/GABA projection disrupts reward behaviors in mice. *Nature Communications*, *14*(1), 1088. https://doi.org/10.1038/s41467-023-36780-x

Block, C. L., Eroglu, O., Mague, S. D., Smith, C. J., Ceasrine, A. M., Sriworarat, C., Blount, C., Beben, K. A., Malacon, K. E., Ndubuizu, N., Talbot, A., Gallagher, N. M., Chan Jo, Y., Nyangacha, T., Carlson, D. E., Dzirasa, K., Eroglu, C., & Bilbo, S. D. (2022). Prenatal environmental stressors impair postnatal microglia function and adult behavior in males. *Cell Reports*, *40*(5), 111161. https://doi.org/10.1016/j.celrep.2022.111161

Boecker, R., Holz, N. E., Buchmann, A. F., Blomeyer, D., Plichta, M. M., Wolf, I., Baumeister, S., Meyer-Lindenberg, A., Banaschewski, T., Brandeis, D., & Laucht, M. (2014). Impact of Early Life Adversity on Reward Processing in Young Adults: EEG-fMRI Results from a Prospective Study over 25 Years. *PLoS ONE*, *9*(8), e104185. https://doi.org/10.1371/journal.pone.0104185

Bolton, J. L., Molet, J., Regev, L., Chen, Y., Rismanchi, N., Haddad, E., Yang, D. Z., Obenaus, A., & Baram, T. Z. (2018). Anhedonia Following Early-Life Adversity Involves Aberrant Interaction of Reward and Anxiety Circuits and Is Reversed by Partial Silencing of Amygdala Corticotropin-Releasing Hormone Gene. *Biological Psychiatry*, *83*(2), 137–147. https://doi.org/10.1016/j.biopsych.2017.08.023

Bolton, J. L., Schulmann, A., Garcia-Curran, M. M., Regev, L., Chen, Y., Kamei, N., Shao, M., Singh-Taylor, A., Jiang, S., Noam, Y., Molet, J., Mortazavi, A., &

Baram, T. Z. (2020). Unexpected Transcriptional Programs Contribute to Hippocampal Memory Deficits and Neuronal Stunting after Early-Life Adversity. *Cell Reports*, *33*(11), 108511. https://doi.org/10.1016/j.celrep.2020.108511

Bolton, J. L., Short, A. K., Othy, S., Kooiker, C. L., Shao, M., Gunn, B. G., Beck, J., Bai, X., Law, S. M., Savage, J. C., Lambert, J. J., Belelli, D., Tremblay, M.-È., Cahalan, M. D., & Baram, T. Z. (2022). Early stress-induced impaired microglial pruning of excitatory synapses on immature CRH-expressing neurons provokes aberrant adult stress responses. *Cell Reports*, *38*(13), 110600. https://doi.org/10.1016/j.celrep.2022.110600

Brieant, A., Vannucci, A., Nakua, H., Harris, J., Lovell, J., Brundavanam, D., Tottenham, N., & Gee, D. G. (2023). Characterizing the dimensional structure of early-life adversity in the Adolescent Brain Cognitive Development (ABCD) Study. *Developmental Cognitive Neuroscience*, *61*, 101256. https://doi.org/10.1016/j.dcn.2023.101256

Brunson, K. L., Kramár, E., Lin, B., Chen, Y., Colgin, L. L., Yanagihara, T. K., Lynch, G., & Baram, T. Z. (2005). Mechanisms of Late-Onset Cognitive Decline after Early-Life Stress. *The Journal of Neuroscience*, *25*(41), 9328–9338. https://doi.org/10.1523/JNEUROSCI.2281-05.2005

Burke, N. J., Hellman, J. L., Scott, B. G., Weems, C. F., & Carrion, V. G. (2011). The impact of adverse childhood experiences on an urban pediatric population. *Child Abuse & Neglect*, *35*(6), 408–413. https://doi.org/10.1016/j.chiabu.2011.02.006

Burns, S. B., Szyszkowicz, J. K., Luheshi, G. N., Lutz, P.-E., & Turecki, G. (2018). Plasticity of the epigenome during early-life stress. *Seminars in Cell &*

Developmental Biology, *77*, 115–132. https://doi.org/10.1016/j.semcdb.2017.09.033

Callaghan, B. L., & Tottenham, N. (2016). The Neuro-Environmental Loop of Plasticity: A Cross-Species Analysis of Parental Effects on Emotion Circuitry Development Following Typical and Adverse Caregiving. *Neuropsychopharmacology*, *41*(1), 163–176. https://doi.org/10.1038/npp.2015.204

Champagne, D. L., Bagot, R. C., Van Hasselt, F., Ramakers, G., Meaney, M. J., De Kloet, E. R., Joels, M., & Krugers, H. (2008). Maternal Care and Hippocampal Plasticity: Evidence for Experience-Dependent Structural Plasticity, Altered Synaptic Functioning, and Differential Responsiveness to Glucocorticoids and Stress. *Journal of Neuroscience*, *28*(23), 6037–6045. https://doi.org/10.1523/JNEUROSCI.0526-08.2008

Cheetham, S. A., Thom, M. D., Jury, F., Ollier, W. E. R., Beynon, R. J., & Hurst, J. L. (2007). The Genetic Basis of Individual-Recognition Signals in the Mouse. *Current Biology*, *17*(20), 1771–1777. https://doi.org/10.1016/j.cub.2007.10.007

Chen, R., Blosser, T. R., Djekidel, M. N., Hao, J., Bhattacherjee, A., Chen, W., Tuesta, L. M., Zhuang, X., & Zhang, Y. (2021). Decoding molecular and cellular heterogeneity of mouse nucleus accumbens. *Nature Neuroscience*, *24*(12), 1757–1771. https://doi.org/10.1038/s41593-021-00938-x

Chen, Y., & Baram, T. Z. (2016). Toward Understanding How Early-Life Stress Reprograms Cognitive and Emotional Brain Networks. *Neuropsychopharmacology*, *41*(1), 197–206. https://doi.org/10.1038/npp.2015.181

Chen, Y., Brunson, K. L., Müller, M. B., Cariaga, W., & Baram, T. Z. (2000). Immunocytochemical distribution of corticotropin-releasing hormone receptor type-1 (CRF1)-like immunoreactivity in the mouse brain: Light microscopy analysis using an antibody directed against the C-terminus. *The Journal of Comparative Neurology*, *420*(3), 305–323. https://doi.org/10.1002/(SICI)1096-9861(20000508)420:3%3C305::AID-CNE3%3E3.0.CO;2-8

Chen, Y., Molet, J., Gunn, B. G., Ressler, K., & Baram, T. Z. (2015). Diversity of Reporter Expression Patterns in Transgenic Mouse Lines Targeting Corticotropin-Releasing Hormone-Expressing Neurons. *Endocrinology*, *156*(12), 4769–4780. https://doi.org/10.1210/en.2015-1673

Chen, Y., Molet, J., Lauterborn, J. C., Trieu, B. H., Bolton, J. L., Patterson, K. P., Gall, C. M., Lynch, G., & Baram, T. Z. (2016). Converging, Synergistic Actions of Multiple Stress Hormones Mediate Enduring Memory Impairments after Acute Simultaneous Stresses. *The Journal of Neuroscience*, *36*(44), 11295–11307. https://doi.org/10.1523/JNEUROSCI.2542-16.2016

Cheng, H. Y., Fournier, D. I., & Todd, T. P. (2024). Retrosplenial cortex and aversive conditioning. *Frontiers in Behavioral Neuroscience*, *18*, 1341705. https://doi.org/10.3389/fnbeh.2024.1341705

Chi, J., Crane, A., Wu, Z., & Cohen, P. (2018). Adipo-Clear: A Tissue Clearing Method for Three-Dimensional Imaging of Adipose Tissue. *Journal of Visualized Experiments*, (137), 58271. https://doi.org/10.3791/58271

Chrousos, G. P., Torpy, D. J., & Gold, P. W. (1998). Interactions between the Hypothalamic-Pituitary-Adrenal Axis and the Female Reproductive System:

Clinical Implications. *Annals of Internal Medicine*, *129*(3), 229–240. https://doi.org/10.7326/0003-4819-129-3-199808010-00012

Cohen, N. J., Lojkasek, M., Zadeh, Z. Y., Pugliese, M., & Kiefer, H. (2008). Children adopted from China: A prospective study of their growth and development. *Journal of Child Psychology and Psychiatry*, *49*(4), 458–468. https://doi.org/10.1111/j.1469-7610.2007.01853.x

Colman, I., Garad, Y., Zeng, Y., Naicker, K., Weeks, M., Patten, S. B., Jones, P. B., Thompson, A. H., & Wild, T. C. (2013). Stress and development of depression and heavy drinking in adulthood: Moderating effects of childhood trauma. *Social Psychiatry and Psychiatric Epidemiology*, *48*(2), 265–274. https://doi.org/10.1007/s00127-012-0531-8

Corral-Frías, N. S., Nikolova, Y. S., Michalski, L. J., Baranger, D. A. A., Hariri, A. R., & Bogdan, R. (2015). Stress-related anhedonia is associated with ventral striatum reactivity to reward and transdiagnostic psychiatric symptomatology. *Psychological Medicine*, *45*(12), 2605–2617. https://doi.org/10.1017/S0033291715000525

Crits-Christoph, P., Wadden, S., Gaines, A., Rieger, A., Gallop, R., McKay, J. R., & Gibbons, M. B. C. (2018). Symptoms of anhedonia, not depression, predict the outcome of treatment of cocaine dependence. *Journal of Substance Abuse Treatment*, *92*, 46–50. https://doi.org/10.1016/j.jsat.2018.06.010

Davis, E. P., Korja, R., Karlsson, L., Glynn, L. M., Sandman, C. A., Vegetabile, B., Kataja, E.-L., Nolvi, S., Sinervä, E., Pelto, J., Karlsson, H., Stern, H. S., & Baram, T. Z. (2019). Across continents and demographics, unpredictable maternal

signals are associated with children's cognitive function. *eBioMedicine*, *46*, 256–263. https://doi.org/10.1016/j.ebiom.2019.07.025

Davis, E. P., Leonard, B. T., Jirsaraie, R. J., Keator, D. B., Small, S. L., Sandman, C. A., Risbrough, V. B., Stern, H. S., Glynn, L. M., Yassa, M. A., Baram, T. Z., & Rasmussen, J. M. (2025). Sex-Specific Effects of Early-Life Unpredictability on Hippocampal and Amygdala Responses to Novelty in Adolescents. *Biological Psychiatry Global Open Science*, *5*(6), 100561. https://doi.org/10.1016/j.bpsgos.2025.100561

Davis, E. P., Stout, S. A., Molet, J., Vegetabile, B., Glynn, L. M., Sandman, C. A., Heins, K., Stern, H., & Baram, T. Z. (2017). Exposure to unpredictable maternal sensory signals influences cognitive development across species. *Proceedings of the National Academy of Sciences*, *114*(39), 10390–10395. https://doi.org/10.1073/pnas.1703444114

Daviu, N., Füzesi, T., Rosenegger, D. G., Rasiah, N. P., Sterley, T.-L., Peringod, G., & Bains, J. S. (2020). Paraventricular nucleus CRH neurons encode stress controllability and regulate defensive behavior selection. *Nature Neuroscience*, *23*(3), 398–410. https://doi.org/10.1038/s41593-020-0591-0

De Guglielmo, G., Kallupi, M., Pomrenze, M. B., Crawford, E., Simpson, S., Schweitzer, P., Koob, G. F., Messing, R. O., & George, O. (2019). Inactivation of a CRF-dependent amygdalofugal pathway reverses addiction-like behaviors in alcohol-dependent rats. *Nature Communications*, *10*(1), 1238. https://doi.org/10.1038/s41467-019-09183-0

De Franceschi, G., Vivattanasarn, T., Saleem, A. B., & Solomon, S. G. (2016). Vision Guides Selection of Freeze or Flight Defense Strategies in Mice. *Current Biology*, *26*(16), 2150–2154. https://doi.org/10.1016/j.cub.2016.06.006

Demaestri, C., Gallo, M., Mazenod, E., Hong, A. T., Arora, H., Short, A. K., Stern, H., Baram, T. Z., & Bath, K. G. (2022). Resource scarcity but not maternal separation provokes unpredictable maternal care sequences in mice and both upregulate Crh-associated gene expression in the amygdala. *Neurobiology of Stress*, *20*, 100484. https://doi.org/10.1016/j.ynstr.2022.100484

Dennison, M. J., Rosen, M. L., Sambrook, K. A., Jenness, J. L., Sheridan, M. A., & McLaughlin, K. A. (2019). Differential Associations of Distinct Forms of Childhood Adversity With Neurobehavioral Measures of Reward Processing: A Developmental Pathway to Depression. *Child Development*, *90*(1), e96–e113. https://doi.org/10.1111/cdev.13011

Dubé, C. M., Molet, J., Singh-Taylor, A., Ivy, A., Maras, P. M., & Baram, T. Z. (2015). Hyper-excitability and epilepsy generated by chronic early-life stress. *Neurobiology of Stress*, *2*, 10–19. https://doi.org/10.1016/j.ynstr.2015.03.001

Dube, S. R., Felitti, V. J., Dong, M., Chapman, D. P., Giles, W. H., & Anda, R. F. (2003). Childhood Abuse, Neglect, and Household Dysfunction and the Risk of Illicit Drug Use: The Adverse Childhood Experiences Study. *Pediatrics*, *111*(3), 564–572. https://doi.org/10.1542/peds.111.3.564

Ducasse, D., Loas, G., Dassa, D., Gramaglia, C., Zeppegno, P., Guillaume, S., Olié, E., & Courtet, P. (2018). Anhedonia is associated with suicidal ideation

independently of depression: A meta-analysis. *Depression and Anxiety*, *35*(5), 382–392. https://doi.org/10.1002/da.22709

East, B. S., Fleming, G., Vervoordt, S., Shah, P., Sullivan, R. M., & Wilson, D. A. (2021). Basolateral amygdala to posterior piriform cortex connectivity ensures precision in learned odor threat. *Scientific Reports*, *11*(1), 21746. https://doi.org/10.1038/s41598-021-01320-4

Evans, E. A., Grella, C. E., & Upchurch, D. M. (2017). Gender differences in the effects of childhood adversity on alcohol, drug, and polysubstance-related disorders. *Social Psychiatry and Psychiatric Epidemiology*, *52*(7), 901–912. https://doi.org/10.1007/s00127-017-1355-3

Fenoglio, K., Brunson, K., & Baram, T. (2006). Hippocampal neuroplasticity induced by early-life stress: Functional and molecular aspects. *Frontiers in Neuroendocrinology*, *27*(2), 180–192. https://doi.org/10.1016/j.yfrne.2006.02.001

Floresco, S. B. (2015). The Nucleus Accumbens: An Interface Between Cognition, Emotion, and Action. *Annual Review of Psychology*, *66*(1), 25–52. https://doi.org/10.1146/annurev-psych-010213-115159

Francés, R., Rabah, Y., Preat, T., & Plaçais, P.-Y. (2024). Diverting glial glycolytic flux towards neurons is a memory-relevant role of Drosophila CRH-like signalling. *Nature Communications*, *15*(1), 10467. https://doi.org/10.1038/s41467-024-54778-x

Francis, T. C., & Lobo, M. K. (2017). Emerging Role for Nucleus Accumbens Medium Spiny Neuron Subtypes in Depression. *Biological Psychiatry*, *81*(8), 645–653. https://doi.org/10.1016/j.biopsych.2016.09.007

Friedmann, D., Pun, A., Adams, E. L., Lui, J. H., Kebschull, J. M., Grutzner, S. M., Castagnola, C., Tessier-Lavigne, M., & Luo, L. (2020). Mapping mesoscale axonal projections in the mouse brain using a 3D convolutional network. *Proceedings of the National Academy of Sciences*, *117*(20), 11068–11075. https://doi.org/10.1073/pnas.1918465117

Garvin, M. M., & Bolton, J. L. (2022). Sex-specific behavioral outcomes of early-life adversity and emerging microglia-dependent mechanisms. *Frontiers in Behavioral Neuroscience*, *16*, 1013865. https://doi.org/10.3389/fnbeh.2022.1013865

Ge, J., Ren, P., Tian, B., Li, J., Qi, C., Huang, Q., Ren, K., Hu, E., Mao, H., Zang, Y., Wu, S., Xue, Q., & Wang, W. (2024). Ventral zona incerta parvalbumin neurons modulate sensory-induced and stress-induced self-grooming via input-dependent mechanisms in mice. *iScience*, *27*(7), 110165. https://doi.org/10.1016/j.isci.2024.110165

Gee, D. G., Gabard-Durnam, L. J., Flannery, J., Goff, B., Humphreys, K. L., Telzer, E. H., Hare, T. A., Bookheimer, S. Y., & Tottenham, N. (2013). Early developmental emergence of human amygdala–prefrontal connectivity after maternal deprivation. *Proceedings of the National Academy of Sciences*, *110*(39), 15638–15643. https://doi.org/10.1073/pnas.1307893110

Gelernter, J., Polimanti, R., Pietrzak, R., Levey, D. F., Bryois, J., Lu, Q., Hu, Y., Li, B., Radhakrishnan, K., Aslan, M., Cheung, K.-H., Li, Y., Rajeevan, N., Sayward, F., Harrington, K., Chen, Q., Cho, K., Pyarajan, S., Sullivan, P. F., … Stein, M. B. (2019). Genome-wide association study of post-traumatic stress disorder

reexperiencing symptoms in >165,000 US veterans. *Nature Neuroscience*, *22*(9), 1394–1401. https://doi.org/10.1038/s41593-019-0447-7

Gildawie, K. R., Wang, K., Budge, K. E., & Byrnes, E. M. (2024). Effects of Maternal Separation on Effort-based Responding for Sucrose Are Associated with c-Fos Expression in the Nucleus Accumbens Core. *Neuroscience*, *537*, 174–188. https://doi.org/10.1016/j.neuroscience.2023.11.030

Glynn, L. M., & Baram, T. Z. (2019). The influence of unpredictable, fragmented parental signals on the developing brain. *Frontiers in Neuroendocrinology*, *53*, 100736. https://doi.org/10.1016/j.yfrne.2019.01.002

Glynn, L. M., Liu, S. R., Golden, C., Weiss, M., Taylor Lucas, C., Cooper, D. M., Ehwerhemuepha, L., Stern, H. S., & Baram, T. Z. (2026). Unpredictability is a childhood adversity that contributes to mental health problems. *Nature Mental Health*, *4*(8), 1219–1226. https://doi.org/10.1038/s44220-026-00681-x

Gongwer, M. W., Klune, C. B., Couto, J., Jin, B., Enos, A. S., Chen, R., Friedmann, D., & DeNardo, L. A. (2023). Brain-Wide Projections and Differential Encoding of Prefrontal Neuronal Classes Underlying Learned and Innate Threat Avoidance. *The Journal of Neuroscience*, *43*(32), 5810–5830. https://doi.org/10.1523/JNEUROSCI.0697-23.2023

Granger, S. J., Glynn, L. M., Sandman, C. A., Small, S. L., Obenaus, A., Keator, D. B., Baram, T. Z., Stern, H., Yassa, M. A., & Davis, E. P. (2021). Aberrant Maturation of the Uncinate Fasciculus Follows Exposure to Unpredictable Patterns of Maternal Signals. *The Journal of Neuroscience*, *41*(6), 1242–1250. https://doi.org/10.1523/JNEUROSCI.0374-20.2020

Green, J. G., McLaughlin, K. A., Berglund, P. A., Gruber, M. J., Sampson, N. A., Zaslavsky, A. M., & Kessler, R. C. (2010). Childhood Adversities and Adult Psychiatric Disorders in the National Comorbidity Survey Replication I: Associations With First Onset of *DSM-IV* Disorders. *Archives of General Psychiatry*, *67*(2), 113. https://doi.org/10.1001/archgenpsychiatry.2009.186

Greiner, E. M., & Petrovich, G. D. (2020). The effects of novelty on food consumption in male and female rats. *Physiology & Behavior*, *223*, 112970. https://doi.org/10.1016/j.physbeh.2020.112970

Griffith, E. C., West, A. E., & Greenberg, M. E. (2024). Neuronal enhancers fine-tune adaptive circuit plasticity. *Neuron*, *112*(18), 3043–3057. https://doi.org/10.1016/j.neuron.2024.08.002

Gunn, B. G., Cox, C. D., Chen, Y., Frotscher, M., Gall, C. M., Baram, T. Z., & Lynch, G. (2017). The Endogenous Stress Hormone CRH Modulates Excitatory Transmission and Network Physiology in Hippocampus. *Cerebral Cortex*, *27*(8), 4182–4198. https://doi.org/10.1093/cercor/bhx103

Gunn, B. G., Sanchez, G. A., Lynch, G., Baram, T. Z., & Chen, Y. (2019). Hyper-diversity of CRH interneurons in mouse hippocampus. *Brain Structure and Function*, *224*(2), 583–598. https://doi.org/10.1007/s00429-018-1793-z

Gupta, P., Galimberti, M., Liu, Y., Beck, S., Wingo, A., Wingo, T., Adhikari, K., Kranzler, H. R., VA Million Veteran Program, Stein, M. B., Gelernter, J., & Levey, D. F. (2024). A genome-wide investigation into the underlying genetic architecture of personality traits and overlap with psychopathology. *Nature Human Behaviour*, *8*(11), 2235–2249. https://doi.org/10.1038/s41562-024-01951-3

Hahn, J., Hopf, F. W., & Bonci, A. (2009). Chronic Cocaine Enhances Corticotropin-Releasing Factor-Dependent Potentiation of Excitatory Transmission in Ventral Tegmental Area Dopamine Neurons. *The Journal of Neuroscience*, *29*(20), 6535–6544. https://doi.org/10.1523/JNEUROSCI.4773-08.2009

Hailes, H. P., Yu, R., Danese, A., & Fazel, S. (2019). Long-term outcomes of childhood sexual abuse: An umbrella review. *The Lancet Psychiatry*, *6*(10), 830–839. https://doi.org/10.1016/S2215-0366(19)30286-X

Han, W., Tellez, L. A., Perkins, M. H., Perez, I. O., Qu, T., Ferreira, J., Ferreira, T. L., Quinn, D., Liu, Z.-W., Gao, X.-B., Kaelberer, M. M., Bohórquez, D. V., Shammah-Lagnado, S. J., De Lartigue, G., & De Araujo, I. E. (2018). A Neural Circuit for Gut-Induced Reward. *Cell*, *175*(3), 665-678.e23. https://doi.org/10.1016/j.cell.2018.08.049

Hardy, K. A., Hart, D. M., & Rosen, M. J. (2023). Early-life stress affects Mongolian gerbil interactions with conspecific vocalizations in a sex-specific manner. *Frontiers in Behavioral Neuroscience*, *17*, 1128586. https://doi.org/10.3389/fnbeh.2023.1128586

Harrold, A., Keating, K., Larkin, F., & Setti, A. (2024). The association between sensory processing and stress in the adult population: A systematic review. *Applied Psychology: Health and Well-Being*, *16*(4), 2536–2566. https://doi.org/10.1111/aphw.12554

Hartley, N. D., Gaulden, A. D., Báldi, R., Winters, N. D., Salimando, G. J., Rosas-Vidal, L. E., Jameson, A., Winder, D. G., & Patel, S. (2019). Dynamic remodeling of a

basolateral-to-central amygdala glutamatergic circuit across fear states. *Nature Neuroscience*, *22*(12), 2000–2012. https://doi.org/10.1038/s41593-019-0528-7

Heshmati, M., & Russo, S. J. (2015). Anhedonia and the Brain Reward Circuitry in Depression. *Current Behavioral Neuroscience Reports*, *2*(3), 146–153. https://doi.org/10.1007/s40473-015-0044-3

Hintiryan, H., Bowman, I., Johnson, D. L., Korobkova, L., Zhu, M., Khanjani, N., Gou, L., Gao, L., Yamashita, S., Bienkowski, M. S., Garcia, L., Foster, N. N., Benavidez, N. L., Song, M. Y., Lo, D., Cotter, K. R., Becerra, M., Aquino, S., Cao, C., … Dong, H.-W. (2021). Connectivity characterization of the mouse basolateral amygdalar complex. *Nature Communications*, *12*(1), 2859. https://doi.org/10.1038/s41467-021-22915-5

Hodes, G. E., & Epperson, C. N. (2019). Sex Differences in Vulnerability and Resilience to Stress Across the Life Span. *Biological Psychiatry*, *86*(6), 421–432. https://doi.org/10.1016/j.biopsych.2019.04.028

Honeycutt, J. A., Demaestri, C., Peterzell, S., Silveri, M. M., Cai, X., Kulkarni, P., Cunningham, M. G., Ferris, C. F., & Brenhouse, H. C. (2020). Altered corticolimbic connectivity reveals sex-specific adolescent outcomes in a rat model of early life adversity. *eLife*, *9*, e52651. https://doi.org/10.7554/eLife.52651

Hughes, K., Bellis, M. A., Hardcastle, K. A., Sethi, D., Butchart, A., Mikton, C., Jones, L., & Dunne, M. P. (2017). The effect of multiple adverse childhood experiences on health: A systematic review and meta-analysis. *The Lancet Public Health*, *2*(8), e356–e366. https://doi.org/10.1016/S2468-2667(17)30118-4

Huot, R. L., Plotsky, P. M., Lenox, R. H., & McNamara, R. K. (2002). Neonatal maternal separation reduces hippocampal mossy fiber density in adult Long Evans rats. *Brain Research*, *950*(1–2), 52–63. https://doi.org/10.1016/S0006-8993(02)02985-2

Hupalo, S., Bryce, C. A., Bangasser, D. A., Berridge, C. W., Valentino, R. J., & Floresco, S. B. (2019). Corticotropin-Releasing Factor (CRF) circuit modulation of cognition and motivation. *Neuroscience & Biobehavioral Reviews*, *103*, 50–59. https://doi.org/10.1016/j.neubiorev.2019.06.010

Hurley, M. M., Robble, M. R., Callan, G., Choi, S., & Wheeler, R. A. (2019). Pituitary adenylate cyclase-activating polypeptide (PACAP) acts in the nucleus accumbens to reduce hedonic drive. *International Journal of Obesity*, *43*(4), 928–932. https://doi.org/10.1038/s41366-018-0154-6

Issler, O., Van Der Zee, Y. Y., Ramakrishnan, A., Wang, J., Tan, C., Loh, Y.-H. E., Purushothaman, I., Walker, D. M., Lorsch, Z. S., Hamilton, P. J., Peña, C. J., Flaherty, E., Hartley, B. J., Torres-Berrío, A., Parise, E. M., Kronman, H., Duffy, J. E., Estill, M. S., Calipari, E. S., … Nestler, E. J. (2020). Sex-Specific Role for the Long Non-coding RNA LINC00473 in Depression. *Neuron*, *106*(6), 912-926.e5. https://doi.org/10.1016/j.neuron.2020.03.023

Itoga, C. A., Chen, Y., Fateri, C., Echeverry, P. A., Lai, J. M., Delgado, J., Badhon, S., Short, A., Baram, T. Z., & Xu, X. (2019). New viral-genetic mapping uncovers an enrichment of corticotropin-releasing hormone-expressing neuronal inputs to the nucleus accumbens from stress-related brain regions. *Journal of Comparative Neurology*, *527*(15), 2474–2487. https://doi.org/10.1002/cne.24676

Ivy, A. S., Brunson, K. L., Sandman, C., & Baram, T. Z. (2008). Dysfunctional nurturing behavior in rat dams with limited access to nesting material: A clinically relevant model for early-life stress. *Neuroscience*, *154*(3), 1132–1142. https://doi.org/10.1016/j.neuroscience.2008.04.019

Ivy, A. S., Rex, C. S., Chen, Y., Dubé, C., Maras, P. M., Grigoriadis, D. E., Gall, C. M., Lynch, G., & Baram, T. Z. (2010). Hippocampal Dysfunction and Cognitive Impairments Provoked by Chronic Early-Life Stress Involve Excessive Activation of CRH Receptors. *The Journal of Neuroscience*, *30*(39), 13005–13015. https://doi.org/10.1523/JNEUROSCI.1784-10.2010

Jo, Y. S., Namboodiri, V. M. K., Stuber, G. D., & Zweifel, L. S. (2020). Persistent activation of central amygdala CRF neurons helps drive the immediate fear extinction deficit. *Nature Communications*, *11*(1), 422. https://doi.org/10.1038/s41467-020-14393-y

Joëls, M., & Baram, T. Z. (2009). The neuro-symphony of stress. *Nature Reviews Neuroscience*, *10*(6), 459–466. https://doi.org/10.1038/nrn2632

Johnson, E. C., Shafer, O. T., Trigg, J. S., Park, J., Schooley, D. A., Dow, J. A., & Taghert, P. H. (2005). A novel diuretic hormone receptor in *Drosophila*: Evidence for conservation of CGRP signaling. *Journal of Experimental Biology*, *208*(7), 1239–1246. https://doi.org/10.1242/jeb.01529

Johnson, J. G., Cohen, P., Kasen, S., & Brook, J. S. (2002). Childhood Adversities Associated With Risk for Eating Disorders or Weight Problems During Adolescence or Early Adulthood. *American Journal of Psychiatry*, *159*(3), 394–400. https://doi.org/10.1176/appi.ajp.159.3.394

Kangas, B. D., Short, A. K., Luc, O. T., Stern, H. S., Baram, T. Z., & Pizzagalli, D. A. (2022). A cross-species assay demonstrates that reward responsiveness is enduringly impacted by adverse, unpredictable early-life experiences. *Neuropsychopharmacology*, *47*(3), 767–775. https://doi.org/10.1038/s41386-021-01250-9

Klein, S., Staring, M., Murphy, K., Viergever, M. A., & Pluim, J. (2010). elastix: A Toolbox for Intensity-Based Medical Image Registration. *IEEE Transactions on Medical Imaging*, *29*(1), 196–205. https://doi.org/10.1109/TMI.2009.2035616

Kolber, B. J., Neugebauer, V., Thorn, C. A., Froemke, R., & Bakalkin, G. (2026). Neuropeptides in control of left–right neural circuits. *Trends in Neurosciences*, *49*(2), 125–140. https://doi.org/10.1016/j.tins.2025.12.003

Koob, G. F., & Le Moal, M. (2005). Plasticity of reward neurocircuitry and the “dark side” of drug addiction. *Nature Neuroscience*, *8*(11), 1442–1444. https://doi.org/10.1038/nn1105-1442

Korosi, A., Shanabrough, M., McClelland, S., Liu, Z.-W., Borok, E., Gao, X.-B., Horvath, T. L., & Baram, T. Z. (2010). Early-Life Experience Reduces Excitation to Stress-Responsive Hypothalamic Neurons and Reprograms the Expression of Corticotropin-Releasing Hormone. *The Journal of Neuroscience*, *30*(2), 703–713. https://doi.org/10.1523/JNEUROSCI.4214-09.2010

Kundakovic, M., & Tickerhoof, M. (2024). Epigenetic mechanisms underlying sex differences in the brain and behavior. *Trends in Neurosciences*, *47*(1), 18–35. https://doi.org/10.1016/j.tins.2023.09.007

Kupchik, Y. M., Brown, R. M., Heinsbroek, J. A., Lobo, M. K., Schwartz, D. J., & Kalivas, P. W. (2015). Coding the direct/indirect pathways by D1 and D2 receptors is not valid for accumbens projections. *Nature Neuroscience*, *18*(9), 1230–1232. https://doi.org/10.1038/nn.4068

Lansbury, E. L., Vana, V., Lund, M. L., Ludwig, M. Q., Mamedova, E., Gautron, L., Arnold, M., Egerod, K. L., Kuhre, R. E., Holst, J. J., Rekling, J., Schwartz, T. W., Pankratova, S., & Dmytriyeva, O. (2025). Neurons Co-Expressing GLP-1, CCK, and PYY Receptors Particularly in Right Nodose Ganglion and Innervating Entire GI Tract in Mice. *International Journal of Molecular Sciences*, *26*(5), 2053. https://doi.org/10.3390/ijms26052053

Lemos, J. C., & Alvarez, V. A. (2020). The upside of stress: A mechanism for the positive motivational role of corticotropin releasing factor. *Neuropsychopharmacology*, *45*(1), 219–220. https://doi.org/10.1038/s41386-019-0510-9

Lemos, J. C., Shin, J. H., & Alvarez, V. A. (2019). Striatal Cholinergic Interneurons Are a Novel Target of Corticotropin Releasing Factor. *The Journal of Neuroscience*, *39*(29), 5647–5661. https://doi.org/10.1523/JNEUROSCI.0479-19.2019

Lemos, J. C., Wanat, M. J., Smith, J. S., Reyes, B. A. S., Hollon, N. G., Van Bockstaele, E. J., Chavkin, C., & Phillips, P. E. M. (2012). Severe stress switches CRF action in the nucleus accumbens from appetitive to aversive. *Nature*, *490*(7420), 402–406. https://doi.org/10.1038/nature11436

LeMoult, J., Humphreys, K. L., Tracy, A., Hoffmeister, J.-A., Ip, E., & Gotlib, I. H. (2020). Meta-analysis: Exposure to Early Life Stress and Risk for Depression in

Childhood and Adolescence. *Journal of the American Academy of Child & Adolescent Psychiatry*, *59*(7), 842–855. https://doi.org/10.1016/j.jaac.2019.10.011

Lenz, K. M., Nugent, B. M., Haliyur, R., & McCarthy, M. M. (2013). Microglia Are Essential to Masculinization of Brain and Behavior. *The Journal of Neuroscience*, *33*(7), 2761–2772. https://doi.org/10.1523/JNEUROSCI.1268-12.2013

Letzkus, J. J., Wolff, S. B. E., Meyer, E. M. M., Tovote, P., Courtin, J., Herry, C., & Lüthi, A. (2011). A disinhibitory microcircuit for associative fear learning in the auditory cortex. *Nature*, *480*(7377), 331–335. https://doi.org/10.1038/nature10674

Leung, B. K., & Balleine, B. W. (2015). Ventral Pallidal Projections to Mediodorsal Thalamus and Ventral Tegmental Area Play Distinct Roles in Outcome-Specific Pavlovian-Instrumental Transfer. *The Journal of Neuroscience*, *35*(12), 4953–4964. https://doi.org/10.1523/JNEUROSCI.4837-14.2015

Levis, S. C., Bentzley, B. S., Molet, J., Bolton, J. L., Perrone, C. R., Baram, T. Z., & Mahler, S. V. (2021). On the early life origins of vulnerability to opioid addiction. *Molecular Psychiatry*, *26*(8), 4409–4416. https://doi.org/10.1038/s41380-019-0628-5

Levis, S. C., Birnie, M. T., Bolton, J. L., Perrone, C. R., Montesinos, J. S., Baram, T. Z., & Mahler, S. V. (2022). Enduring disruption of reward and stress circuit activities by early-life adversity in male rats. *Translational Psychiatry*, *12*(1), 251. https://doi.org/10.1038/s41398-022-01988-w

Lichtenberg, N. T., & Wassum, K. M. (2017). Amygdala mu-opioid receptors mediate the motivating influence of cue-triggered reward expectations. *European Journal of Neuroscience*, *45*(3), 381–387. https://doi.org/10.1111/ejn.13477

Liss, M., Timmel, L., Baxley, K., & Killingsworth, P. (2005). Sensory processing sensitivity and its relation to parental bonding, anxiety, and depression. *Personality and Individual Differences*, *39*(8), 1429–1439. https://doi.org/10.1016/j.paid.2005.05.007

Liu, S. R., Kia-Keating, M., & Nylund-Gibson, K. (2018). Patterns of adversity and pathways to health among White, Black, and Latinx youth. *Child Abuse & Neglect*, *86*, 89–99. https://doi.org/10.1016/j.chiabu.2018.09.007

Luby, J. L., Baram, T. Z., Rogers, C. E., & Barch, D. M. (2020). Neurodevelopmental Optimization after Early-Life Adversity: Cross-Species Studies to Elucidate Sensitive Periods and Brain Mechanisms to Inform Early Intervention. *Trends in Neurosciences*, *43*(10), 744–751. https://doi.org/10.1016/j.tins.2020.08.001

Lüthi, A., & Lüscher, C. (2014). Pathological circuit function underlying addiction and anxiety disorders. *Nature Neuroscience*, *17*(12), 1635–1643. https://doi.org/10.1038/nn.3849

Maccari, S., Krugers, H. J., Morley-Fletcher, S., Szyf, M., & Brunton, P. J. (2014). The Consequences of Early-Life Adversity: Neurobiological, Behavioural and Epigenetic Adaptations. *Journal of Neuroendocrinology*, *26*(10), 707–723. https://doi.org/10.1111/jne.12175

Machado, T. D., Dalle Molle, R., Laureano, D. P., Portella, A. K., Werlang, I. C. R., Benetti, C. D. S., Noschang, C., & Silveira, P. P. (2013). Early life stress is

associated with anxiety, increased stress responsivity and preference for “comfort foods” in adult female rats. *Stress*, *16*(5), 549–556. https://doi.org/10.3109/10253890.2013.816841

Maddern, X. J., Pearl, A. J., Tan, Q. T., Dempsey, H., Ursich, L. T., Huckstep, K. L., Richards, B. K., Anversa, R. G., Lawrence, A. J., Campbell, E. J., Brown, R. M., & Walker, L. C. (2026). Sex differences in neural circuits driving binge-like drinking: A female-specific role for an amygdalo-striatal pathway. *Neuropsychopharmacology*. https://doi.org/10.1038/s41386-026-02513-z

Mahler, S. V., Brodnik, Z. D., Cox, B. M., Buchta, W. C., Bentzley, B. S., Quintanilla, J., Cope, Z. A., Lin, E. C., Riedy, M. D., Scofield, M. D., Messinger, J., Ruiz, C. M., Riegel, A. C., España, R. A., & Aston-Jones, G. (2019). Chemogenetic Manipulations of Ventral Tegmental Area Dopamine Neurons Reveal Multifaceted Roles in Cocaine Abuse. *The Journal of Neuroscience*, *39*(3), 503–518. https://doi.org/10.1523/JNEUROSCI.0537-18.2018

Mahler, S. V., Vazey, E. M., Beckley, J. T., Keistler, C. R., McGlinchey, E. M., Kaufling, J., Wilson, S. P., Deisseroth, K., Woodward, J. J., & Aston-Jones, G. (2014). Designer receptors show role for ventral pallidum input to ventral tegmental area in cocaine seeking. *Nature Neuroscience*, *17*(4), 577–585. https://doi.org/10.1038/nn.3664

Malter Cohen, M., Jing, D., Yang, R. R., Tottenham, N., Lee, F. S., & Casey, B. J. (2013). Early-life stress has persistent effects on amygdala function and development in mice and humans. *Proceedings of the National Academy of Sciences*, *110*(45), 18274–18278. https://doi.org/10.1073/pnas.1310163110

Marlin, B. J., Mitre, M., D'amour, J. A., Chao, M. V., & Froemke, R. C. (2015). Oxytocin enables maternal behaviour by balancing cortical inhibition. *Nature*, *520*(7548), 499–504. https://doi.org/10.1038/nature14402

Matikainen-Ankney, B. A., Earnest, T., Ali, M., Casey, E., Wang, J. G., Sutton, A. K., Legaria, A. A., Barclay, K. M., Murdaugh, L. B., Norris, M. R., Chang, Y.-H., Nguyen, K. P., Lin, E., Reichenbach, A., Clarke, R. E., Stark, R., Conway, S. M., Carvalho, F., Al-Hasani, R., … Kravitz, A. V. (2021). An open-source device for measuring food intake and operant behavior in rodent home-cages. *eLife*, *10*, e66173. https://doi.org/10.7554/eLife.66173

Mazi, A. R., Karakoc, Y., Demirtas, C., Aykin, U., & Yildirim, M. (2025). Extracellular Matrix Alterations Due to Early-Life Adversity: Implications for Auditory Learning in Male Sprague–Dawley Rats. *Molecular Neurobiology*, *62*(5), 6490–6502. https://doi.org/10.1007/s12035-025-04690-2

McCarthy, M. M., Arnold, A. P., Ball, G. F., Blaustein, J. D., & De Vries, G. J. (2012). Sex Differences in the Brain: The Not So Inconvenient Truth. *The Journal of Neuroscience*, *32*(7), 2241–2247. https://doi.org/10.1523/JNEUROSCI.5372-11.2012

McCullough, K. M., Chatzinakos, C., Hartmann, J., Missig, G., Neve, R. L., Fenster, R. J., Carlezon, W. A., Daskalakis, N. P., & Ressler, K. J. (2020). Genome-wide translational profiling of amygdala Crh-expressing neurons reveals role for CREB in fear extinction learning. *Nature Communications*, *11*(1), 5180. https://doi.org/10.1038/s41467-020-18985-6

McEwen, B. S. (1998). Stress, Adaptation, and Disease: Allostasis and Allostatic Load. *Annals of the New York Academy of Sciences*, *840*(1), 33–44. https://doi.org/10.1111/j.1749-6632.1998.tb09546.x

McEwen, B. S., & Stellar, E. (1993). Stress and the Individual: Mechanisms Leading to Disease. *Archives of Internal Medicine*, *153*(18), 2093. https://doi.org/10.1001/archinte.1993.00410180039004

McKay, M. T., Kilmartin, L., Meagher, A., Cannon, M., Healy, C., & Clarke, M. C. (2022). A revised and extended systematic review and meta-analysis of the relationship between childhood adversity and adult psychiatric disorder. *Journal of Psychiatric Research*, *156*, 268–283. https://doi.org/10.1016/j.jpsychires.2022.10.015

Mehta, M. A., Gore-Langton, E., Golembo, N., Colvert, E., Williams, S. C. R., & Sonuga-Barke, E. (2010). Hyporesponsive Reward Anticipation in the Basal Ganglia following Severe Institutional Deprivation Early in Life. *Journal of Cognitive Neuroscience*, *22*(10), 2316–2325. https://doi.org/10.1162/jocn.2009.21394

Merrick, M. T., Ford, D. C., Ports, K. A., & Guinn, A. S. (2018). Prevalence of Adverse Childhood Experiences From the 2011-2014 Behavioral Risk Factor Surveillance System in 23 States. *JAMA Pediatrics*, *172*(11), 1038. https://doi.org/10.1001/jamapediatrics.2018.2537

Millan, M. A., Jacobowitz, D. M., Hauger, R. L., Catt, K. J., & Aguilera, G. (1986). Distribution of corticotropin-releasing factor receptors in primate brain. *Proceedings of the National Academy of Sciences*, *83*(6), 1921–1925. https://doi.org/10.1073/pnas.83.6.1921

Miller, C. H., Reichard, T. M., Yang, J., Carlson-Clarke, B., Vogt, C. C., Warden, M. R., & Sheehan, M. J. (2025). *Pregnancy Modulates Responses to Male Odors in House Mice*. SSRN. https://doi.org/10.2139/ssrn.5177383

Mitre, M., Marlin, B. J., Schiavo, J. K., Morina, E., Norden, S. E., Hackett, T. A., Aoki, C. J., Chao, M. V., & Froemke, R. C. (2016). A Distributed Network for Social Cognition Enriched for Oxytocin Receptors. *The Journal of Neuroscience*, *36*(8), 2517–2535. https://doi.org/10.1523/JNEUROSCI.2409-15.2016

Molet, J., Heins, K., Zhuo, X., Mei, Y. T., Regev, L., Baram, T. Z., & Stern, H. (2016). Fragmentation and high entropy of neonatal experience predict adolescent emotional outcome. *Translational Psychiatry*, *6*(1), e702–e702. https://doi.org/10.1038/tp.2015.200

Molet, J., Maras, P. M., Avishai-Eliner, S., & Baram, T. Z. (2014). Naturalistic rodent models of chronic early-life stress. *Developmental Psychobiology*, *56*(8), 1675–1688. https://doi.org/10.1002/dev.21230

Molet, J., Maras, P. M., Kinney-Lang, E., Harris, N. G., Rashid, F., Ivy, A. S., Solodkin, A., Obenaus, A., & Baram, T. Z. (2016). MRI uncovers disrupted hippocampal microstructure that underlies memory impairments after early-life adversity. *Hippocampus*, *26*(12), 1618–1632. https://doi.org/10.1002/hipo.22661

Nelson, C. A., Zeanah, C. H., Fox, N. A., Marshall, P. J., Smyke, A. T., & Guthrie, D. (2007). Cognitive Recovery in Socially Deprived Young Children: The Bucharest Early Intervention Project. *Science*, *318*(5858), 1937–1940. https://doi.org/10.1126/science.1143921

Nelson, R. J., Bumgarner, J. R., Walker, W. H., & DeVries, A. C. (2021). Time-of-day as a critical biological variable. *Neuroscience & Biobehavioral Reviews*, *127*, 740–746. https://doi.org/10.1016/j.neubiorev.2021.05.017

Nestler, E. J. (2015). ΔFosB: A transcriptional regulator of stress and antidepressant responses. *European Journal of Pharmacology*, *753*, 66–72. https://doi.org/10.1016/j.ejphar.2014.10.034

Nestler, E. J., & Carlezon, W. A. (2006). The Mesolimbic Dopamine Reward Circuit in Depression. *Biological Psychiatry*, *59*(12), 1151–1159. https://doi.org/10.1016/j.biopsych.2005.09.018

Ochi, S., & Dwivedi, Y. (2023). Dissecting early life stress-induced adolescent depression through epigenomic approach. *Molecular Psychiatry*, *28*(1), 141–153. https://doi.org/10.1038/s41380-022-01907-x

Oomen, C. A., Soeters, H., Audureau, N., Vermunt, L., Van Hasselt, F. N., Manders, E. M. M., Joëls, M., Krugers, H., & Lucassen, P. J. (2011). Early maternal deprivation affects dentate gyrus structure and emotional learning in adult female rats. *Psychopharmacology*, *214*(1), 249–260. https://doi.org/10.1007/s00213-010-1922-8

Oomen, C. A., Soeters, H., Audureau, N., Vermunt, L., Van Hasselt, F. N., Manders, E. M. M., Joëls, M., Lucassen, P. J., & Krugers, H. (2010). Severe Early Life Stress Hampers Spatial Learning and Neurogenesis, but Improves Hippocampal Synaptic Plasticity and Emotional Learning under High-Stress Conditions in Adulthood. *The Journal of Neuroscience*, *30*(19), 6635–6645. https://doi.org/10.1523/JNEUROSCI.0247-10.2010

Parel, S. T., & Peña, C. J. (2022). Genome-wide Signatures of Early-Life Stress: Influence of Sex. *Biological Psychiatry*, *91*(1), 36–42. https://doi.org/10.1016/j.biopsych.2020.12.010

Peciña, S., Schulkin, J., & Berridge, K. C. (2006). Nucleus accumbens corticotropin-releasing factor increases cue-triggered motivation for sucrose reward: Paradoxical positive incentive effects in stress? *BMC Biology*, *4*(1), 8. https://doi.org/10.1186/1741-7007-4-8

Peña, C. J., Kronman, H. G., Walker, D. M., Cates, H. M., Bagot, R. C., Purushothaman, I., Issler, O., Loh, Y.-H. E., Leong, T., Kiraly, D. D., Goodman, E., Neve, R. L., Shen, L., & Nestler, E. J. (2017). Early life stress confers lifelong stress susceptibility in mice via ventral tegmental area OTX2. *Science*, *356*(6343), 1185–1188. https://doi.org/10.1126/science.aan4491

Peña, C. J., Smith, M., Ramakrishnan, A., Cates, H. M., Bagot, R. C., Kronman, H. G., Patel, B., Chang, A. B., Purushothaman, I., Dudley, J., Morishita, H., Shen, L., & Nestler, E. J. (2019). Early life stress alters transcriptomic patterning across reward circuitry in male and female mice. *Nature Communications*, *10*(1), 5098. https://doi.org/10.1038/s41467-019-13085-6

Perens, J., Salinas, C. G., Skytte, J. L., Roostalu, U., Dahl, A. B., Dyrby, T. B., Wichern, F., Barkholt, P., Vrang, N., Jelsing, J., & Hecksher-Sørensen, J. (2021). An Optimized Mouse Brain Atlas for Automated Mapping and Quantification of Neuronal Activity Using iDISCO+ and Light Sheet Fluorescence Microscopy. *Neuroinformatics*, *19*(3), 433–446. https://doi.org/10.1007/s12021-020-09490-8

Perrault, T. J., Vaughan, J. W., Stein, B. E., & Wallace, M. T. (2005). Superior Colliculus Neurons Use Distinct Operational Modes in the Integration of Multisensory Stimuli. *Journal of Neurophysiology*, *93*(5), 2575–2586. https://doi.org/10.1152/jn.00926.2004

Pizzagalli, D. A. (2014). Depression, Stress, and Anhedonia: Toward a Synthesis and Integrated Model. *Annual Review of Clinical Psychology*, *10*(1), 393–423. https://doi.org/10.1146/annurev-clinpsy-050212-185606

Pizzagalli, D. A. (2022). Toward a Better Understanding of the Mechanisms and Pathophysiology of Anhedonia: Are We Ready for Translation? *American Journal of Psychiatry*, *179*(7), 458–469. https://doi.org/10.1176/appi.ajp.20220423

Pizzagalli, D. A., Jahn, A. L., & O'Shea, J. P. (2005). Toward an objective characterization of an anhedonic phenotype: A signal-detection approach. *Biological Psychiatry*, *57*(4), 319–327. https://doi.org/10.1016/j.biopsych.2004.11.026

Plotsky, P. M., & Meaney, M. J. (1993). Early, postnatal experience alters hypothalamic corticotropin-releasing factor (CRF) mRNA, median eminence CRF content and stress-induced release in adult rats. *Molecular Brain Research*, *18*(3), 195–200. https://doi.org/10.1016/0169-328X(93)90189-V

Ramm, S. A., Cheetham, S. A., & Hurst, J. L. (2008). Encoding choosiness: Female attraction requires prior physical contact with individual male scents in mice. *Proceedings of the Royal Society B: Biological Sciences*, *275*(1644), 1727–1735. https://doi.org/10.1098/rspb.2008.0302

Rice, C. J., Sandman, C. A., Lenjavi, M. R., & Baram, T. Z. (2008). A Novel Mouse Model for Acute and Long-Lasting Consequences of Early Life Stress. *Endocrinology*, *149*(10), 4892–4900. https://doi.org/10.1210/en.2008-0633

Richardson, N. R., & Roberts, D. C. S. (1996). Progressive ratio schedules in drug self-administration studies in rats: A method to evaluate reinforcing efficacy. *Journal of Neuroscience Methods*, *66*(1), 1–11. https://doi.org/10.1016/0165-0270(95)00153-0

Risbrough, V. B., Glynn, L. M., Davis, E. P., Sandman, C. A., Obenaus, A., Stern, H. S., Keator, D. B., Yassa, M. A., Baram, T. Z., & Baker, D. G. (2018). Does Anhedonia Presage Increased Risk of Posttraumatic Stress Disorder?: Adolescent Anhedonia and Posttraumatic Disorders. In E. Vermetten, D. G. Baker, & V. B. Risbrough (Eds.), *Behavioral Neurobiology of PTSD* (Vol. 38, pp. 249–265). Springer International Publishing. https://doi.org/10.1007/7854_2018_51

Rivest, S. (1995). The role of corticotropin-releasing factor and interleukin-1 in the regulation of neurons controlling reproductive functions. *Endocrine Reviews*, *16*(2), 177–199. https://doi.org/10.1210/er.16.2.177

Roberto, M., Cruz, M. T., Gilpin, N. W., Sabino, V., Schweitzer, P., Bajo, M., Cottone, P., Madamba, S. G., Stouffer, D. G., Zorrilla, E. P., Koob, G. F., Siggins, G. R., & Parsons, L. H. (2010). Corticotropin Releasing Factor–Induced Amygdala Gamma-Aminobutyric Acid Release Plays a Key Role in Alcohol Dependence. *Biological Psychiatry*, *67*(9), 831–839. https://doi.org/10.1016/j.biopsych.2009.11.007

Roberts, S. A., Simpson, D. M., Armstrong, S. D., Davidson, A. J., Robertson, D. H., McLean, L., Beynon, R. J., & Hurst, J. L. (2010). Darcin: A male pheromone that stimulates female memory and sexual attraction to an individual male's odour. *BMC Biology*, *8*(1), 75. https://doi.org/10.1186/1741-7007-8-75

Robins, M. T., Li, J., & Ryabinin, A. E. (2020). Effects of Housing Conditions and Circadian Time on Baseline c-Fos Immunoreactivity in C57BL/6J Mice. *Neuroscience*, *431*, 143–151. https://doi.org/10.1016/j.neuroscience.2020.02.006

Rocks, D., Jaric, I., Bellia, F., Cham, H., Greally, J. M., Suzuki, M., & Kundakovic, M. (2023). Early-life stress and ovarian hormones alter transcriptional regulation in the nucleus accumbens resulting in sex-specific responses to cocaine. *Cell Reports*, *42*(10), 113187. https://doi.org/10.1016/j.celrep.2023.113187

Roozendaal, B., Brunson, K. L., Holloway, B. L., McGaugh, J. L., & Baram, T. Z. (2002). Involvement of stress-released corticotropin-releasing hormone in the basolateral amygdala in regulating memory consolidation. *Proceedings of the National Academy of Sciences*, *99*(21), 13908–13913. https://doi.org/10.1073/pnas.212504599

Rothschild, G., Nelken, I., & Mizrahi, A. (2010). Functional organization and population dynamics in the mouse primary auditory cortex. *Nature Neuroscience*, *13*(3), 353–360. https://doi.org/10.1038/nn.2484

Shansky, R. M., & Woolley, C. S. (2016). Considering Sex as a Biological Variable Will Be Valuable for Neuroscience Research. *The Journal of Neuroscience*, *36*(47), 11817–11822. https://doi.org/10.1523/JNEUROSCI.1390-16.2016

Short, A. K., & Baram, T. Z. (2019). Early-life adversity and neurological disease: Age-old questions and novel answers. *Nature Reviews Neurology*, *15*(11), 657–669. https://doi.org/10.1038/s41582-019-0246-5

Silberman, Y., & Winder, D. G. (2013). Corticotropin releasing factor and catecholamines enhance glutamatergic neurotransmission in the lateral subdivision of the central amygdala. *Neuropharmacology*, *70*, 316–323. https://doi.org/10.1016/j.neuropharm.2013.02.014

Smith, K. E., & Pollak, S. D. (2020). Early life stress and development: Potential mechanisms for adverse outcomes. *Journal of Neurodevelopmental Disorders*, *12*(1), 34. https://doi.org/10.1186/s11689-020-09337-y

Smith, K. S., Bucci, D. J., Luikart, B. W., & Mahler, S. V. (2016). DREADDS: Use and application in behavioral neuroscience. *Behavioral Neuroscience*, *130*(2), 137–155. https://doi.org/10.1037/bne0000135

Sohal, V. S., Zhang, F., Yizhar, O., & Deisseroth, K. (2009). Parvalbumin neurons and gamma rhythms enhance cortical circuit performance. *Nature*, *459*(7247), 698–702. https://doi.org/10.1038/nature07991

Spadoni, A. D., Vinograd, M., Cuccurazzu, B., Torres, K., Glynn, L. M., Davis, E. P., Baram, T. Z., Baker, D. G., Nievergelt, C. M., & Risbrough, V. B. (2022). Contribution of early-life unpredictability to neuropsychiatric symptom patterns in adulthood. *Depression and Anxiety*, *39*(10–11), 706–717. https://doi.org/10.1002/da.23277

Stein, B. E., Meredith, M. A., Huneycutt, W. S., & McDade, L. (1989). Behavioral Indices of Multisensory Integration: Orientation to Visual Cues is Affected by Auditory

Stimuli. *Journal of Cognitive Neuroscience*, *1*(1), 12–24. https://doi.org/10.1162/jocn.1989.1.1.12

Stuber, G. D. (2023). Neurocircuits for motivation. *Science*, *382*(6669), 394–398. https://doi.org/10.1126/science.adh8287

Stuber, G. D., Sparta, D. R., Stamatakis, A. M., Van Leeuwen, W. A., Hardjoprajitno, J. E., Cho, S., Tye, K. M., Kempadoo, K. A., Zhang, F., Deisseroth, K., & Bonci, A. (2011). Excitatory transmission from the amygdala to nucleus accumbens facilitates reward seeking. *Nature*, *475*(7356), 377–380. https://doi.org/10.1038/nature10194

Surmeier, D. J., Song, W.-J., & Yan, Z. (1996). Coordinated Expression of Dopamine Receptors in Neostriatal Medium Spiny Neurons. *The Journal of Neuroscience*, *16*(20), 6579–6591. https://doi.org/10.1523/JNEUROSCI.16-20-06579.1996

Swedo, E. A., Aslam, M. V., Dahlberg, L. L., Niolon, P. H., Guinn, A. S., Simon, T. R., & Mercy, J. A. (2023). Prevalence of Adverse Childhood Experiences Among U.S. Adults—Behavioral Risk Factor Surveillance System, 2011–2020. *MMWR. Morbidity and Mortality Weekly Report*, *72*(26), 707–715. https://doi.org/10.15585/mmwr.mm7226a2

Taniguchi, H., He, M., Wu, P., Kim, S., Paik, R., Sugino, K., Kvitsani, D., Fu, Y., Lu, J., Lin, Y., Miyoshi, G., Shima, Y., Fishell, G., Nelson, S. B., & Huang, Z. J. (2011). A Resource of Cre Driver Lines for Genetic Targeting of GABAergic Neurons in Cerebral Cortex. *Neuron*, *71*(6), 995–1013. https://doi.org/10.1016/j.neuron.2011.07.026

Taniguchi, L., Goodpaster, C. M., Chen, Y., De Carvalho, G. B., Birnie, M. T., Paul, A., Chiang, A., Chen, L. Y., Baram, T. Z., & DeNardo, L. A. (2026). Sex and Stress Govern the Function and Innervation of a Basolateral Amygdala to Nucleus Accumbens Corticotropin-Releasing Hormone/GABA-Expressing Projection. *The Journal of Neuroscience*, *46*(2), e1239252025. https://doi.org/10.1523/JNEUROSCI.1239-25.2025

Taylor, S. E. (2010). Mechanisms linking early life stress to adult health outcomes. *Proceedings of the National Academy of Sciences*, *107*(19), 8507–8512. https://doi.org/10.1073/pnas.1003890107

Tian, Z., Song, J., Zhao, X., Zhou, Y., Chen, X., Le, Q., Wang, F., Ma, L., & Liu, X. (2024). The interhemispheric amygdala-accumbens circuit encodes negative valence in mice. *Science*, *386*(6722), eadp7520. https://doi.org/10.1126/science.adp7520

Torres-Berrío, A., Issler, O., Parise, E. M., & Nestler, E. J. (2019). Unraveling the epigenetic landscape of depression: Focus on early life stress. *Dialogues in Clinical Neuroscience*, *21*(4), 341–357. https://doi.org/10.31887/DCNS.2019.21.4/enestler

Tracy, M., Salo, M., Slopen, N., Udo, T., & Appleton, A. A. (2019). Trajectories of childhood adversity and the risk of depression in young adulthood: Results from the Avon Longitudinal Study of Parents and Children. *Depression and Anxiety*, *36*(7), 596–606. https://doi.org/10.1002/da.22887

Turecki, G., Ota, V. K., Belangero, S. I., Jackowski, A., & Kaufman, J. (2014). Early life adversity, genomic plasticity, and psychopathology. *The Lancet Psychiatry*, *1*(6), 461–466. https://doi.org/10.1016/S2215-0366(14)00022-4

Van Den Dries, L., Juffer, F., Van IJzendoorn, M. H., & Bakermans-Kranenburg, M. J. (2010). Infants' Physical and Cognitive Development After International Adoption From Foster Care or Institutions in China. *Journal of Developmental & Behavioral Pediatrics*, *31*(2), 144–150. https://doi.org/10.1097/DBP.0b013e3181cdaa3a

Vann, S. D., Aggleton, J. P., & Maguire, E. A. (2009). What does the retrosplenial cortex do? *Nature Reviews Neuroscience*, *10*(11), 792–802. https://doi.org/10.1038/nrn2733

Vegetabile, B. G., Stout-Oswald, S. A., Davis, E. P., Baram, T. Z., & Stern, H. S. (2019). Estimating the Entropy Rate of Finite Markov Chains With Application to Behavior Studies. *Journal of Educational and Behavioral Statistics*, *44*(3), 282–308. https://doi.org/10.3102/1076998618822540

Volkow, N. D., Wang, G., Fowler, J. S., Tomasi, D., Telang, F., & Baler, R. (2010). Addiction: Decreased reward sensitivity and increased expectation sensitivity conspire to overwhelm the brain's control circuit. *BioEssays*, *32*(9), 748–755. https://doi.org/10.1002/bies.201000042

Wahlstrom, K. L., Huff, M. L., Emmons, E. B., Freeman, J. H., Narayanan, N. S., McIntyre, C. K., & LaLumiere, R. T. (2018). Basolateral Amygdala Inputs to the Medial Entorhinal Cortex Selectively Modulate the Consolidation of Spatial and Contextual Learning. *The Journal of Neuroscience*, *38*(11), 2698–2712. https://doi.org/10.1523/JNEUROSCI.2848-17.2018

Walker, C.-D., Bath, K. G., Joels, M., Korosi, A., Larauche, M., Lucassen, P. J., Morris, M. J., Raineki, C., Roth, T. L., Sullivan, R. M., Taché, Y., & Baram, T. Z. (2017). Chronic early life stress induced by limited bedding and nesting (LBN) material in rodents: Critical considerations of methodology, outcomes and translational potential. *Stress*, *20*(5), 421–448. https://doi.org/10.1080/10253890.2017.1343296

Wallace, D. J., Greenberg, D. S., Sawinski, J., Rulla, S., Notaro, G., & Kerr, J. N. D. (2013). Rats maintain an overhead binocular field at the expense of constant fusion. *Nature*, *498*(7452), 65–69. https://doi.org/10.1038/nature12153

Walsh, J. J., Friedman, A. K., Sun, H., Heller, E. A., Ku, S. M., Juarez, B., Burnham, V. L., Mazei-Robison, M. S., Ferguson, D., Golden, S. A., Koo, J. W., Chaudhury, D., Christoffel, D. J., Pomeranz, L., Friedman, J. M., Russo, S. J., Nestler, E. J., & Han, M.-H. (2014). Stress and CRF gate neural activation of BDNF in the mesolimbic reward pathway. *Nature Neuroscience*, *17*(1), 27–29. https://doi.org/10.1038/nn.3591

Wang, Q., Ding, S.-L., Li, Y., Royall, J., Feng, D., Lesnar, P., Graddis, N., Naeemi, M., Facer, B., Ho, A., Dolbeare, T., Blanchard, B., Dee, N., Wakeman, W., Hirokawa, K. E., Szafer, A., Sunkin, S. M., Oh, S. W., Bernard, A., … Ng, L. (2020). The Allen Mouse Brain Common Coordinate Framework: A 3D Reference Atlas. *Cell*, *181*(4), 936-953.e20. https://doi.org/10.1016/j.cell.2020.04.007

Wang, X., Chou, X., Zhang, L. I., & Tao, H. W. (2020). Zona Incerta: An Integrative Node for Global Behavioral Modulation. *Trends in Neurosciences*, *43*(2), 82–87. https://doi.org/10.1016/j.tins.2019.11.007

Wang, Z., Yu, L., Xu, J., Stein, B. E., & Rowland, B. A. (2020). Experience Creates the Multisensory Transform in the Superior Colliculus. *Frontiers in Integrative Neuroscience*, *14*, 18. https://doi.org/10.3389/fnint.2020.00018

Wassum, K. M., & Izquierdo, A. (2015). The basolateral amygdala in reward learning and addiction. *Neuroscience & Biobehavioral Reviews*, *57*, 271–283. https://doi.org/10.1016/j.neubiorev.2015.08.017

Watanabe, H., Kobikov, Y., Nosova, O., Sarkisyan, D., Galatenko, V., Carvalho, L., Maia, G. H., Lukoyanov, N., Lavrov, I., Ossipov, M. H., Hallberg, M., Schouenborg, J., Zhang, M., & Bakalkin, G. (2024). The Left-Right Side-Specific Neuroendocrine Signaling from Injured Brain: An Organizational Principle. *Function*, *5*(4), zqae013. https://doi.org/10.1093/function/zqae013

Watanabe, H., Nosova, O., Sarkisyan, D., Andersen, M. S., Zhang, M., Rorick-Kehn, L., Clausen, F., Gawel, K., Kehr, J., Hallberg, M., Schouenborg, J., Marklund, N., & Bakalkin, G. (2020). Ipsilesional *versus* contralesional postural deficits induced by unilateral brain trauma: A side reversal by opioid mechanism. *Brain Communications*, *2*(2), fcaa208. https://doi.org/10.1093/braincomms/fcaa208

Weaver, I. C. G., Cervoni, N., Champagne, F. A., D'Alessio, A. C., Sharma, S., Seckl, J. R., Dymov, S., Szyf, M., & Meaney, M. J. (2004). Epigenetic programming by maternal behavior. *Nature Neuroscience*, *7*(8), 847–854. https://doi.org/10.1038/nn1276

Whitton, A. E., Kakani, P., Foti, D., Van't Veer, A., Haile, A., Crowley, D. J., & Pizzagalli, D. A. (2016). Blunted Neural Responses to Reward in Remitted Major Depression: A High-Density Event-Related Potential Study. *Biological Psychiatry:*

Cognitive Neuroscience and Neuroimaging, *1*(1), 87–95. https://doi.org/10.1016/j.bpsc.2015.09.007

Winter, J. J., Rodríguez-Acevedo, K. L., Dittrich, M., & Heller, E. A. (2023). Early life adversity: Epigenetic regulation underlying drug addiction susceptibility. *Molecular and Cellular Neuroscience*, *125*, 103825. https://doi.org/10.1016/j.mcn.2023.103825

Yan, X.-X., Toth, Z., Schultz, L., Ribak, C. E., & Baram, T. Z. (1998). Corticotropin-releasing hormone (CRH)-containing neurons in the immature rat hippocampal formation: Light and electron microscopic features and colocalization with glutamate decarboxylase and parvalbumin. *Hippocampus*, *8*(3), 231–243. https://doi.org/10.1002/(SICI)1098-1063(1998)8:3%3C231::AID-HIPO6%3E3.0.CO;2-M

Yang, X., Liu, Q., Zhong, J., Song, R., Zhang, L., & Wang, L. (2020). A simple threat-detection strategy in mice. *BMC Biology*, *18*(1), 93. https://doi.org/10.1186/s12915-020-00825-0

Yang, Y., & Wang, J.-Z. (2017). From Structure to Behavior in Basolateral Amygdala-Hippocampus Circuits. *Frontiers in Neural Circuits*, *11*, 86. https://doi.org/10.3389/fncir.2017.00086

Yarur, H. E., Vega-Quiroga, I., González, M. P., Noches, V., Thomases, D. R., Andrés, M. E., Ciruela, F., Tseng, K. Y., & Gysling, K. (2020). Inhibitory Control of Basolateral Amygdalar Transmission to the Prefrontal Cortex by Local Corticotrophin Type 2 Receptor. *International Journal of Neuropsychopharmacology*, *23*(2), 108–116. https://doi.org/10.1093/ijnp/pyz065

Ye, Q., Nunez, J., & Zhang, X. (2023). Zona incerta dopamine neurons encode motivational vigor in food seeking. *Science Advances*, *9*(46), eadi5326. https://doi.org/10.1126/sciadv.adi5326

Yilmaz, M., & Meister, M. (2013). Rapid Innate Defensive Responses of Mice to Looming Visual Stimuli. *Current Biology*, *23*(20), 2011–2015. https://doi.org/10.1016/j.cub.2013.08.015

Zhou, H., Xiang, W., & Huang, M. (2021). Inactivation of Zona Incerta Blocks Social Conditioned Place Aversion and Modulates Post-traumatic Stress Disorder-Like Behaviors in Mice. *Frontiers in Behavioral Neuroscience*, *15*, 743484. https://doi.org/10.3389/fnbeh.2021.743484